NASA CR-122453

(NASA-CR-122453) DESIGN STUDY FOR A HIGH RELIABILITY FIVE-YEAR SPACECRAFT TAPE TRANSPORT Final Report G.S.L. Benn, et al (IIT Research Inst.) Nov. 1971 235 p CSCL 14C G3/07

N72-30146

Unclas 39554

IITRI

DESIGN STUDY FOR A HIGH RELIABILITY FIVE-YEAR SPACECRAFT TAPE TRANSPORT

Final Report
IITRI Project No. E6179
Contract No. NAS5-21556

Goddard Space Flight Center
Greenbelt, Maryland

Prepared by

G.S.L. Benn
Dr. R.L. Eshleman

IIT Research Institute
10 West 35th Street
Chicago, Illinois 60616

November 1971

FOREWORD

This is the Final Report on IIT Research Institute Project No. E6179 entitled, "Design Study for a High Reliability Five-Year Spacecraft Tape Recorder." The work was performed for the National Aeronautics and Space Administration, Goddard Space Flight Center, under Contract No. NAS5-21556.

The work, completed over a nine month period, was monitored by Mr. Carl Powell of GSFC. IITRI personnel contributing to the technical content of this report include Dr. R.L. Eshleman, Dr. E.E. Hahn, W.J. Courtney, E. Swider, D.W. Hanify, R.J. Owen and G.S.L. Benn. Special acknowledgement is due to T.M. Scopelite, Manager, Mechanical Systems for his assistance and direction throughout the program.

Respectfully submitted,
IIT RESEARCH INSTITUTE

G.S.L. Benn

G.S.L. Benn
Research Engineer

Approved:

J. T. Jacobi, Director of Research

G.T. Jacobi
Assistant Director
Electronics Research

ABSTRACT

The main objective of this design study was the development of a design for a spacecraft tape transport which inherently possessed high reliability and was capable of unattended operation at 100% duty cycle over a period of five years. The initial establishment of a philosophy of approach that life should predominate and that the design should not be constrained by imposed specifications, differed from that normally followed in the design of a magnetic tape transport for unattended use in space. This philosophy generated a set of reliability guidelines and program goals that were applied to a transport configuration study from which a coplanar reel to reel concept with independently motor driven reels and capstans was considered to be the most desirable candidate for a high reliability five-year tape transport.

Following the establishment of the overall transport concept a detailed study of all of the life limiting constraints associated with the transport were carefully analyzed using modeling techniques. These design techniques included a response analysis from which the performance of the transport could be determined under operating conditions for a variety of conceptual variations both in a new and aged condition; an analysis of a double cone guidance technique which yielded an optimum design for maximum guidance with minimum tape degradation; an analysis of the tape pack design to eliminate spoking caused by negative tangential stress within the pack; a detailed evaluation of the stress levels experienced by the magnetic tape throughout the system; a general review of the bearing and lubrication technology as applied to satellite recorders and hence the recommendation for using standard load carrying antifriction ball bearings coupled with a lubricant replenishment system; and finally, a detailed kinetic analysis to determine the change in kinetic properties of the transport during operation.

The results of these various analyses were then applied to a conceptual layout of the tape transport, which is functionally described in modular form, and from this, a system performance analysis was conducted which indicated that the transport performance compared favorably with existing satellite recorders. Finally, a testing technique to assure long life was established. This technique does not rely upon accelerated test procedures or the unrealistic requirement of life testing for the full term. It does, however, make it possible to establish the usable life of the transport with a high level of confidence and hence may be applied to confirm the design practices developed during this design study.

The design of a spacecraft tape transport resulting from this study, clearly illustrates that the survivability of mechanical devices for unattended operation over a five year period is within the capability of the state of the art. Although the proposed system is similar to those used in ground based transports, its application to the space environment is unique. This represents a major redirection of engineering techniques for the design of magnetic tape transports, where all of the design criteria have been selectively directed towards maximizing the operational life of the machine.

TABLE OF CONTENTS

TABLE OF CONTENTS (CONT'D)

TABLE OF CONTENTS (CONT'D)

TABLE OF CONTENTS (CONT'D)

LIST OF FIGURES

LIST OF FIGURES (CONT'D)

LIST OF FIGURES (CONT'D)

LIST OF TABLES

DESIGN STUDY FOR A HIGH RELIABILITY FIVE-YEAR SPACECRAFT TAPE TRANSPORT

1. INTRODUCTION

1.1 Program Objectives

The purpose of a tape recorder is to store and retrieve data without significantly degrading the information content. Although tape recorders may be used to either expand or compress data in time, the principal reason for their widespread use in satellite systems is the large storage capacity provided. In comparison with other techniques for achieving large memories, tape recorders have proven to be efficient on a size, weight, and cost basis. In order to provide access to the data stored, it is necessary for the tape transport to move tape past the read and/or write head and to provide intimate contact between the tape and heads. Historically, satellite transports have experienced difficulty in fulfilling these requirements.

Traditionally, space transport systems have been designed to satisfy the requirements of the signal processing system as well as being contained by severe weight, volume, and power limitations. The broad goal of this study was to provide the maximum engineering latitude in the development of a design which would lead to a transport with a five year mission life. Clearly, to achieve this goal, it was necessary to adopt a general approach of reducing mechanical complexity and operational constraints and, where possible, to shift the demand of high critical performance from the mechanical subsystem to the electronics subsystem.

The objective of this program was, therefore, to develop a design for a tape transport which inherently possessed high reliability and was capable of unattended operation over a five-year period at a data storage capacity commensurate with future mission requirements. In order to fulfill this requirement it was necessary at the commencement of this study to specify a philosophy of approach, and establish certain goals, which would lead to a logical derivation of a design which possessed the required reliability as prescribed in the Goddard Space Flight Center specification No. S-731-P-105. These goals included:

- The identification of a transport configuration in which all considerations were made on the basis of long life.
- The identification of a set of specifications that were compatible with satellite operation, but were not life limiting and, therefore, were not self defeating. This implied identification of life limiting constraints.
- The identification of a course of action which would maximize life and, if the need be, a series of alternatives.

In order to achieve these goals of this design study, it was necessary to formulate a set of guidelines. These guidelines together with the engineering strategy involved in the fulfillment of the program objectives are outlined in more detail in a later section.

The tape transport configuration selected during this program is discussed in greater detail in Section 2 of this report. It is, however, necessary to establish at this point that although the selected configuration has been chosen on the basis of careful engineering judgement, the choice of configuration is only a small but important part of the prime objective. Of equal significance, and yet not so obvious, are such factors as the choice, installation, and lubrication of the bearings; the minimization of stress levels in the magnetic tape; the concept and advantages of modularization techniques; overall fabrication methods; the relative size and position of the various transport elements; and the selection of critical subelements. Also of importance is the understanding that the term 'five year life' used throughout this report is meant to represent continuous operation at 100% duty cycle. An arbitrary value of 10,000 tape passes per year has been assigned which is typical of the earth orbital requirements. The major significance is that the long life requirement of the transport may be defined as the ability to record and reproduce data successfully for 50,000 full tape passes.

This study program has resulted in a tape transport design where all considerations of its design were made on the basis of maximizing life. It will be seen that the transport configuration is not in itself unique, however, all criteria leading to its formulation have been arrived at by maximizing all of the analytical techniques currently available and insuring that the imposed reliability guidelines were adhered to throughout the program. This represents a major redirection of engineering techniques for the design of magnetic tape transports, where all of the design criteria have been selectively directed towards maximizing the operational life of the machine.

1.2 Report Organization

The technical discussion in Section 2 of this report is divided into four parts. The first describes the general philosophy and method of approach that was used throughout the Design Study. This section also describes the major goals of the program and outlines a set of guidelines that were established in order to successfully achieve these goals. This is followed by a definition of the proposed modularization technique and a description of the analytical modeling of the mechanical system. The second part outlines the various methods of approach that were undertaken in the prior selection of the transport configuration, various trade off studies are explained, and reasons for the final choice of configuration are stated. The third part describes in detail the high reliability five-year tape transport that resulted from this Design Study. The functional layout is described, followed by a description of the major critical areas of bearings and tape stresses throughout the system. This is followed by a description of the overall system performance and a proposed testing technique for five-year life.

Section 3 of this report, entitled Design Techniques and Results, contains the indepth analytical work that was undertaken in a variety of subject areas. Included in this section are the formulation of the mathematical models derived during the program, the computer programs used, and the analytical results that were obtained and later applied to the overall design study.

2. TECHNICAL DISCUSSION

2.1 General Philosophy

In order to achieve the main objective of this design study an overall philosophy was established together with a set of program goals which differed from those normally followed in the design of a magnetic tape transport for unattended use in space.

In the past, satellite receivers have by necessity been designed to conform to a set of stringent specifications. These specifications not only established performance criteria but contained fundamental specification values for power, weight, and volume. Such values were obviously necessary in terms of payload and limited available power, but it implied that the system mechanics were slave to unusually tight limitations. Many such recorders were produced and it is a tribute to engineering ingenuity that these transports fulfilled these stringent specifications. Recently, however, greater emphasis has been placed on extending the operational life of such systems and it is here that failures have occurred. It is not unreasonable to conclude that the heavy burden placed on the mechanical system in achieving the unusual specifications resulted in the life limitations that have been experienced. Mechanical failures have been observed, the weakest link generally failing first such as the magnetic tape, belts, bearings, etc. Certain failures are not always catastrophic such as an increase in tape flutter or deterioration in guidance, but even these can be related to failures in the mechanical system.

It was for this reason that the underlying philosophy of approach established during this study was that the transport design should be directed towards maximizing life without the constraints of imposed specifications. Obviously, for operation in space, tape recorders must conform to an envelope of general specifications but these should not be imposed. Implied in this is that the design study would identify a set of specifications that were compatible with life but were not life limiting. This would, therefore, allow the mechanical system to operate in a regime where it can exist for five years. Operational regime implies dimensional as well as performance areas in which the mechanics can operate in a realm of reasonable capability.

Coupled with the identification of a set of specifications was the need to identify a transport configuration where all consideration was made on the basis of long life. In the past, the need to conform to specific geometric form factors and limited power availability have generated a family of satellite recorders which include novel configurations, such as the negator spring coaxial reel type. Long operating life was not, however, a primary consideration and although much effort has subsequently been expended in extending the operational life of these and other transport designs so that now one year operation is possible and two probable, life beyond two years is considered unproven and probably unobtainable.

It was mandatory, therefore, in considering a high reliability five-year transport design to identify a transport configuration which was in no way influenced by an factor other than those related to maximizing life. Realistically, trade offs between life and even the broad envelope of specifications were bound to occur and infact did.

The philosophy that life shall predominate over all other requirements led to a set of program goals necessary to achieve the prime objective. These goals were:

- The identification of a set of specifications within a broad envelope that were compatible with satellite operation, and were not life limiting.

- The identification of a transport configuration in which all considerations were made on the basis of long life.

- The identification of life limiting aspects of the transport as a whole.

- The identification of a design procedure using analytical modeling to maximize life.

In order to achieve these goals and objectives it was necessary to establish a set of rules or guidelines, the use of which would allow trade off decision-criteria to be consistent throughout the program. These Machine System Reliability Guidelines were:

- To recognize the limitations of applying traditional reliability analysis to satellite tape recorders.

- To maximize all of the analytical capabilities relevent to the overall system.

- Ensure adaptability to modularization.

- To adhere to minimum mechanical complexity, but to temper this with minimum interactive mechanical functions.

- To select a system and components well within historically proven performance regimes.

- To acquire components from the largest production population possible, therefore attempting to obtain not a unique sample but a statistically average sample.

- To recognize the need to establish realistic life testing techniques throughout the system.

Many of these guidelines are self explanatory, but one or two require a brief explanation. There is a drawback to applying traditional reliability analysis to satellite tape recorders, this is primarily one of limited knowledge. There is only a small amount of failure rate information available and little or no knowledge on the prognosis relative to life of a running system. A failure in orbit may be due to a multiplicity of causes but the exact cause usually remains unknown or uncertain. Clearly the construction of models for failure when information is so sparce is difficult. The lack of relevant information with regards to failure can be attributed to two main reasons. First, the difficulty and therefore the expense of testing and evaluating mechanical systems is prohibitive. This is coupled with the inexactitude in mechanical systems to successfully duplicate accelerated life tests in real time. Second and more important is that the accuracy of correlating test data with prediction is questionable. The reliability of mechanical components is related not only to fabrication of the element but to the installation of that element into the system. The success of a mechanical element such as a belt or bearing in achieving many mission lifetimes on a life test model appears to have little relationship to the failure of an identical element installed in another system, and therefore the ability to generalize test data is very difficult. What is needed to overcome this severe limitation in mechanical systems for long term unattended use is a radically new approach both in the analytical design stage and in the subsequent life testing, so that a mechanical element can be selected on the basis of its own behavior rather than on the premise that an identical element behaved well in life tests. To realize this approach requires modularization of the transport.

2.1.1 Modularization

Modularization was the key design strategy selected to overcome the insufficiency of failure information connected with products of extremely limited number such as satellite tape recorders.

Modularization in this context implies unitizing a functional subsystem. Storage of the tape is one example of a function; its related subsystem is not the reel alone, it is the reel, the bearings, the bearing supports, and the drive system. All of these are designed to form a module which can then be inserted as a unit into the principal tape transport.

The advantages to such a system are many but the prime advantage is associated with a new approach to pre-flight testing to ensure long life. Modularization of a transport, to be effective, requires fabrication of several modules of the same function. Let us say, for example, that six or eight reel assemblies are fabricated. Each one is then subjected as a subsystem to a burn in period of 10% of the total operational life required, in this case six months. Burn in periods are used in electronics but not well established in mechanical systems. This is the way that long life mechanisms should be evaluated to eliminate short term failures. During this burn in period all the modules are continually evaluated so that a running signature of performance is established for each over a five to six month period. At the end of this multi-month evaluation period, one or two modules are then selected on the basis of performance, i.e., drag, torque, acoustic signature, etc. In this way there is some evidence that a module will continue without a major change or serious degradation which would indicate that an early failure is likely to occur.

The set of modules selected would then be assembled into the transport as a whole and qualification testing would begin.

While this transport is being qualified as a complete mechanical system, the remainder of the modularized subsystems would continue to be tested as individual units. In this way, at the end of the qualification period all modules would still have an equal life evaluation time and any component degradation may be observed. If component failure occurred during qualification in the assembled transport, then only the module responsible for the failure need be replaced by an equivalent module that is still performing satisfactorily.

2.1.2 Analytical Modeling

To overcome the severe limitations of a mechanical system for long term unattended use, emphasis was placed on analytical modeling of mechanical systems. The analytical model of the tape transport is an integral portion of the design approach. The model allows the maximization of the conceptual design by variation of model parameters. In this way a design can be obtained that requires minimum hardware development.

The design procedure using the analytical model begins with the selection of a concept. This concept was selected on the basis of minimizing the number of critical elements in the system. The analytical model of this concept is used to select dimensions, materials, and components based on long life and performance. The stresses in the various components are compared to their strengths, the performance of the system is, with typical error sources, compared to that of normal transports. In addition, the degraded (with respect to wear) transport performance is compared to that of the new transport. In this way the performance of the transport after a finite time interval can be assessed.

During the study, as the mechanical system was functionally described, each of the main subsystems were analytically designed to maximize the systems mission life reliability.

In this context, reliability is meant to encompass:

- Structural integrity in withstanding the shock, vibration, and thermal environment.
- The maintenance of system performance within acceptable bounds, e.g., the tape motion irregularities such as time base error and skew must not exceed a specified limit due to the effects of operational aging.
- The design against catastrophic fatigue failure of elements such as belts and bearings.

Relative to the reliability analyses, the first step involved is defining the function of each component in the tape transport system, parameter limits for satisfactory operation, and functional relationships and interaction with other components. The second step consisted of an analysis of all possible failure and degradation modes which would be applicable to individual system components or combinations of components, and an evaluation of design and application factors which could contribute to specific failure modes. Complete analysis of failure modes require a quantative, or at least a qualitative, evaluation of likelihood of occurrence. The information necessary to conduct such an analysis came from engineering design and stress analysis, published reliability handbook data, component and equipment manufacturer data, and specific although limited information on failures in present tape transport systems. Further failure mode evaluation was obtained by means of criticality analysis, where probability of each failure was combined with some measure of its effect on system operation to rank each possible failure according to a criticality index.

Comparison of various subsystems in terms of reliability characteristics was made on the basis of a number of possible failure modes for each system, comparison of effects on performance, and a comparison of failure criticalities of each element. This evaluation also gave an indication of points where redesign, derating, improved quality control and inspection would be most effective in improving reliability. For portions of the tape transport system where varying amounts of failure rate data were available, evaluations and comparisons were made on the basis of subsystem reliability analyses based on such data, utilizing standard reliability modeling, and prediction techniques.

In evaluating the long term operating performance, it was essential to simulate the design in dynamic terms and then to study the influence of error source generators, such as bearings and eccentricity in film guiding surfaces, as well as predict the implications of aging effects due to wear and lubricant viscosity variations. To this end, use was made of fundamental analytical techniques[1], developed at IITRI for the computer simulation of a transport system as affected by error and system parameter variations. This analysis, was effective in portraying how certain performance parameters degrade with operational life; and more particularly focused the design on those areas to which system performance was most sensitive.

Thus an approach selected to meet the prime requirement, a five-year life expectancy, emerged in a program of design of modules with adequate margins against all stresses to minimize all possible failure modes.

2.2 Configuration Study

2.2.1 Tape Management

Inevitably, the initial design of a high reliability tape transport system focused upon the resolution of three main design areas; namely, tape storage, tape tensioning, and tape metering. For higher storage capacities, the technique successful to date has been the reel-to-reel system. Other approaches, such as cartridges and bin storage, produce exceptionally large and random tension pulsations; and in general violate the axiom of stringent control of tape tension and tape velocity throughout the systems operational history. The objective in designing a reel system is to provide sufficient structural integrity to the reel itself and its support so that precise motion can be achieved. This point cannot be over-emphasized, since the main dynamic errors of any transport result from poor reeling and inadequate tensioning.

Two basic reel positions have been traditionally utilized in previous satellite transports; coaxial and coplanar. The choice between these configurations, strongly influences the final tape path. The principal differences between these two main configurations are the change in tape elevation (as required in coaxial systems), and the complexity of the tape tensioning and guiding system. Variations on these two basic types together with several other configurations were the basis of the initial configuration study.

The singular objective of the configuration study was to identify a transport whose potential for achieving an unattended five-year mission life was established through historical performance, and where possible, through engineering analytics. In this study, the central trade-off decision focused on performance reliability; that is, when given a choice between several functionally acceptable alternatives, the selection was made on the basis of the component, module, or system which had the greatest chance of achieving a five-year life. At the onset of this effort, it was recognized that to identify a system whose life would be unquestionably the maximum among all possible choices could not be absolutely ascertained either theoretically or experimentally. But, by utilizing the reliability criteria, the system selected at least represented the best first approximation based on good engineering judgements and practices.

To initiate this task, several basic transport configurations were described in the terms of the following:

- Reel configuration, e.g., co-planar or coaxial;
- reel drive technique, e.g., electric motors, spring motor, or peripheral belt;
- tape path trajectory;
- tape metering technique

Further, these configurations were selected from those systems that had been, or were in the process of being, used in satellite applications. The basic transports considered were:

1. Co-Planar, Reel-to-Reel. Tape metering achieved by servo controlled reel speeds.
2. Co-Planar, Reel-to-Reel, with capstan metering systems, i.e., single capstan, dual capstan, a differential capstan. Further, reel drives and tape pack tensioning achieved by spring motors or individual reel motors.
3. Co-Axial Reel-to-Reel, with capstan and reel drives similar to (2).
4. Co-Planar Reel-to-Reel with tape metering and reel drive achieved with a peripheral belt.
5. Newell Drive, with a single capstan driving both tape and reels.

To delineate a high reliability five-year design from either one or a combination of the above concepts, the following elements of "designed-in" mechanical reliability were established as a means for evaluating the intrinsic reliability of a particular configuration.

2.2.2 Reliability Criteria

2.2.2.1 Minimum Mechanical Complexity

For the function required, e.g., for multiple speeds, it is essential to transform speed changing functions to motor and electric controls and away from belt drive-complex mechanical transmissions.

2.2.2.2 Minimum Interacting Mechanical Functions

This criteria emphasizes the need for assuring against serially adding functions, that is, each component is independent from an adjacent failure probability. For example:

- Using a capstan to drive the tape;
- the tape to drive the reel;
- the reels to drive a tachometer;
- the tachometer to drive a motor controller; and
- the motor controller to control the motor speed.

Failure anywhere in this serial loop results in failure of the total system. Further, there is no possibility for filtering or impeding incipient failures or their impact in the system. Therefore, minimum interacting mechanical functions were deemed crucial to successfully achieving a sound uncomplicated mechanical design.

2.2.2.3 Select and Design System Components Well Within Historically Proven Applications and Performance Regimes

This factor focuses upon specific elements within a transport to assure the proper application of mechanical components from the points of view of function and life. In this study, this implied that use could not be made of a mechanical system that had neither performance experience nor manufacturing quality control history behind it. It was, therefore, essential that the mechanical system have some historical evidence of successful operation in the multi-year area. When components are not chosen in this regime then the effective prediction of life is difficult and there is no operational justification or experimental evidence whatsoever to substantiate long life.

2.2.2.4 Component Acquisition from Largest Population Possible

It is essential that a specific configuration does not require exotic or limited available components, since these elements have little or no performance history from which to judge life. Selection from a large population insures that not a unique sample by a statistically average sample is obtained that has a record of proven performance.

2.2.2.5 Adaptability to Modularization

To bring a five-year life design through the development and system qualification phases, it was essential to the development scheme to separately test and evaluate subsystems such as capstan modules and reel-to-reel drive subassemblies. This approach became particularly cogent when it was recognized that component run in and evaluation might require 10% of the mission life. Hence, it was anticipated that the testing and qualification cycle would entail the simultaneous testing of several identical models of all transport subsystems. Subsequent testing of the total system could progress into the qualification phase. When a subsystem fails in this critical period, it is impossible, because of time limitations, to recycle the whole transport. Thus, the modularization strategy permits the failed module to be removed and replaced by a qualified substitute, thereby permitting the transport qualification to progress without a major setback or delay.

2.2.2.6 Minimum Tape Handling Stress

For a transport that is expected to produce at least 50,000 tape passes, a critical limitation of the system is in the tape handling area. To minimize tape oriented problems, it is important to reduce to an absolute minimum, the mechanically induced stresses. There are two main areas in which high stress levels occur in the magnetic tape system; namely, the tape pack itself and that associated with the tape handling and guidance. This is an extremely critical area which has been somewhat neglected throughout the industry in the past.

Therefore, all of the configurations were carefully examined during this study and compared for their ability to handle the tape in a manner which minimizes the tape stresses thoughout the system. There is little doubt that when the magnetic tape experiences severe stress levels while being handled, premature degradation often follows. To meet the prime objective of a five-year operational life high stress levels had to be eliminated throughout the tape pack system.

2.2.3 Transport Comparisons

The first step in the choice of a configuration for a high reliability five-year tape transport was a general comparison of the five basic reel configuration concepts shown in Figure 1. This entailed listing all of the advantages and disadvantages of each system and examining the various implications with regard to the reliability criteria and guidelines that had been established. As an example, a short form concept comparison is shown in Table 1, indicating the major advantages and disadvantages of the five concepts.

The next step was a comparison of alternative reel drive systems. Reel drives for the five basic concepts may be categorized into four basic types:

Type 1 Spring Devices

Type 2 Servo Controlled Motors

Type 3 Newell System

Type 4 Peripheral Belt

Table 1

CONCEPT COMPARISON

Concept	Advantages	Disadvantages
Concept No. 1 (Coplanar, Reel-to-Reel No Capstans)	1. Mechanical simplicity.	1. Difficult to control tape speed and tape tension simultaneously. 2. Lack of isolation between head and tape pack.
Concept No. 2 (Coplanar, Reel-to-Reel with Capstans)	1. Tape speed control and tape tension control.	1. Mechanical complexity.
Concept No. 3 (Coaxial, Reel-to-Reel with Capstans)	1. Use of negator. 2. Compactness in the linear dimension. (Geometric form factor)	1. High stress in tape owing to a change in tape elevation. 2. Unreliability of negator spring. 3. Tape guidance, e.g., corrective guidance to directive guidance.

Table 1

CONCEPT COMPARISON (Cont.)

Concept	Advantages	Disadvantages
Concept No. 4 (Coplanar, Reel-to-Reel with Peripheral Belt Drive)	1. Reel configuration very simple.	1. Load on isobelt bearings.
		2. High tension in p-belt.
		3. Control of tape tension.
		4. Variable tape tension profile.
		5. Tape to p-belt friction
		6. No head/reel isolation.
Concept No. 5 (Coplanar, Reel-to-Reel with Single Drive Capstan)	1. Conceptually simple.	1. Tension disturbance in tape pack unknown.
		2. Critical elements unknown.
		3. Tension-compliance of capstan and pressure on reels.
		4. Low frequency flutter - no damping.
		5. Lack of tape guidance.
		6. Severe mechanical tolerances.
		7. Mechanism reliability unknown.
		8. Moving tape hubs.

An interesting comparison results when each of the four basic drive systems are delineated into their major components as follows:

		Quantity	Component
1.	Spring Device	0	Motors
		1	Negator Spring
		1	Belt
		1	Differential Transmission
2.	Motors	2	Motors
3.	Newell	1	Motor
		1	Spring
		1	Moveable Reel System
4.	P-Belt	1	Motor
		1	Belt
		Several	Guide Elements

Use of this essential component division then allowed further comparison by listing the advantages and disadvantages of each reel drive system; three examples of which are shown below.

REEL DRIVE COMPARISON

a. Spring Comparison

Advantages	Disadvantages
1. Low power requirement.	1. Poor history of negator spring.
	2. Mechanical complexity.
	3. Gear or linkage pertubations.
	4. Uneven tension profile.
	5. Intricate assembly.

b. Two Variable Speed Motors

Advantages

1. Constructional simplicity.
2. Ease of modularization.
3. Electro/mechanical emphasis.
4. Large population.

Disadvantages

1. Increased power.
2. Increased weight.
3. Increased volume.
4. Small population without brushes.
5. Electronic control required.
6. Tension sensing problems.
7. Tape speed ratio require high ratio for direct drive motor.
8. Alignment of reels to motor shaft.

c. P-Belt with Constant Speed Motor

Advantages

1. Low power requirement.
2. Reel simplicity.

Disadvantages

1. P-belt must be guided.
2. Uneven tension profile.
3. High stress in p-belt.
4. Many bearings.
5. Frictional coupling.
6. Small population (motors).
7. Difficult to inspect belt.
8. Belt installation problems.
9. Difficult to control tension.

Obviously it was difficult to include every detail of the complex evaluation in this report, a great deal of which relied upon experience and engineering judgement, but the overall results are summarized in Table 2 where the transport configurations (1) through (5) are evaluated with respect to the long life mechanical characteristics previously described. This evaluation is reported in the form of numerical ratings 0 through 10 with ten indicating best compliance with the goals of the program. Numerical values are included to simplify

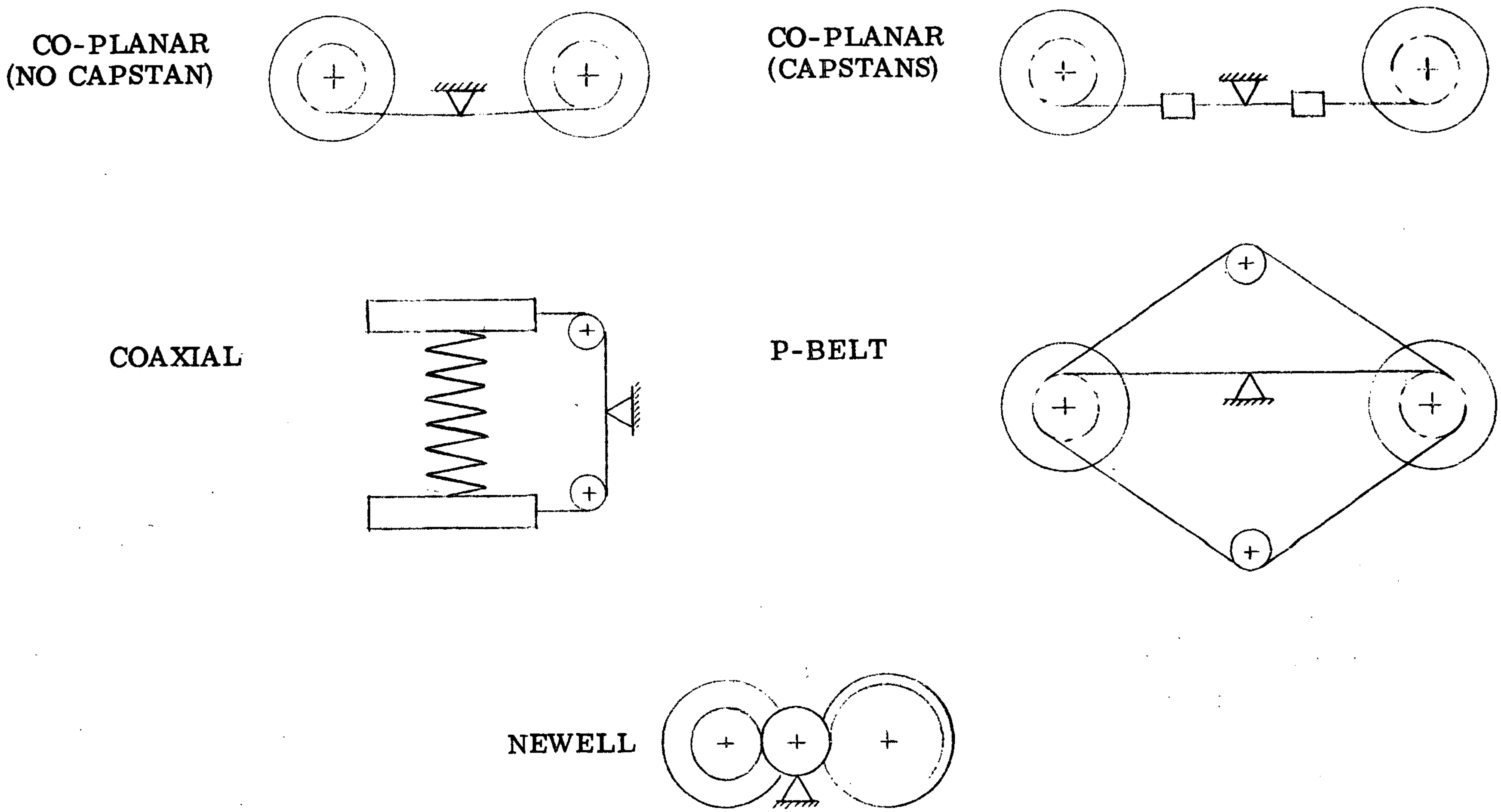

Figure 1

BASIC REEL CONFIGURATION CONCEPTS

Table 2 TRANSPORT CONFIGURATION DESIGN EVALUATION

	Reel-To-Reel Transport Configuration	Long Life Recorder Mechanical Characteristics									
		Simplicity	Single Function Elements	Elements with Historically Proven Applications	Component Availability From Large Population	Modularization	Tape Handling	Reliability Merit Rating	Geometric Form Factor	Power Consumption	Total System Rating
1	Co-Planar No Capstan	10*	3	3	10	7	8	41	5	5	51
2	Co-Planar With Capstan and (a) Motor Reel Drive	6	10	10	8	9	8	51	5	5	61**
	(b) Spring Reel Drive	3	8	7	8	7	8	41	5	10	56
3	Co-Axial With Capstan and (a) Motor Reel Drive	5	9	10	7	8	2	41	10	5	56
	(b) Spring Reel Drive	3	7	7	7	6	2	32	10	10	52
4	Co-Planar Peripheral Belt Reel Drive	7	4	3	5	4	6	29	5	10	44
5	Co-Planar Newell Reel Drive	9	3	2	4	6	6	30	5	10	45

*Best Rating 10
Poorest Application 0

**Selected System

interpretation of comparative rank. The table illustrates the design team's collective judgement on the relative importance of various characteristics, such as reel configuration and drive techniques and their influence on the total system's reliability rating. No attempt was made to weight the relative significance between the elements of the design criteria. In designing a system to survive five times longer than previous transport life, a relaxation in any of the design goals could lead to failure. If a weighting factor were to be applied, clearly tape handling would represent the critical factor for long mission periods.

By including additional evaluation points, such as geometric form and power consumption, Table 2 demonstrates the reason spring driven co-axial reel systems have been selected for missions where limited volume, low power, and moderate tape life were required. For extended mission durations, mechanical component reliability and tape integrity must be maintained. In this application, the system with the greatest "designed-in" reliability should be selected. Therefore, system No. 2a, which consists of individually servo motor controlled, co-planar reels and capstans was selected as the candidate transport configuration.

In summary, five basic transport configurations were identified and described in terms of their reel configuration, reel drive technique, tape path trajectory, and tape metering technique. By establishing a set of reliability criteria together with the overall program guidelines, the five concepts were then compared for their "intrinsic reliability". This comparison resulted in a choice of concept No. 2a, that is, a reel-to-reel coplanar configuration with independently motor driven reels and capstans as the most desirable candidate for a high reliability five-year tape transport.

2.3 Five Year Tape Transport

2.3.1 Functional Layout

Following the choice of the most desirable concept as a reel-to-reel coplanar configuration with independently motor driven reels and capstans, the next stage in the design study was a conceptual layout of such a configuration. Consideration was given to obtain maximum reliability for required performance, and as such, all assemblies were designed for mechanical simplicity, minimum constructional error and for ease of fabrication and assembly. In order to satisfy the guideline of minimum mechanical complexity, and also to reduce inherent error and failure sources, the minimum number of rotating elements were chosen that were compatible with meeting the performance specifications of guidance and tape speed irregularities. The IITRI coplanar tape transport concept is shown in Figure 2 and contains the following modules:

- reels for tape storage
- double cone idlers for tape guidance
- capstans for filtering and tape metering
- head for recording and reproduction

Although the functional layout of the transport as conceived is readily adaptable to a variety of tape widths and tape lengths. Specific dimensions were assumed in order to allow the system performance and response analysis to be undertaken. The tape dimensions used for illustration throughout for this report are therefore:

Width	0.5 inches
Thickness	0.001 inches
Length	1200 feet

These dimensions, although not directly aimed at a specific mission requirement, are adequate enough to be applicable to a generalized earth orbiting mission. Although pertinent, the head/tape interface and the magnetic tape were not directly studied during this effort. Use was made of the recent Head/Tape Interface Study[2] conducted for Goddard Space Flight Center, and the Magnetic Tape for Five-Year Life[3] is currently being studied for Goddard in a separate program.

It can be seen that this conceptual layout requires minimum space consistent with high reliability and acceptable performance. The exact size and arrangement of the subsystems within the tape deck were established by applying the results obtained from the various detailed designed studies in Section 3 of this report. These included both system and individual component analyses as well as stress analyses on the tape and bearings to show reliability of critical components. This technique is shown diagrammatically in Figure 3.

The initial step in the engineering development of this five-year transport was the selection of a tape handling system that has the following characteristics:

- Satisfies basic transport requirements of tape storage, tracking, and metering
- Excludes the main failure modes common to many satellite recorders, e.g., gears belts, and clutches
- Meets or exceeds the head/tape interface guidelines established under NASA/GSFC Contract No. NAS5-11622
- Meets or exceeds the tape handling guidelines of Contract No. NAS5-11622
- Has provisions in the tape loop to isolate and filter from the head area, errors resulting from wear out and other aging effects that can be anticipated after 50,000 hours of operation
- Exhibits high probability of survival against catastrophic component failure

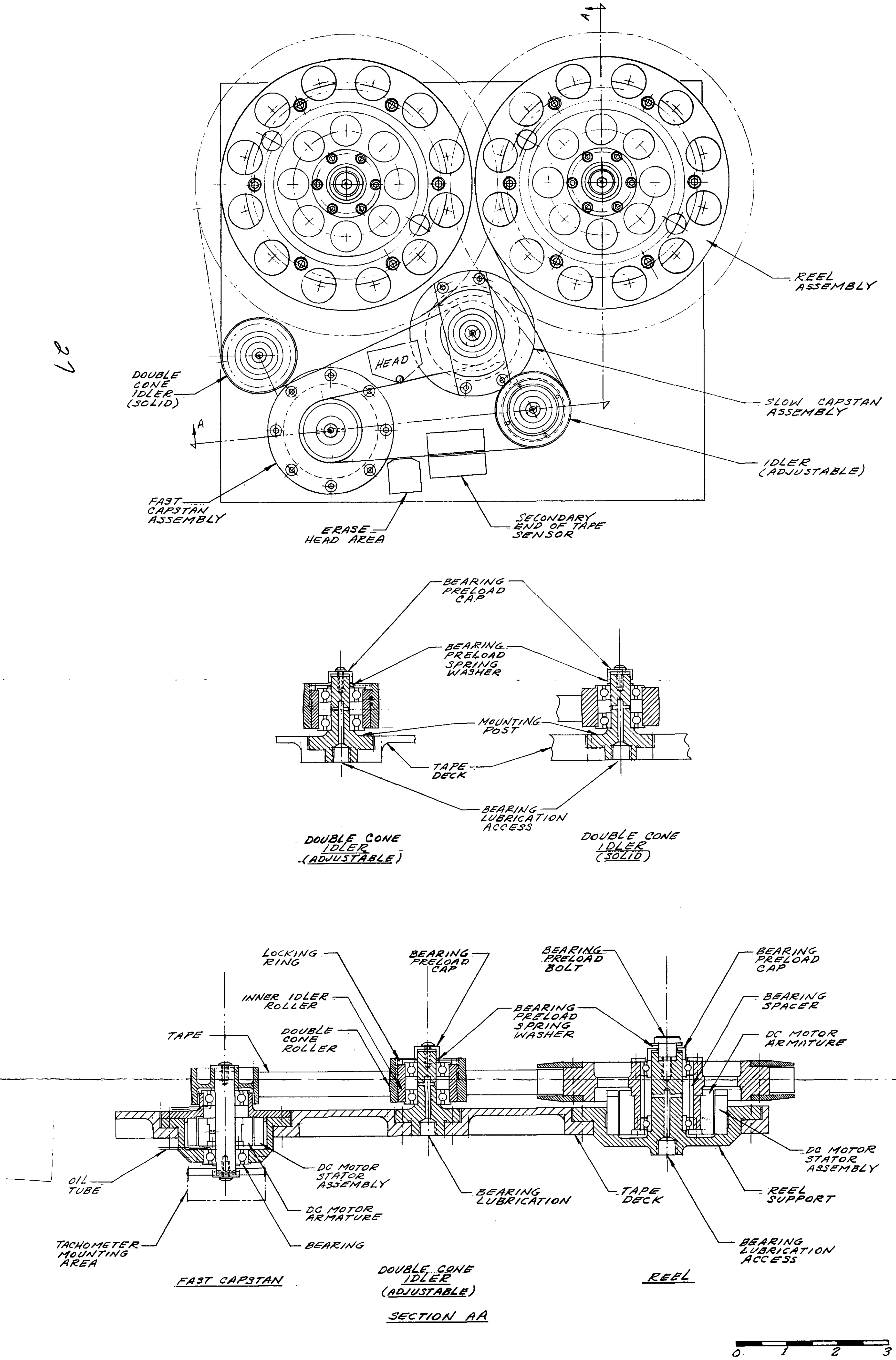

FIGURE 2 COPLANAR TAPE TRANSPORT CONCEPT

27

FOLDOUT FRAME 1

FOLDOUT FRAME 2

Preceding page blank

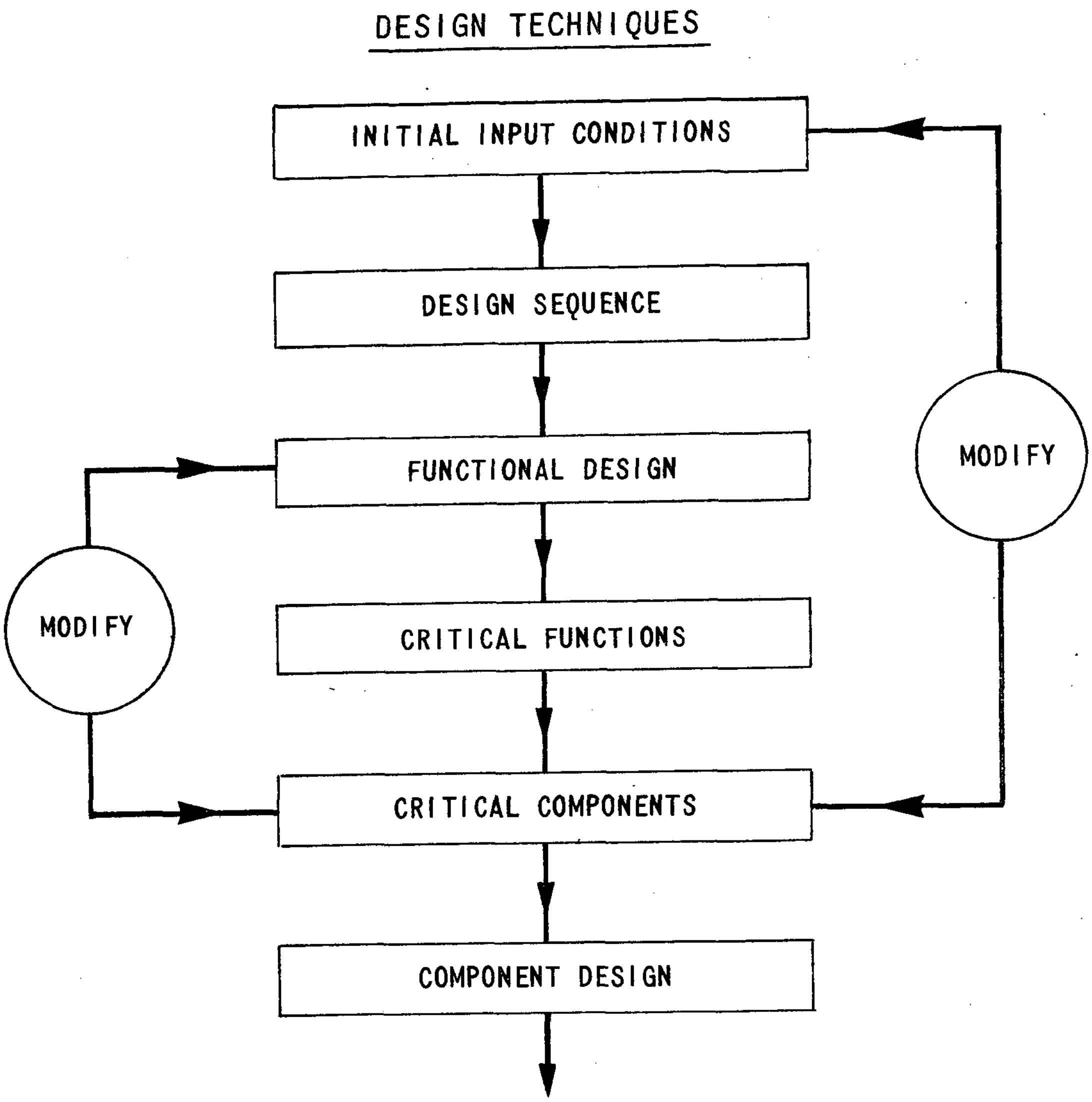

Figure 3

FLOW DIAGRAM OF APPLIED DESIGN TECHNIQUES

Figure 2 illustrates the basic transport configuration that satisifies the above goals. This system has coplanar motor driven reels that straddle the tape handling area. Tracking is accomplished by the incorporation of two double coned idlers. Also, the head is isolated from the reels and idlers by a set of individually driven dual capstans. To satisfy the tape handling and head/tape interface guidelines, independently driven reels are employed to assure tape pack integrity and to effect constant tape tensions in the regime of 8 ounces per inch width. Double coned idlers are utilized to minimize tracking errors resulting from the reels and from within the tape loop. The technique of individually driven dual capstans provides a method for precisely metering the tape past the head as well as providing the means for fine tuning the head/tape contact pressure. Further, the dual capstans straddling the head are the primary means of filtering from the head regime, dynamics disturbances emanating from the reel and idler assemblies. These disturbances are anticipated to be originally the result of bearing torque pulsations and component machining variations; but in the latter stages of life, major errors will result from aging and wear out.

From the computer simulation models (Section 3.3) the reel-tape system was designed to assure tape pack integrity, i.e., that no clinching occurs. Also to effect the precision tracking required at the head, the IITRI tracking model was utilized to size the free tape lengths and idler geometry. The tape path geometry and tension profile was selected so that tape stresses will be under 3500 psi throughout the transport.

As a means for further insuring against catastrophic component failure, all bearings are lubricated with both a grease (Andoc C) and periodically, a liquid lubricant, that will replenish the bearing lubricant supply. Specific details on lubricant techniques and bearing selection are discussed in depth in Section 3.5. It is sufficient to note that all mechanical elements have been derated so that the total mechanical failure rate will not diminish the transport reliability to less that 99.9% for the mission life.

2.3.1.1 Reel Assembly

Storage of the magnetic tape is provided by the reel assembly shown in Figure 2. The reel assembly is an independent module that includes the reel, a reel support structure and bearings, lubricant seals and re-supply lines, and a D-C drive motor. This compact configuration is obtained by directly attaching the D-C motor armature to the reel. The D-C motor field housing is an integral part of the module's support housing. Substantial bearings of the Precision Class 7 type are preloaded to a 1/2 to 1 lb level by using the calibrated preload spring technique. Preloadings is employed to assure effective bearing performance as well as to minimize the run-out effects resulting from internal bearing clearances. Reel shaft run-out errors are directly translated into gross tape tracking errors. To minimize the reel generated tracking errors and hence to negate the necessity for severe tracking idler configurations, pre-loading and precision mechanical assembly procedures are employed to control reel hub run-out to less than $\pm$ .001 inch.

2.3.1.2 Idler Assembly

Tape guidance (control of vertical tracking error) is performed by the double cone idler assembly modified by crowning the apex shown in Figure 2. The double cone roller is mounted on an inner roller to provide vertical adjustment to the dynamic center of the roller. A locking ring maintains the relative position of the two rollers. A support post to the tape deck provides bearing mounting facility, direct bearing lubrication and bearing preload support. Two antifriction ball bearings preload by a bolt and spring washer are used to mount the idler. The integral mounting post assure a tape path parallel to the deck.

2.3.1.3 Capstan Assemblies

Capstan assemblies are provided for low and high speed tape metering. Both assemblies utilize direct drive DC motors to control the tension of the tape in the vicinity of the head and to mechanically filter tape propagated disturbances. The DC motors induce damping from the electrical field and help to control tensions through drive or drag (back emf).

The fast capstan is driven directly by a direct driven DC motor with the motor armature mounted directly on the capstan shaft. This shaft also contains a tachometer mounting position. The driven shaft is mounted to the structure that attaches to the tape deck through two ball bearings. In addition, the motor field is an integral part of this structure which provides bearing lubrication access.

Alternate means are available for obtaining slow capstan speeds, but these are mechanically complex (Section 3.7). Mechanical simplicity is achieved with the use of a low speed DC motor in the fast capstan assembly. The low speed motor must be governed by a tachometer in a control system that achieves acceptable slow speed performance. This mode of operation fulfills one of the objectives of this program, i.e., the replacement of low reliability mechanical components with electrical components.

2.3.1.4 Recording Heads

The location of the recording head between the two capstan assemblies is shown in Figure 2. A single head stack is indicated over that of a multiple head stack arrangement in order to conform with the guidelines for head selection and operational constraints[2] established under Contract No. NAS5-11622. The guidelines applicable to the recording head are as follows:

- The core and block materials used in the front face of the head in the contact area should fall in the category of "hard" materials, i.e., greater than 100 Rockwell B; brass should be avoided.

- Voids or gaps between laminations or other discontinuities on the front face should be less than 50 microinches in width.

- There should be no scratch in the direction of tape motion on the contact surface of the head that is deeper than 12 microinches. Also, there should be no scratches perpendicular to the direction of tape motion.

- A break-in period of 200 passes is advisable. Following this break-in the head should meet the surface finish guidelines above. Observation of a deep scratch, indicating repeated damage by debris in the same area, should be cause for replacing the tape and relapping the head.

- The maximum tape tension should be defined by the tape path and tape pack stress considerations.

- The required normal force at the gap line should be defined by maximizing the reproduce output signal of the shortest wavelength being reproduced.

- Tape wrap angle should be minimized.

- The minimum head radius consistent with the packing density of the information being stored should be utilized.

- The number of heads should be minimized. Erase heads should be out of contact when possible.

These guidelines were established in order to negate the frictional drag and debris problems that occur at the head tape interface and hence improve the probability of successful operation of satellite recorder systems operating for a period of one year or 10,000 tape passes.

Many of these guidelines were confirmed in a separate study[4] where a safe operating area for the head tape interface was postulated. This operating area was defined by the maximum torque capability of the transport, the minimum tension required for guidance and reproduce signal response, the maximum tape stress throughout the tape path and the change in the physical parameters between the head and tape. It is essential therefore, that when considering a recording head for use over a period of five years or 50,000 tape passes, that all of these guidelines by strictly adhered to and that a safe operating area is defined during the early stages of the transport design.

Another major consideration with regard to the recording head for use in a five year transport is that of wear. Wear is directly related to the quantity of tape passing over head, which for a five year mission may approach 60 million feet of tape. Rates of wear of various head materials in general use are difficult to establish exactly, because of the variety of conditions that influence the wear rate. However, a typical rate of wear for hard core materials, such as Alfesil, is in the order of 50×10^{-6} inches for the first million feet of tape. Although this rate of wear may decrease for each successive million feet of tape, use of this initial wear rate allows a maximum expected head wear to be established. For five year continuous operation where 60×10^{6} feet of tape will pass over the head surface, a maximum expected wear of 0.003 inches would be anticipated. Such total wear may not be serious for low packing density systems, however if high linear packing densities are encountered such a wear rate may be a high proportion of the available interface depth. As such, changes in the electrical and performance specifications of the head must be anticipated and the drive and reproduce electronics designed to accomodate such changes. Equally essential is that any wear experienced on the front face of the recording head in no way interferes with the tracking requirement of the magnetic tape. Anticlastic curvature of the tape generally leads to increased wear at the tape edges. Tracking abnormalities may be avoided by removing the head material in this region of high wear.

Another form of wear which strongly influences the reliability of a recording head is gap smear. Gap smear, or loss of gap integrity, is caused by the movement of the core material across the working gap of the head until a condition is reached where it shorts out the effective gap length resulting in a serious reduction in the head efficiency. In order to negate this wear phenomena it is essential that the head chosen for unattended operation for a period of five years has a core material that is the least susceptable to smearing (such as the hard materials) and that the gap length specified for data reproduction be no smaller than 50 microinches.

2.3.2 Critical Areas

2.3.2.1 Bearings and Lubrication System

Bearings are one of the principal sources of transport system failure, either by degradation of performance or catastrophic failure. Therefore, special emphasis has been placed on long life bearing design with proper lubrication. The following considerations discussed in detail in Section 3.5, govern long life bearing design.

- bearing contact stresses
- preload effects
- shaft misalignment
- bearing torque
- bearing life
- materials
- lubrication and environment

These considerations were observed in the selection, mounting, and preloading of the bearings detailed in Table 3 and used in the long life transport concept. The considerations of misalignment, ball and retainer materials and lubricant are discussed in Section 3.5. Recommendations are listed below.

Shaft Misalignment	Less than 0.3 milliradians or 3×10^{-4} inches off center per axial inch of shaft center.
Ball Material	440C stainless steel (high humidity) 52100 Steel (low humidity)
Retainer Material	Bronze

The bearing lubrication system for the five year tape transport is schematically shown in Figure 4. It consists of storage reservoirs, dispensers, and lubricant feeder lines which provide periodic, incremental lubrication of the tape transport bearings. Periodic lubrication will insure bearing performance after long period of inactivity and long life.

The reservoir and dispenser are basically constructed the same way. The large reservoirs pistons maintain a constant spring load on the oil while the small reservoirs pistons are pulled back by solenoids and forced forward by springs during an oiling sequence.

The reservoirs body are made of plastic and are used to separate the inert gas of the environment from the oil. These diaphragms are commercially available. Proper fabric and elastomeric sealant will be selected to be compatible with the environmental gas and fluids used. This will provide a non-porous membrane or wall between the two substances.

The feeder lines (stainless steel hypodermic tubing) insure proper oil delivery. When not in use the solenoid is de-energized with the small rolling diaphragm keeping the oil contained in the large reservoir due to the forward position of the piston with its diaphragm sealing off the intake part until the oiling sequence.

To oil the bearings, the solenoid is energized and the piston pulls back allowing the oil from the large reservoir to fill the small reservoir and loading a spring. At the same time the upper check valve (see drawings) opens to allow the oil to flow between the two reservoirs, while the lower valve closes to prevent sucking the oil back from the feeder lines.

When the solenoid is de-energized the spring pushes the plunger forward, forcing the oil into the feeder lines and thereby lubricating the bearings. This time, however, the

Table 3

BEARINGS FOR LONG LIFE TRANSPORT

Bearing Description	Location (Number)	Static Load (lb)				Torque (in-oz)		Power Loss (Watts)	Life (Cycles) 99% Reliability
		Allowable		Actual		Thrust 0.5 lb Per Load	Radial 1.0 lb		
		Thrust	Radial	Thrust	Radial				
Barden A 538T	Reel (2)	950	315	100**	< 1	7.0×10^{-3}	11.3×10^{-3}	3.27×10^{-3}	6.0×10^{12}
Barden SFR6	Idler (2)	252	167	neg*	< 1	4.15×10^{-3}	7.0×10^{-3}	6.72×10^{-3}	1.4×10^{11}
Barden SFR6	Fast Capstan (2)	252	167	neg*	< 1	4.15×10^{-3}	7.0×10^{-3}	5.6×10^{-3}	1.4×10^{11}
Barden SFR6	Slow Capstan (3)	252	167	neg*	< 1	4.15×10^{-3}	7.0×10^{-3}	$.525\times10^{-3}$	1.4×10^{11}
Barden SR6	Slow Capstan (1)	252	167	neg*	< 1	4.15×10^{-3}	7.0×10^{-3}	$.175\times10^{-3}$	1.4×10^{11}
Barden VSR-1012	Slow Capstan (2)	—	—	—	—	—	—	—	—

*neg - Negligible

**Maximum axial load during launch

FOLDOUT FRAME 1

FOLDOUT FRAME 2

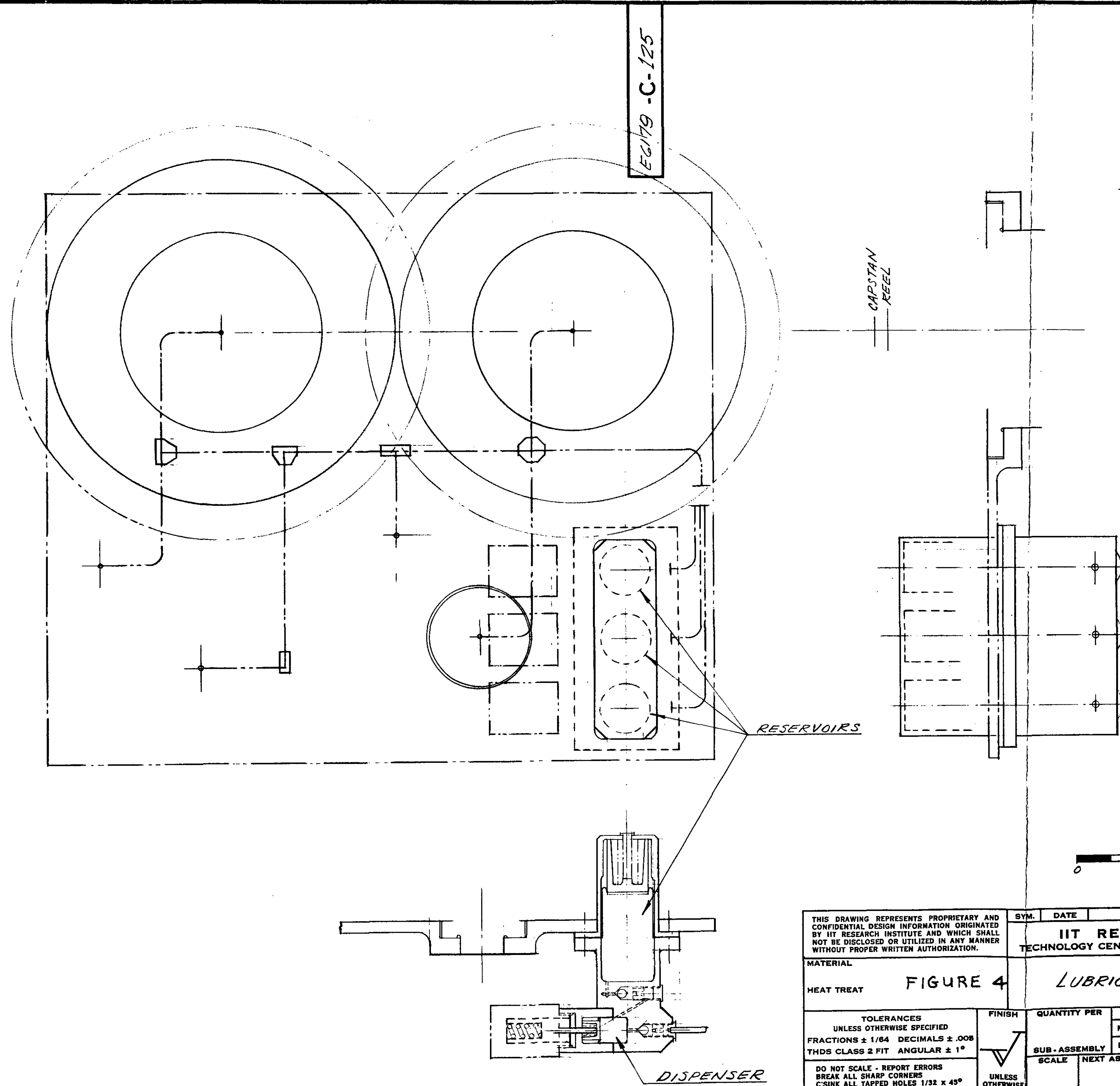

THIS DRAWING REPRESENTS PROPRIETARY AND CONFIDENTIAL DESIGN INFORMATION ORIGINATED BY IIT RESEARCH INSTITUTE AND WHICH SHALL NOT BE DISCLOSED OR UTILIZED IN ANY MANNER WITHOUT PROPER WRITTEN AUTHORIZATION.

SYM.	DATE	DESCRIPTION OF REVISION	NAME

IIT RESEARCH INSTITUTE
TECHNOLOGY CENTER — CHICAGO, ILLINOIS 60616

MATERIAL

HEAT TREAT — FIGURE 4

LUBRICATION SYSTEM

TOLERANCES
UNLESS OTHERWISE SPECIFIED
FRACTIONS ± 1/64 DECIMALS ± .005
THDS CLASS 2 FIT ANGULAR ± 1°

DO NOT SCALE - REPORT ERRORS
BREAK ALL SHARP CORNERS
C'SINK ALL TAPPED HOLES 1/32 x 45°
REMOVE BURRS

FINISH — UNLESS OTHERWISE NOTED

QUANTITY PER — SUB-ASSEMBLY

	DESIGNED	DRAWN	CHECKED	APPROVED
NAME	E.S.	E.S.		
DATE	6-14-71			

SCALE	NEXT ASSEMBLY NO.	PROJECT DRAWING NO.
		E6179-C-125

upper valve closes to prevent any flow between reservoirs while the lower valve opens to allow the oil to flow in the feeder lines. When the small plunger reaches the forward position the oiling cycle is completed.

2.3.2.2 Tape Stress

The second major long life reliability constraining item is the tape. Unfortunately, the fatigue data needed to realistically assess tape life is not available at this time. In view of this fact, the mechanical components involved in tape storage, handling, and tensioning were designed to minimize tape degradation. Material constants for presently available tapes were used in the analysis of the design concept. Double cone idlers were designed to minimize tape stress (static considerations) yet achieve acceptable guidance. This involves a trade off between guidance and reliability because increased tape tension and cone angle yields increased guidance and decreased life. In addition increased tape tension increases bearing radial loads lowering bearing life. Capstan roller diameters were selected to minimize tape stress. The tape packs were designed to enable storage of 1200 feet of tape without spoking or cinching. Stresses in the tape pack were found in the design analysis.

Tape tension profiles shown in Figure 5 were selected to achieve adequate handling and control of the tape. Four ounces of tension is maintained by the reel motors to achieve good tape packing without spoking. In addition the reel motors maintain four ounces around the idlers which insures the required guidance performance. Five to six ounces of tape tension are maintained at the head by the capstans to achieve control and metering during record and reproduce.

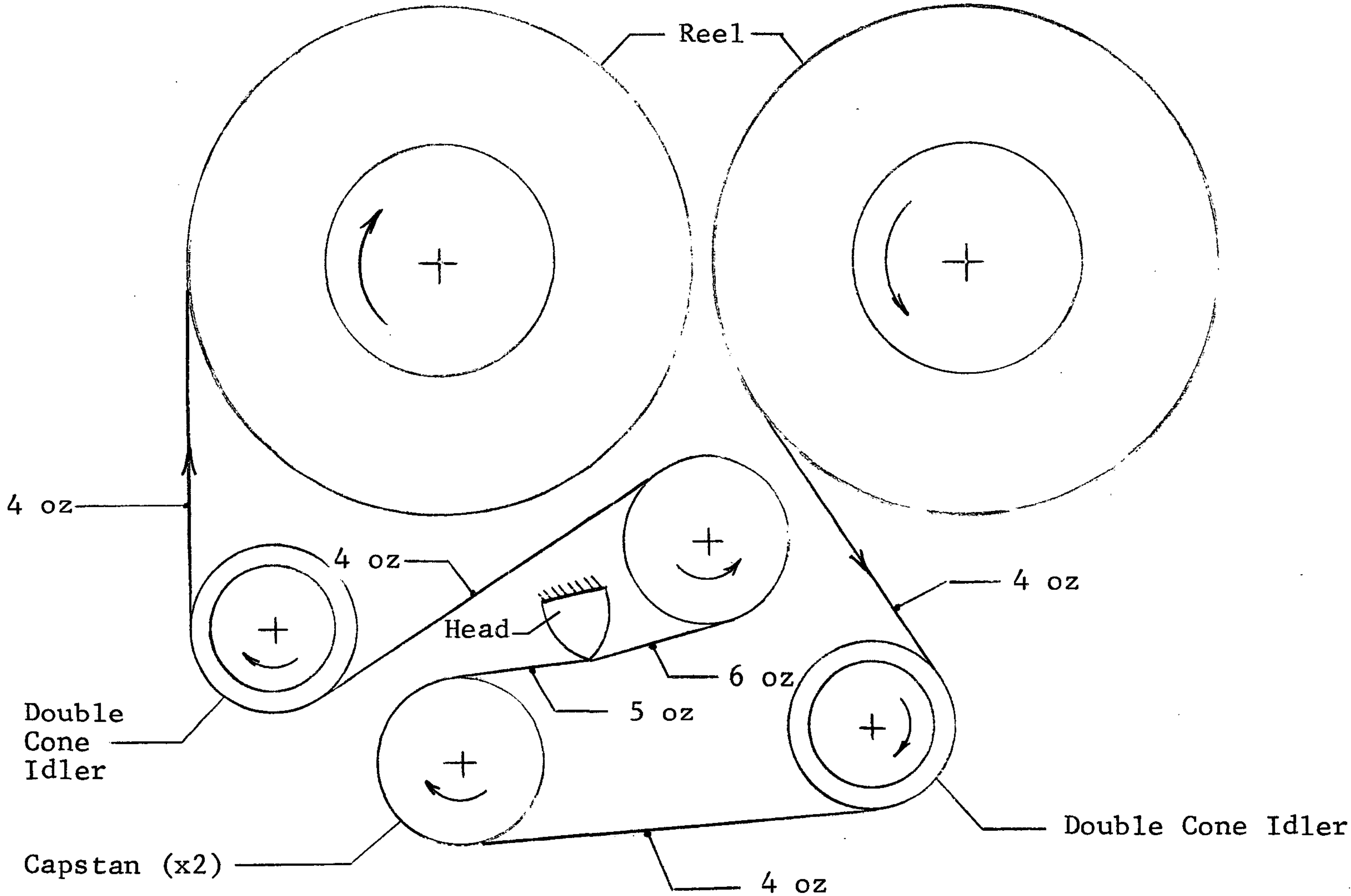

Figure 5

DYNAMIC TAPE TENSION PROFILE

The tape tension profile shown in Figure 5 was used to design the:

- tape packs to minimize stress and avoid spoking
- capstans to minimize tape stress
- idlers to achieve guidance with minimum tape stress

Tape pack design was based on the analysis reported in Section 3.3. The computer program in Section 3.3 determines tape pack stresses for varied hub diameter, hub thickness, hub material, tape width, tape material, tape length, and tape tension. A parameter variation was run to obtain the design data shown in Section 3.3. Tape pack spoking is avoided by maintaining a positive tangential stress throughout the tape pack. Figure 6 illustrates allowable and nonallowable tape pack stress distributions. From the design data shown in Section 3.3 the following tape pack parameters were selected:

Hub diameter - 4.0 inches

Hub thickness - 0.5 inches

Hub material - Aluminum

Tape tension - Four ounces

Figure 7 shows the stress distribution in the aforementioned tape pack.

The capstan outside diameters were selected on the basis of the tape stress induced by six ounces of tension. The results of Figures 8 and 9 were obtained from a computer program developed in a recent Head/Tape Interface Study[2]. Tape stresses over cylindrical rollers with 1 inch and 1-1/2 inch diameter were obtained for varied tape tensions. Since the oxide faces the capstan in one instance, these results are also shown on Figure 9. A 1.25 inch diameter capstan resulted in the following maximum stresses in the Mylar and oxide materials of the tape.

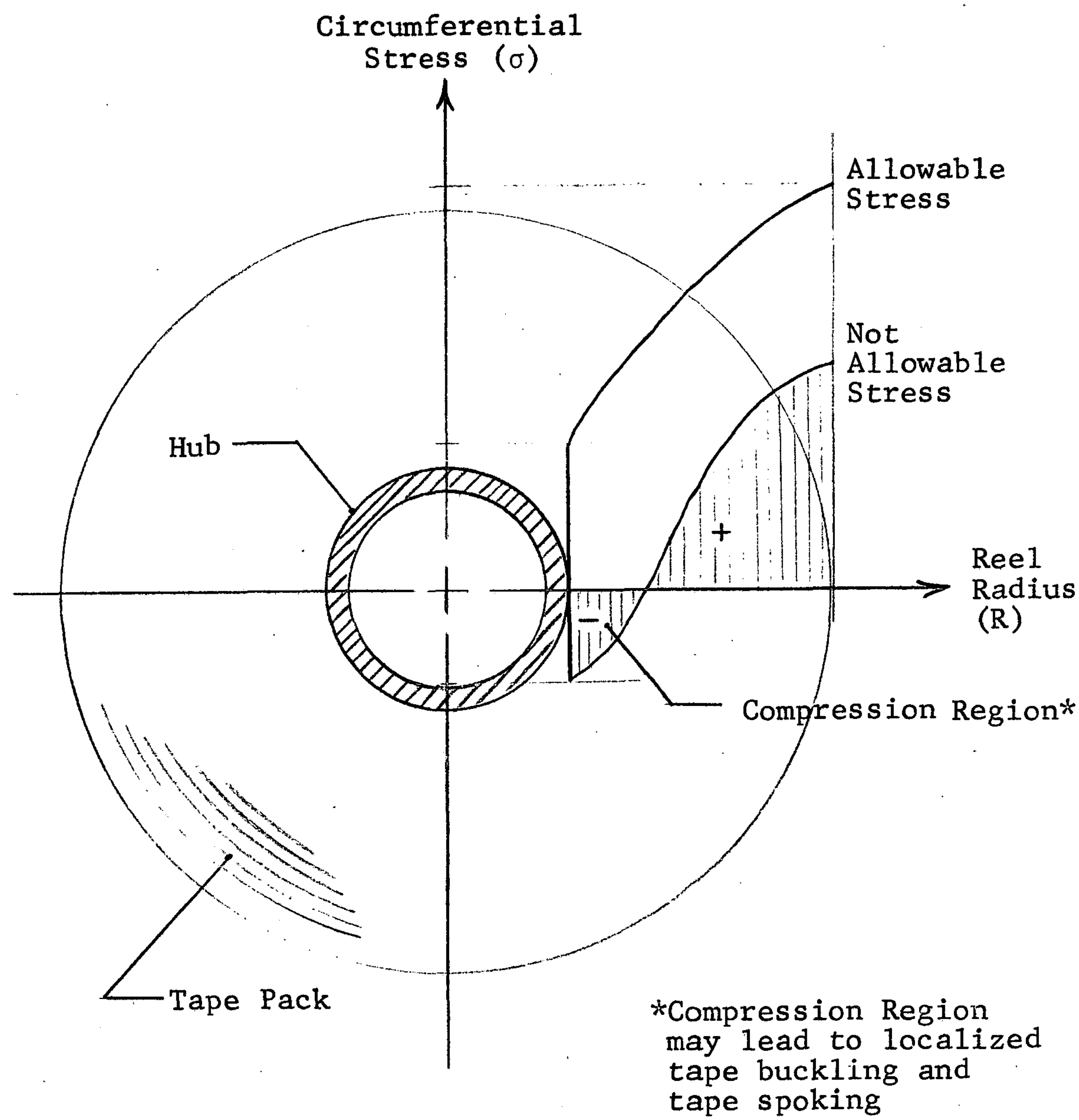

Figure 6

ALLOWABLE TAPE PACK STRESS DISTRIBUTIONS

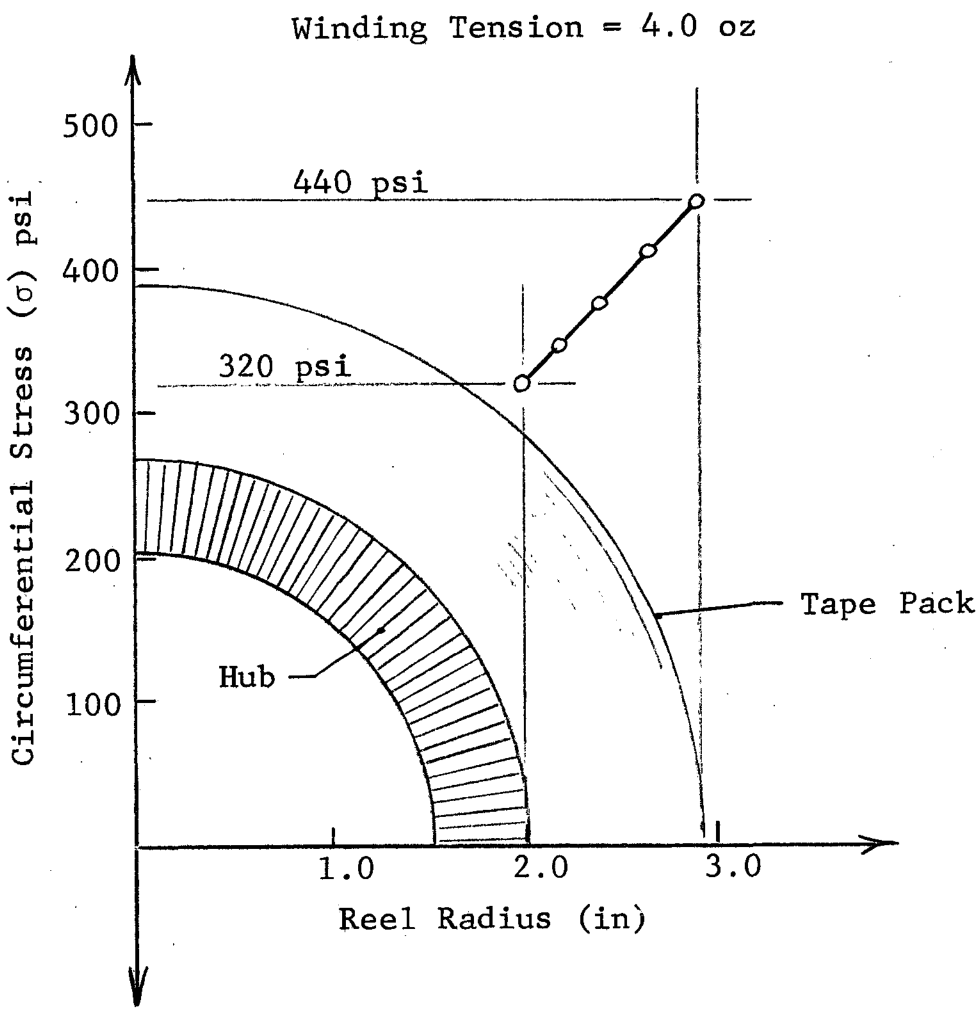

Figure 7

ACTUAL TAPE PACK STRESS DISTRIBUTION

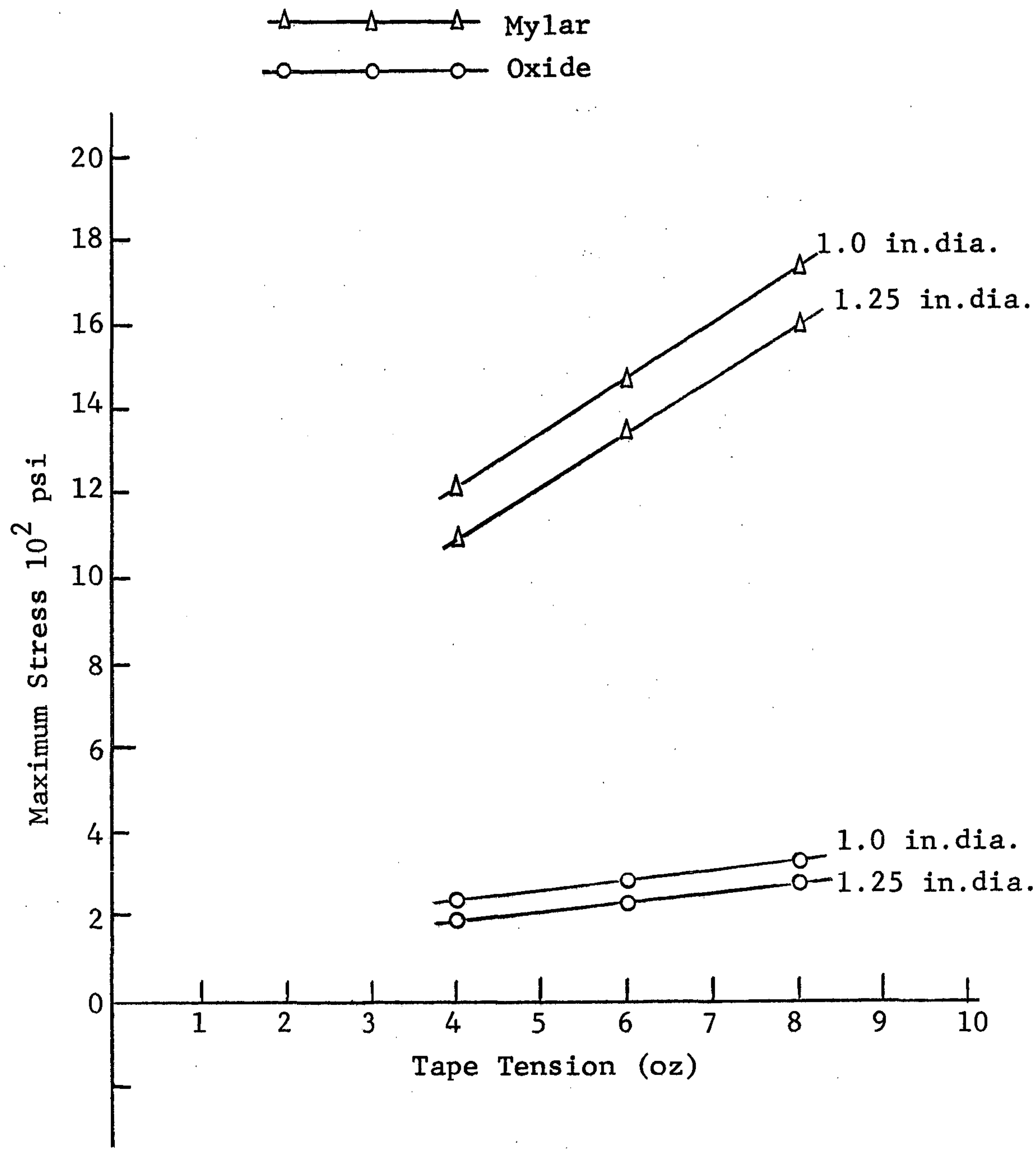

Figure 8

TAPE STRESS PASSING OVER CAPSTAN, MYLAR ON CAPSTAN SURFACE

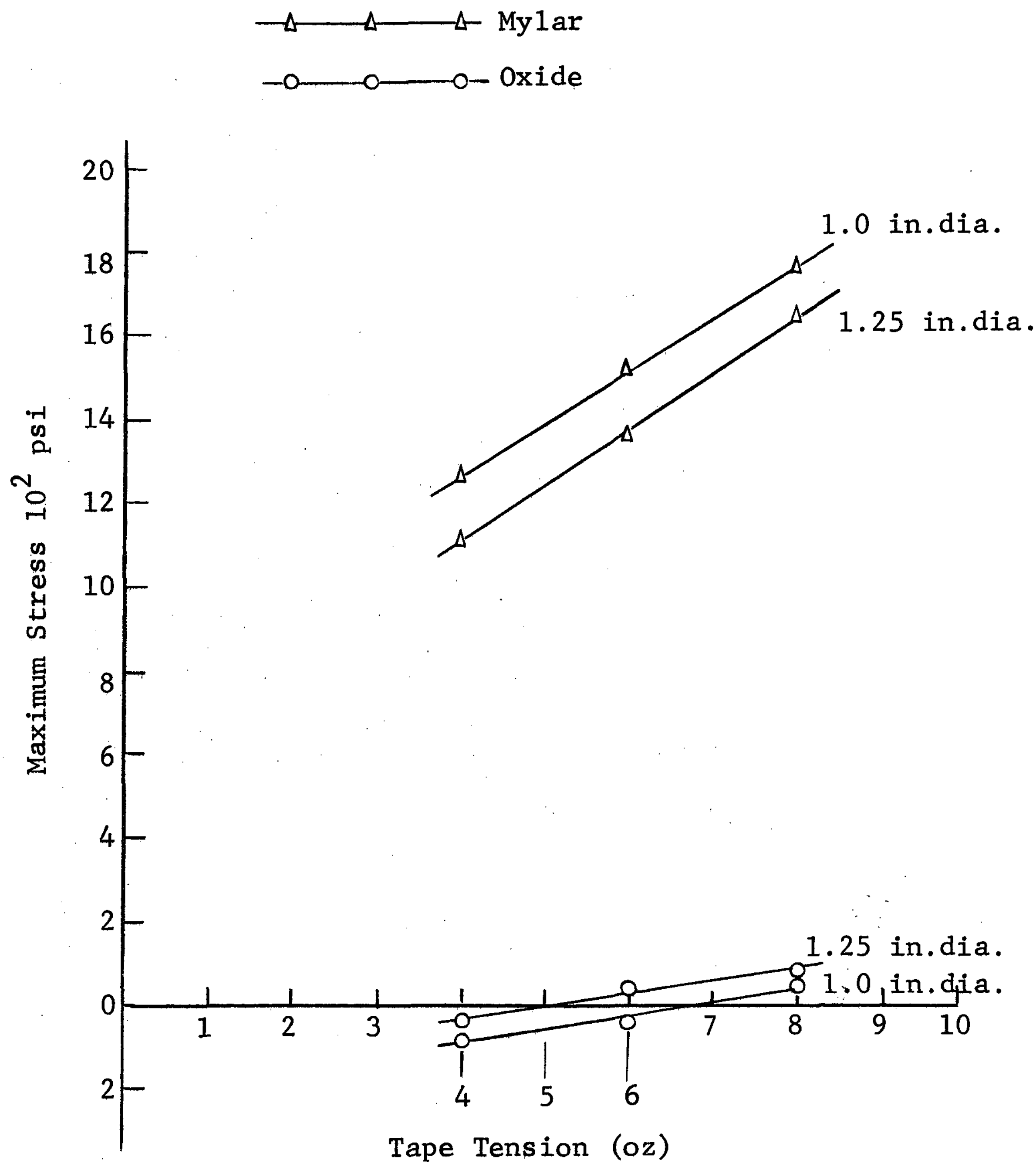

Figure 9

TAPE STRESS PASSING OVER CAPSTANS, OXIDE FACING CAPSTAN SURFACE

C 2

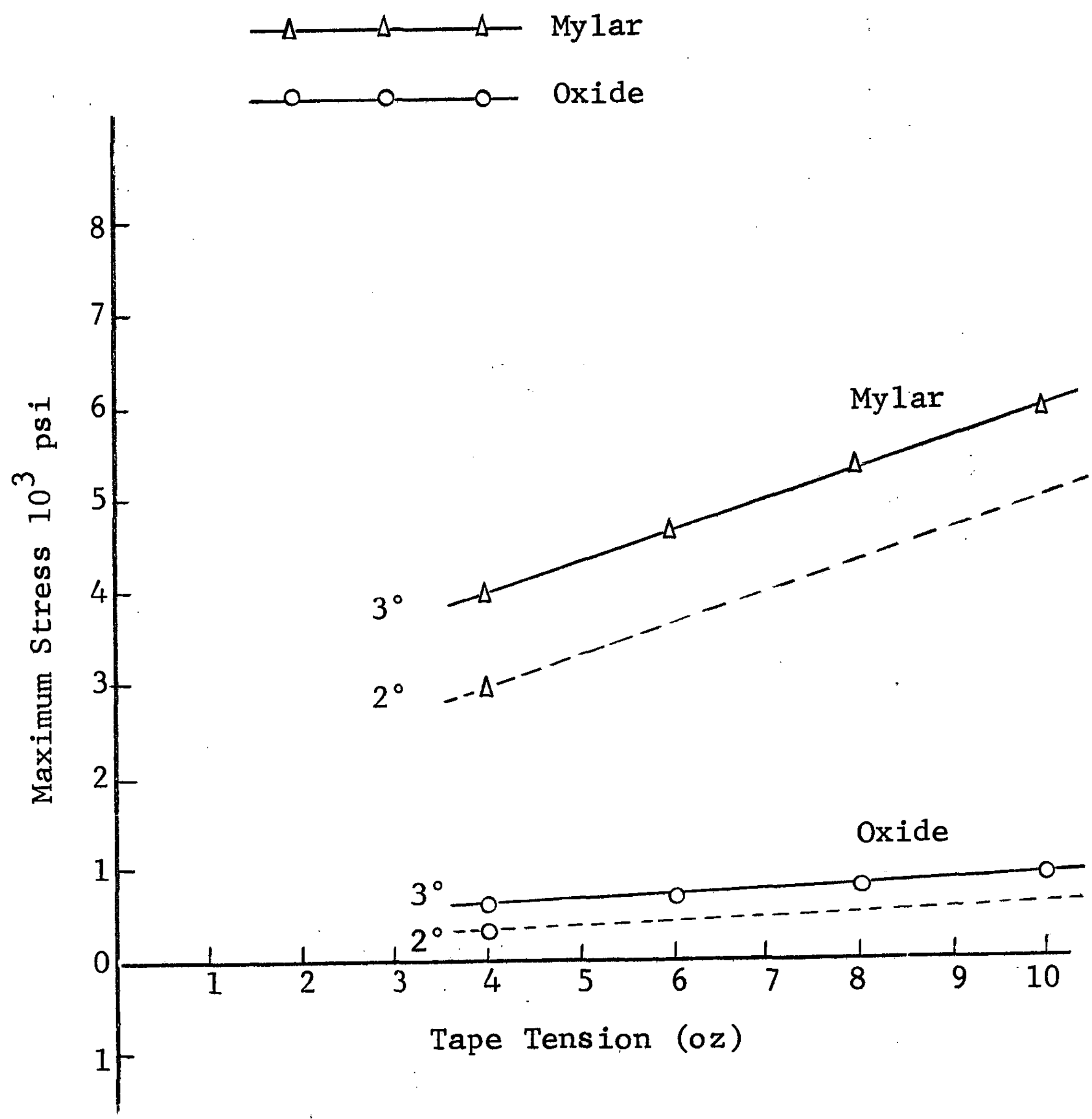

Figure 10

TAPE STRESS PASSING OVER DOUBLE CONED IDLER

	Mylar	Oxide
Oxide Facing Capstan	1350 psi	25 psi
Mylar Facing Capstan	1325	225

The double cone idlers induce tape stress due to the cone angle, diameter, and apex radius. See Section 3.4 for details.

The values of tape tension, 4 oz.; of the cone angle, 2°; and of the idler major diameter, 1-1/2 in.; were selected to achieve adequate guidance. The computer program in Section 3.4 was used to calculate stress values shown in Figure 10. The effect of tape tension on tape stress and for an apex radius of 1 inch for a cone angle of 2° and 3° is plotted. The stresses in the tape are 3400 psi in the Mylar, and 568 psi in the oxide for the selected idler. Therefore, the balance between tape stress and proper guidance has been achieved.

2.3.3 System Performance

Reliability and long life have been the major concerns in the design of the five year tape transport. Within the framework of the highly reliable design, some minimum mechanical system performance must be achieved. This section is devoted to the analysis of the transport to determine its performance as a function of its life. The analysis of the transport consisted of:

- Determination of the transport inertia, power requirements, and momentum
- Examination of the tape guidance for stated performance and probably error disturbance
- Calculation of transport system natural frequencies and comparison of these frequencies to system excitation frequencies
- Calculation of system response (specifically the tape at the head) for varied input disturbances including bearing pertubations, motor cogging and part rotational eccentricities.

These analyses are used to show where trade offs could be made to maintain performance and to determine the effect of possible component failures on performance. The following physical quantities provide a measure of the transport performance.

<u>Jitter</u> is the time displacement between successive bits of information

<u>Flutter</u> is the (rms) vibration velocity of the tape (low frequency range 0-50 Hz, high frequency range - above 50 Hz)

<u>Lateral Tracking Error</u> is the vertical alignment error between tape and head due to tracking perturbations.

2.3.3.1 General Analysis

The gross kinetic properties of the transport were calculated as a function of time using the computer programs given in Section 3.6. The following transport operational characteristics were determined.

- Reel inertia as a function of quantity of tape storage.
- Motor torque requirements to meter and store tape. (Friction losses estimated in a separate calculation).
- Reel angular momentum.
- Rotational kinetic energy.
- Power.

The results of the computer calculations of the kinetic properties for the given transport using a tape speed of 32 ips are shown below:

- Power (in-lb/sec) 0.5×10^{-3}
- Torque (in-lb) 0.53×10^{-4}
- Momentum (in-lb-sec) 0.884×10^{-1}

- Energy (in-lb) 0.476
- Inertia (in-lb-sec^2) 0.82×10^{-2}

It is of interest to note in Figure 11 that these properties remain relatively constant during the operation of the transport. For more detail of these results, see Section 3.6.

The additional torque and power required due to friction and tensioning is given in Table 4.

The total mechanical power requirements for the mechanical operation of the transport is 3.5 watts. The torque available is compared to the calculated required torque in Table 5. This table shows that adequate motor torque is available to operate all transport components.

2.3.3.2 Guidance

Tape transport lateral error is introduced by errors in reel and capstan runout due to machining and assembly tolerances. These errors can never be completely eliminated but they can be minimized. The function of the guidance element (double cone roller) is to attenuate these errors and to minimize them at the head. Good guidance depends on the inlet tape length (to the idler), the tape elastic properties, the tape geometry, the double cone idler geometry, and tape tension. The idlers were designed through the use of the computer program given in Section 3.2. The parameters noted above were varied to obtain a design that would give the required guidance for anticipated input errors at the reels. Figure 12 shows the double cone idler with the appropriate dimensions. Error attenuation must be achieved with a minimum of 4 ounces of tape tension. The minimum inlet tape length to the idlers is 3 inches and standard 1 mil 1/2 inch magnetic tape was used.

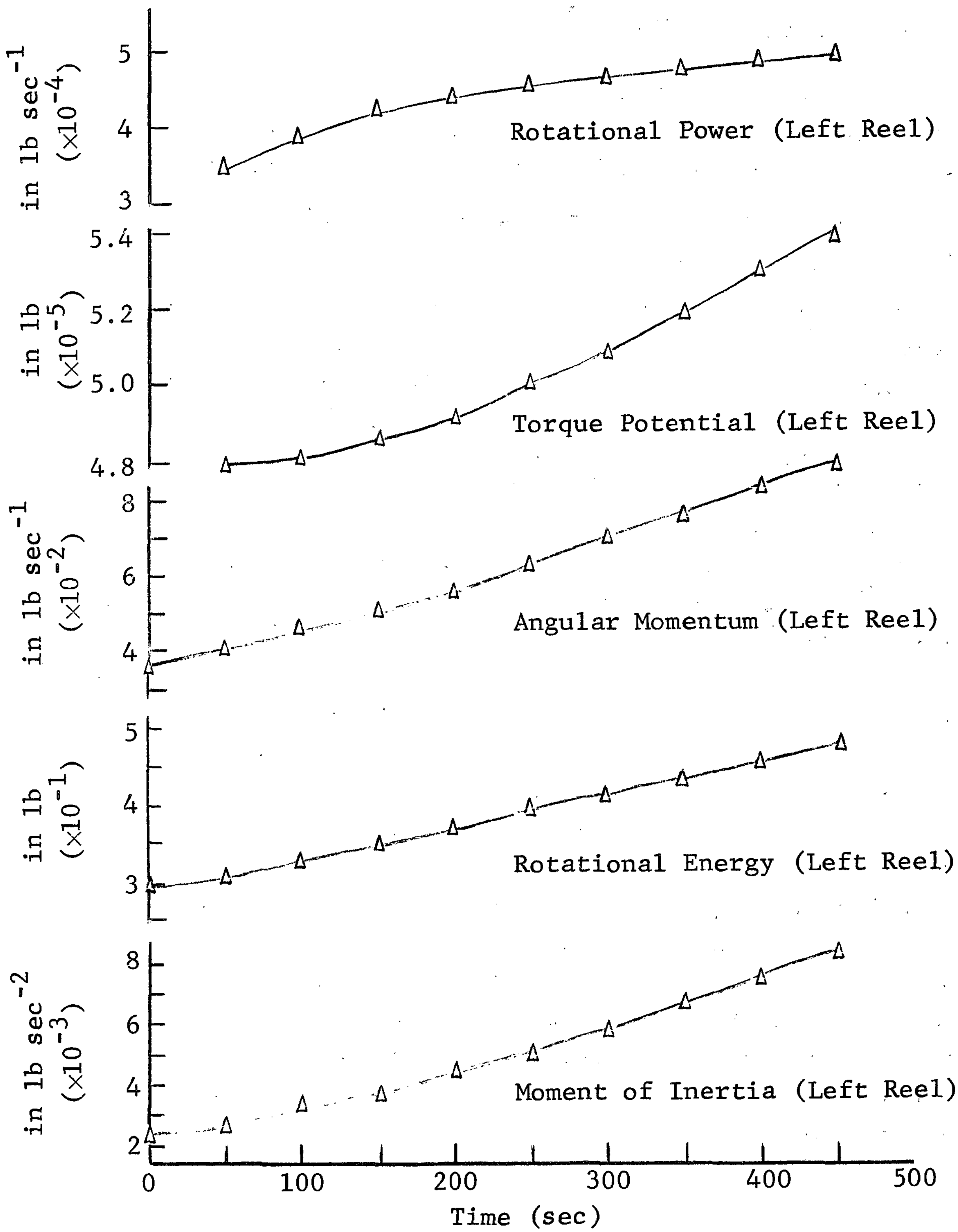

Figure 11

KINETIC PROPERTIES DURING OPERATION

Table 4

TORQUE AND MECHANICAL POWER REQUIREMENTS OF FIVE YEAR TAPE TRANSPORT DUE TO FRICTION AND TENSIONING AT 32 IPS

Component/Purpose	Torque (in-oz) Load (oz)	Milliwatts
Reel/Packing	10 in-oz	.900
Reel/Bearings	36×10^{-3} in-oz	6.5
Capstan/Tensioning	8 oz	1792
Capstan/Bearings	22×10^{-3} in-oz	11.2
Idler/Bearings	22×10^{-3} in-oz	13.4
Head/Drag	1 oz	224
Other	—	500

Total for Transport ~ 3.5 watts

Table 5

MOTOR SIZES

Motor	Power Watts	Torque Available	Torque Required
Reel	1.66	60 in-oz	10 in-oz
Capstan	1.73	15 in-oz	2.5 in-oz

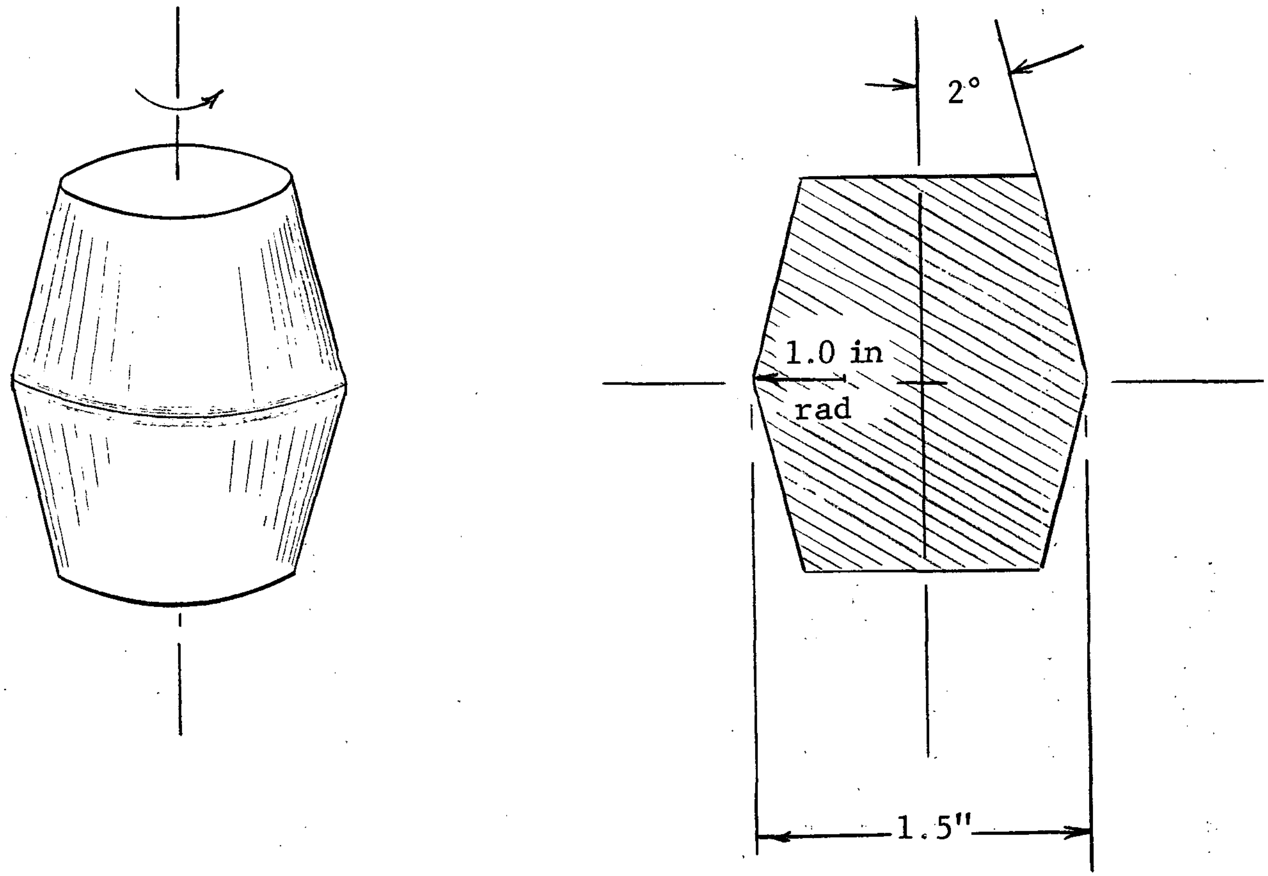

Figure 12

DOUBLE CONE IDLER

The important dimensionless handling parameters given in Section 3.2 are:

$$P = \frac{\alpha t L^4}{DI} = 182 \tag{1}$$

$$Q = L\sqrt{\frac{T}{EI}} = 0.52 \tag{2}$$

where

$\alpha = 2° =$ cone angle

$t = .001$ in = tape thickness

$L = 3$ in = head/tape length

$D = 1.5$ in = major roller diameter

$E = 8 \times 10^5$ lb/in^2 tape modulus of elasticity

$I = \frac{1}{12} tw^3 = 1.04 \times 10^{-5}$ in^4 tape moment of inertia

$T = 4$ oz = tape tension

The dimensionless handling parameters were obtained from the tracking model developed in Section 3.2. The tracking model uses the geometry of a rigid double-coned roller with a length of flexible tape leading into the roller to determine how the double cone stabilizes the tape lateral motion. Using the displacement response of the tape with the rigid tracking of the roller, the effectiveness of the roller can be assessed.

Guidance analysis of these handling parameters P and Q yields an idler output response of .0005 inches for an input error of .005 inches. Hence, the double cone idler provides a 90% attenuation of the input error.

2.3.3.3 Local Dynamic Analysis

Tape flutter and jitter at the head are caused by mechanical and electrical system errors such as bearing torque perturbations, component eccentricities, and motor cogging. Flutter and jitter magnitudes are determined by the simulation model described in Section 3.1 for the newly constructed recorder and for recorders degraded through usage. In addition to response calculation, the local dynamic analysis includes system natural frequency analysis. The process of moving the tape from reel to reel produces the tape excitation. Therefore, flutter and jitter are tape velocity sensitive.

Figure 13 shows the schematic diagram of the five year tape transport. The physical description of the transport is given in Table 6 . The general element used to simulate each component of the simulation model is shown in Figure 14. Inertia, damping to ground, damping across the tape, tape elasticity, and general excitation are allowed for each element. The transport dynamic behavior is then simulated by a model composed of as many of these elements as are required to achieve the desired simulation. The detail of the response obtained from the simulation model increases with the number of components utilized; however, the computer time required also increases.

2.3.3.4 System Natural Frequency

System natural frequencies were calculated and compared to mechanical excitation frequencies to avoid difficulties in performance because the coincidence of the two generates resonance. Resonance can deteriorate system performance and/or cause mechanical failures. The system natural frequencies were calculated using the dynamic simulation model described in Section 3.1. Table 7 shows the first five system natural frequencies of the tape transport concept. These results show little change in natural frequency when the tape distribution on the reels is varied, the higher natural frequencies are associated with the tape mass. These frequencies can be calculated from the model shown in Figure 15. Since the ratio of the mass of the tape to the mass of its constraining elements is less than .01, the longitudinal vibration of a fixed bar simulates the higher vibration modes of the tape. The mass of a four inch length of tape is:

$$m_t = \frac{W_t}{g} \tag{3}$$

where W_t = tape weight

g = gravitational constant

$$m_t = \frac{.05 \times .001 \times .5 \times 4}{386}$$

$$m_t = 2.59 \times 10^{-7} \; \frac{\text{lb sec}^2}{\text{in}}$$

The equivalent mass of the idler supporting the tape is

$$M_{eq} = \frac{J}{r^2} = \frac{.853 \times 10^{-4} \text{ lb sec}^2 \text{ in}}{(.75)^2 \text{ in}^2} \tag{4}$$

where J = idler inertia

r = idler radius

$$M_{eq} = 1.54 \times 10^{-4}$$

The ratio of the tape mass to its end connected mass

$$M = \frac{2.59 \times 10^{-7}}{1.54 \times 10^{-4}} = .0016 \tag{5}$$

is an order of magnitude less than the allowable mass ratio established through sensitivity analysis of mass-spring systems[5].

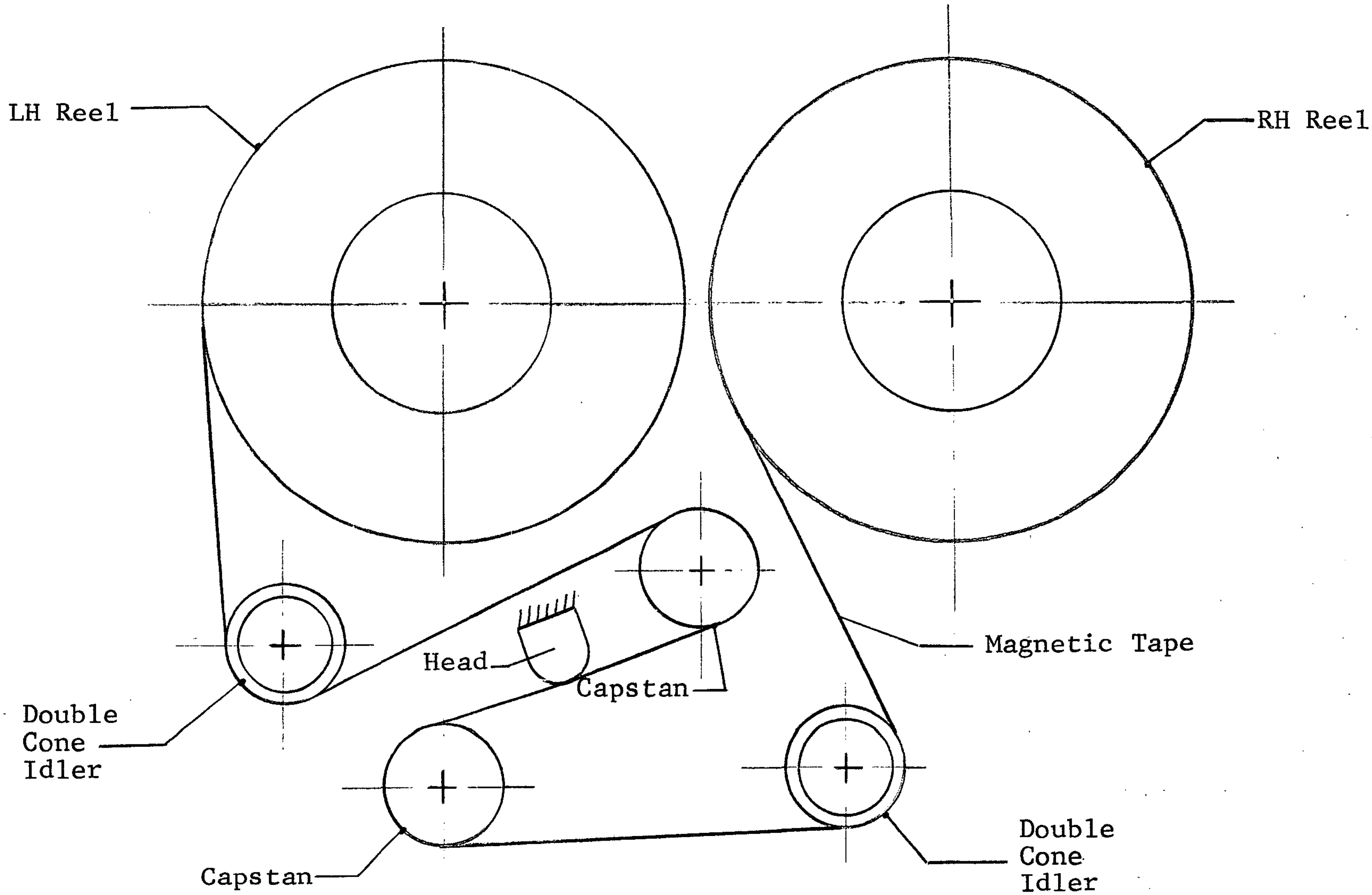

Figure 13

SCHEMATIC DIAGRAM OF FIVE-YEAR HIGH RELIABILITY TAPE TRANSPORT

Table 6

DYNAMIC DESCRIPTION OF FIVE YEAR
HIGH RELIABILITY TAPE TRANSPORT

Component	Radius (in)	Inertia (in lb sec^2)	Damping Constant (in lb sec)	Tape Length (in)
Reel	2.53	0.81×10^{-2}	0.18×10^{-3}	3.375
Idler	0.75	0.853×10^{-4}	0.33×10^{4}	4.0
Capstan	0.625	0.91×10^{-4}	0.27×10^{-4}	1.6
Head	1.0*	0.2×10^{-6}	0.002	1.6
Capstan	0.625	0.277×10^{-3}	0.27×10^{-4}	4.0
Idler	0.75	0.853×10^{-4}	0.33×10^{-4}	3.375
Reel	2.53	0.81×10^{-2}	0.18×10^{-3}	—

*Equivalent Radius

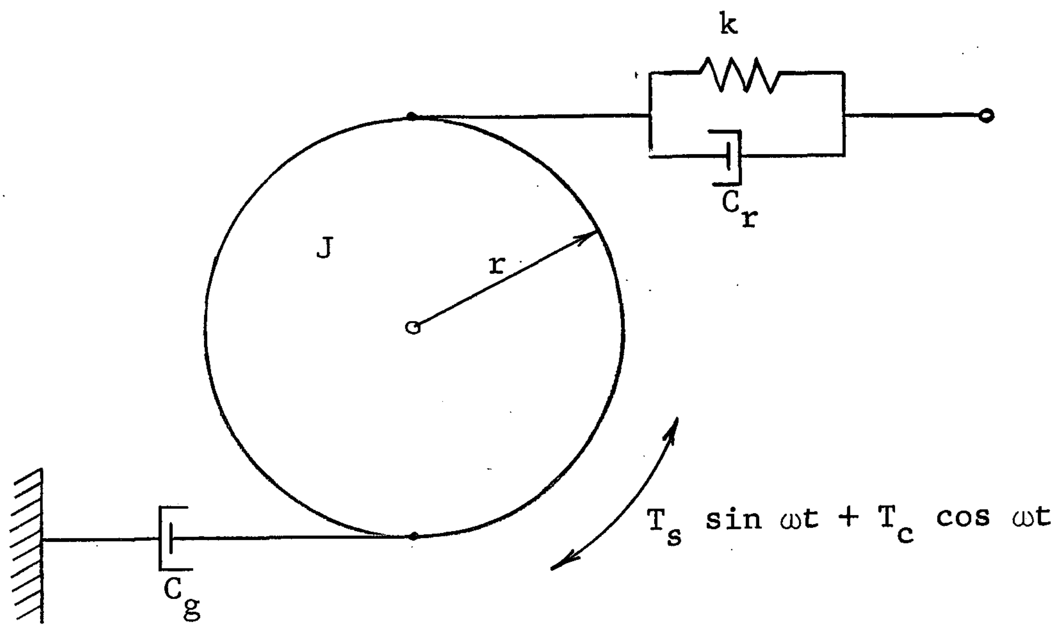

Where: k = tape stiffness

C_r = tape damping

J = reel, idler, or capstan inertia

r = reel, idler, or capstan radius

C_g = external damping

T_s, T_c, ω = external disturbance description

Figure 14

MODEL OF ANY TAPE TRANSPORT COMPONENT

Table 7

FIVE YEAR TAPE TRANSPORT SYSTEM NATURAL FREQUENCIES (Hz)
(NO TAPE MASS INCLUDED)

Natural Frequencies	% Tape on Reel No. 1		
	100	75	50
1	25.18	25.83	26.02
2	50.05	52.25	52.3
3	100.77	100.65	100.58
4	177.44	178.96	179.90
5	186.16	182.5	—

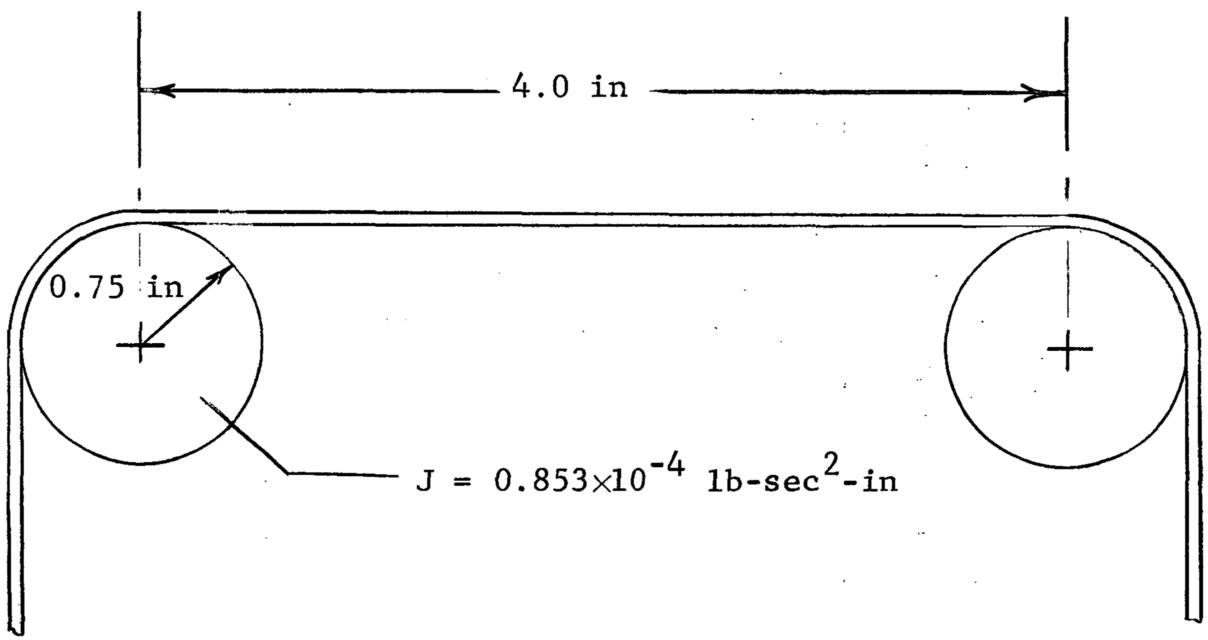

Figure 15

HIGH FREQUENCY MODEL

The formula for the natural frequencies of a fixed rod is:

$$f_n = \frac{n}{4\ell}\sqrt{\frac{E}{\rho}} \tag{6}$$

where f_n = the n^{th} natural frequency (Hz)

n = 1, 2, 3, ...

ℓ = unsupported tape length

E = tape modulus of elasticity

ρ = tape density

Using a tape modulus of 8×10^5 lb/in^2 and a specific weight of .05 lb/in^3, the following formula for natural frequencies is obtained.

$$f = 19600\ \frac{n}{\ell} \tag{7}$$

This formula is written in this form because of changing tape lengths (at the reels) during operation and differing tape lengths between components. Table 8 shows the range of natural frequencies obtained from the five year transport concept.

Table 8

HIGH SYSTEM NATURAL FREQUENCIES

Tape Length	Natural Frequency (Hz)
4	4900n
3.125	6250n
2-7/8 to 4	4900n to 6800n

It is obvious that short tape spans raise the natural frequencies. From an operational point of view, it is important to minimize the number of natural frequencies. Therefore, equal unchanging tape lengths between components is the optimum design solution because only one set of natural frequencies (f_n) need be avoided by proper selection of the system excitations (tape velocity). Changing lengths (i.e., between the reels and idlers) cause changing frequencies and the liklihood of excitation. Different spacing of components yields a set of natural frequencies for each different spacing.

Figure 16 shows a plot of the natural frequencies and excitation frequencies (above 10 Hz) for the five year tape transport concept.

2.3.3.5 Response

The response calculation gives a quantitative analysis of the performance of the tape transport which is preferable to the qualitative measure of the natural frequency calculation. Using the computer program discussed in Section 3.1, the transport tape response for inherent system excitations was computed. Three types of excitations were applied to the dynamic model of the transport.

- Component once-per-revolution bearing torque perturbation excitations
- Component once-per-revolution eccentricities
- Motor twice-per-revolution perturbation excitations
- motor 2000-per-revolution perturbation tachometer excitations

The torque excitations are directly entered in the simulation program while the displacement (eccentricities) must be related to torque through the tape constants. Figure 17 is a free body diagram showing the relationship between eccentricity, ε, and related tape length, $\Delta\delta$. The change in torque as a result of tape lengths A and B due to the eccentricity are:

$$\Delta\tau_A = (T_A + \frac{EA \quad \Delta\delta}{\delta_A}) \ (R + \Delta R) - T_A \ R \tag{8}$$

$$\Delta\tau_B = (T_B + \frac{EA \ \Delta\delta}{\delta_B}) \ (R - \Delta R) - T_B \ R \tag{9}$$

with

$$\Delta\tau = \Delta\tau_A - \Delta\tau_B \text{ , and} \tag{10}$$

combining equations and dropping second order terms, $\Delta\tau$ becomes

$$\Delta\tau = EA\Delta\delta \ R \ (\frac{1}{\delta_A} - \frac{1}{\delta_B}) + (T_A + T_B) \ \Delta R \tag{11}$$

$$\Delta\delta = f(\varepsilon,\theta) = \varepsilon \sin \omega t$$

$$\Delta R = f(\varepsilon,\theta) = \frac{\varepsilon}{2} \sin \omega t$$

therefore

$$\Delta\tau = EA \ \varepsilon \ R \ (\frac{1}{\delta_A} - \frac{1}{\delta_B}) \sin \omega t + (T_A + T_B) \ \frac{\varepsilon}{2} \sin \omega t \tag{12}$$

The torque perturbation for the following idler configuration with an .0001 eccentricity becomes 0.25×10^{-2} in-lb.

$E = 8 \times 10^5$ lb-in

$A = .0005$ in^2

$\varepsilon = .0001$ in

$T_A = T_B = 4$ oz

$R = 0.75$ in

$\delta_A = 3.0$ in

$\delta_B = 4.0$ in

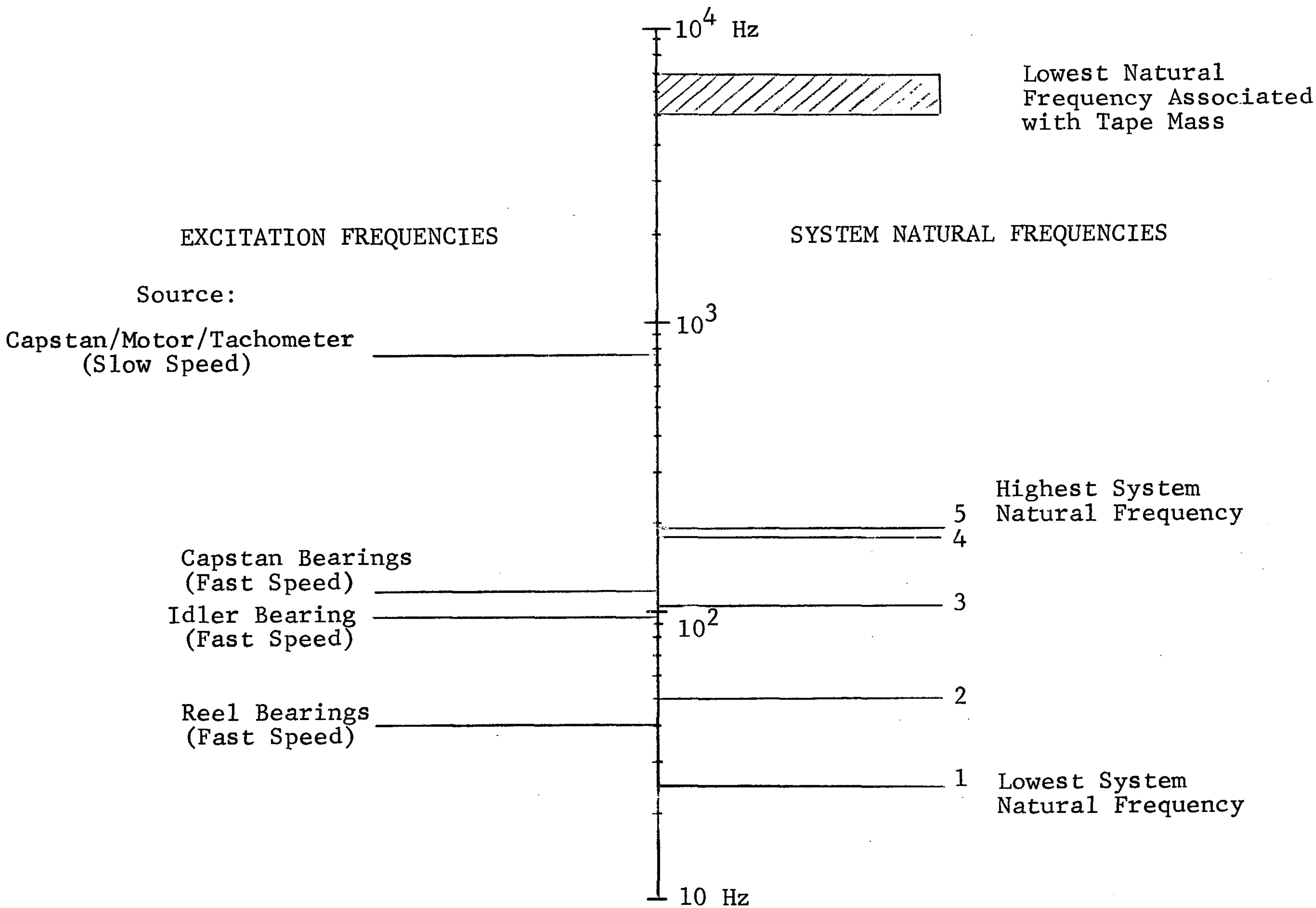

Figure 16

COMPARISON OF NATURAL FREQUENCIES AND EXCITATION FREQUENCIES ABOVE 10 Hz

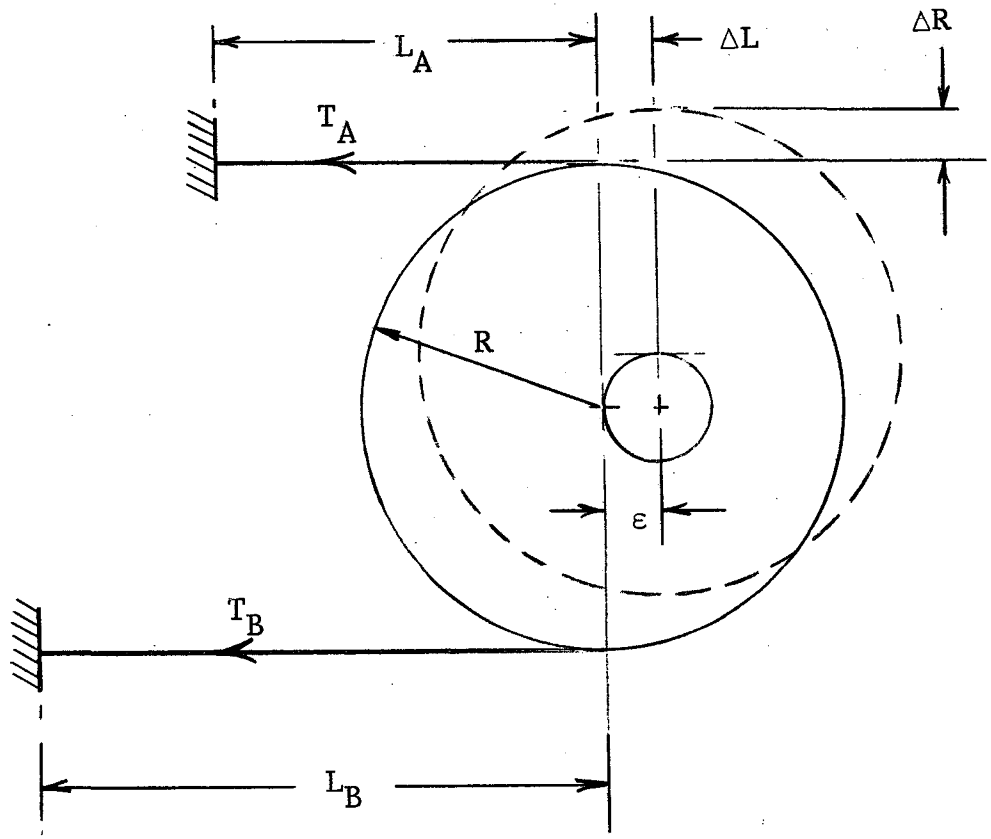

Figure 17

RELATIONSHIP BETWEEN ECCENTRICITY AND CHANGE IN TAPE LENGTH

Table 9 shows tape vibration response due to bearing torque perturbations, component eccentricities, and motor cogging for tape speeds of 1-1/2 and 32 ips. The response is shown in terms of instantaneous absolute displacement and flutter (rms velocity). These responses were calculated for a newly constructed transport.

In order to determine the jitter from the vibration response data, the relative tape displacement between bits is obtained from the following relationship:

$$\text{Jitter} = \sum_{i=1}^{n} \chi_i \ (t + \tau) - \chi_i(\tau) \tag{13}$$

where

$\chi_i(t + \tau)$ = tape displacement at time = $t + \tau$ due to i th disturbance

τ = bit spacing in seconds

$\chi_i \ (t)$ = instantaneous tape displacement due to i th disturbance

For a given disturbance, the tape displacement is harmonic and, therefore

$$\chi_i = a_i \sin (\omega_i t - \phi_i) \tag{14}$$

where

a_i = disturbances amplitude

ϕ_i = disturbance phase angle

ω_i = disturbance frequency

Then the jitter for the i th disturbance is

$$\tau_i = a_i \left[\sin \omega_i \ (t + \tau) - i\right] - a_i \sin \left[\omega_i t - \phi_i\right] \tag{15}$$

Table 9 TAPE VIBRATION RESPONSE AT HEAD

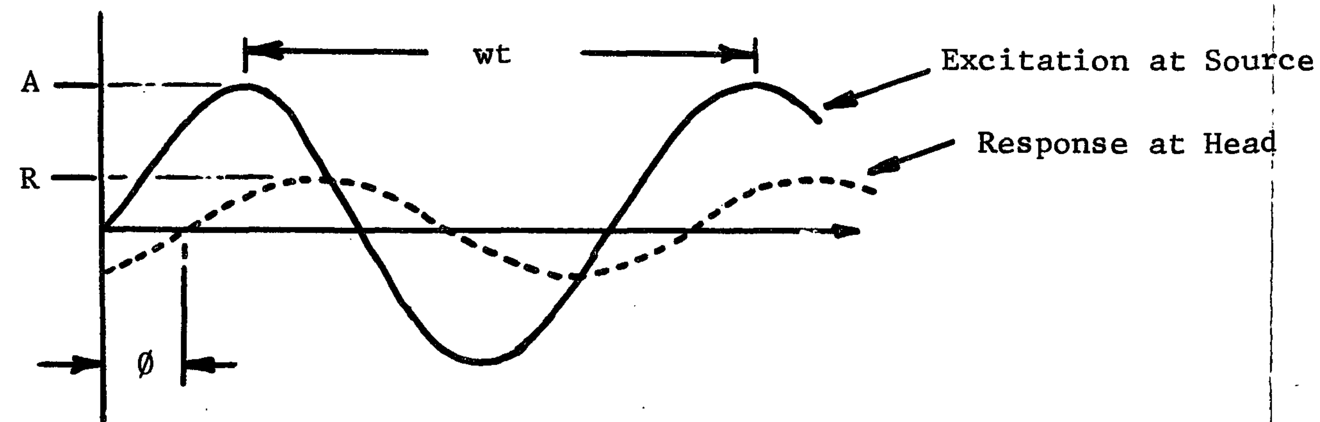

Component	Excitation Source	Tape Speed (ips): 1.5 ips (Flutter 0.0018 ips) — Excitation: Amplitude (A) in-lb	Excitation: Frequency (wt) rad-sec	Response at Head: Amplitude (R) in	Response at Head: Phase (Ø) rad	Tape Speed (ips): 32.0 ips (Flutter 0.027 ips) — Excitation: Amplitude (A) in-lb	Excitation: Frequency (wt) rad-sec	Response at Head: Amplitude (R) in	Response at Head: Phase (Ø) rad
Reels	Bearings	0.113×10^{-2}	11.84	0.335×10^{-5}	-0.667	0.113×10^{-2}	253	0.68×10^{-2}	-1.417
Idlers	Bearings	0.696×10^{-3}	28.00	0.47×10^{-5}	-1.2876	0.696×10^{-3}	595	0.23×10^{-5}	+1.197
Capstan	Bearings	0.696×10^{-3}	33.60	0.561×10^{-5}	-1.37	0.696×10^{-3}	717	0.322×10^{-5}	+0.416
Roller	Eccentricity (0.0001 in)	0.24×10^{-2}	2.00	0.608×10^{-3}	-0.0122	0.24×10^{-2}	42.6	0.418×10^{-3}	+0.467
Capstan	Eccentricity	0.24×10^{-2}	2.40	0.522×10^{-3}	-0.0248	0.24×10^{-2}	51.2	0.389×10^{-3}	+0.481
Capstan Reducer	Motor	0.23×10^{-4}	28800	0.15×10^{-13}	+0.247				
Reel	Motor	0.63×10^{-3}	1.18	0.13×10^{-3}	+0.0029				
Reel	Motor	0.63×10^{-3}	0.59	0.484×10^{-3}	+0.007				
Reel	Motor	0.663×10^{-4}	1186.0	0.165×10^{-7}	-0.739				
Capstan	Motor	0.23×10^{-3}	2.40	0.25×10^{-4}	-0.059				
Capstan	Motor	0.23×10^{-3}	4.80	0.66×10^{-5}	-0.2628				
Capstan	Motor	0.23×10^{-4}	4800.0	0.36×10^{-8}	+1.529				
Capstan Reducer	Motor	0.23×10^{-3}	14.40	0.717×10^{-6}	+0.020				
Capstan Reducer	Motor	0.23×10^{-3}	28.00	0.18×10^{-6}	+0.033				

Expanding the transcendental functions and making small angle assumptions the jitter is

$$\tau_i = a_i \omega_i \tau \cos (\omega_i t - \emptyset_i) \tag{16}$$

with a maximum value of

$$|\tau_i| \max = a_i \omega_i \tau \tag{17}$$

and

$$\omega_i = \frac{V}{r_i} n_i$$

$$\tau = \frac{B}{V}$$

$$B = \text{in/Bit}$$

$$V = \text{tape speed}$$

$$r_i = \text{disturbing component radius}$$

$$n_i = \text{disturbance order of tape speed}$$

then

$$|\tau_i| \max = \frac{a_i n_i}{r_i} B \tag{18}$$

For a conservative answer, the random addition is bounded by:

$$|\tau_i| \max = \sum_{i=1}^{n} \frac{a_i n_i}{r_i} B \tag{19}$$

Table 10 shows values of jitter computed from results of Table 9 for a 3000 bit/in spacing at 1-1/2 and 32 ips tape speed. The first column shows results for a newly constructed recorder while the second column shows the jitter for a recorder subject to extensive wear. Thus the local dynamic model provides a measure of the tape recorder performance as a function of its life.

Table 10

COMPUTED VALUES OF JITTER

		Jitter (microinches)		
Tape Speed	Time (sec)	New	Degraded (.0005 in Tolerances)	Flutter (in/sec) (new)
1-1/2 ips	.000222	.75	2.9	.0018 in/sec
32 ips	.0000104	.45	2.0	.027 in/sec

The results of Table 10 for the non-degraded state correlate with the analytical predictions of other investigations[6] as well as with published performance ratings of existing satellite recorders. The degraded performance is a factor of four increase in the jitter level, but still only represents a 1% variation in this bit cell spacing. This variation is clearly acceptable from a data processing standpoint.

2.4 Testing Techniques for Five Year Life

2.4.1 General

In attempting to establish the required testing techniques to assure long life for an unattended period of five years, two specific problems are encountered. The first relates to the unrealistic requirement of life testing for the full time period of five years. Even attempting to life test for a significant proportion of the total life period is clearly impractical. The second problem arises from the inability to accelerate the life test in a way which would allow correlation between accelerated and real time. Although accelerated life tests are well documented in certain fields, the application of these techniques to rotating mechanisms such as antifriction ball bearings is not applicable. Life accelerating in this case means rotational acceleration, and hence an overall change in the required mode of operation with a corresponding change in all known wear and degradation mechanisms.

The need for establishing a life assurance testing technique is essential in attempting to verify many of the design procedures developed in this study. As both actual life and accelerated life testing cannot be directly applied, it has been necessary to develop a strategy which could be adopted at some later date to verify the overall design concept. This section outlines such a strategy and indicates how it may be implemented by the combination of a wear model, which relates disturbance errors to time; and a performance model, which relates system performance to disturbance errors; so that an overall life model may be generated so relating the performance of a system to time.

2.4.2 Simple Model for Life

Although the prime requisite of long life has been the major goal of this design study, it is necessary at this point in time to define this statement in terms of system performance. End of life should therefore be related to the inability of the total system to adequately recover data in a form which would allow meaningful interpretation. End of life may, therefore, be defined in relationship to the ability of the machine to record or reproduce, or the degradation of the bit error rate of the signal output, or an increase in the time base error of the system which would influence the recovery of the recorded data. It is not necessary to absolutely define end of life in these terms at this time, what is essential, however, is to acknowledge that a transport that is successfully recording and reproducing data after 50,000 tape passes (i.e., 10,000 passes per year, 100% duty cycle) fulfills the prime objective of the program irrespective of its actual mechanical condition.

The successful recovery of the data, termed data integrity, is therefore related to end of life

$$\text{End of Life} = f\ (\text{Data Integrity})$$

This statement, however, is of little or no value in assessing the condition of the transport with regards to time. Data integrity is effectively a digital condition, that is, there are only two possible levels. The data is either recoverable (e.g., a one level) or it is not (e.g., a zero level). There is not a condition between these two levels which has an identifiable value that can be used to interpret the condition of the overall transport. The reason for this is obviously associated with the data processing electronics such as squaring and buffering circuits, which are used to manipulate and mold the reproduced output signal into the required form for data collection.

In order to assess the condition of the transport and hence interpret the degradation of life, an analog condition as opposed to a digital condition is required. Such an analog condition is available at a point in the reproduce electronics prior to any form of signal processing. The recovery of a signal at this point is termed signal integrity and its analog nature is meant to represent a gradual change with respect to time. The position of observing signal integrity and data integrity and their respective relationship with time is diagrammatically shown in Figure 18.

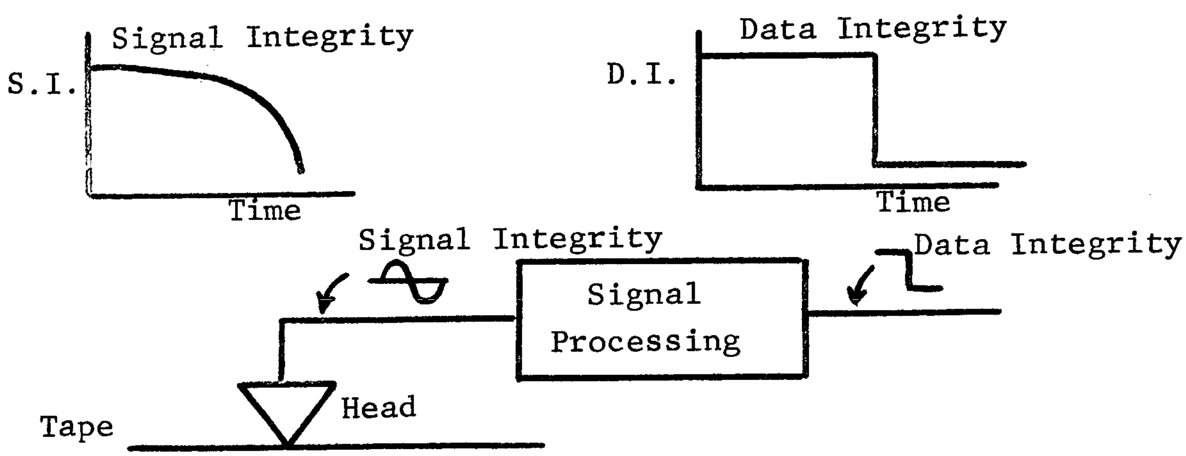

Figure 18

EVALUATORY POSITIONS OF SIGNAL AND DATA INTEGRITY

The measurement of signal integrity by observing a variety of reproduce parameters such as flutter, time displacement error, wavelength response, signal to noise level, etc., allows the performance of the transport to be monitored and hence its short term degradation to be assessed even though the reduced performance level of signal integrity in no way influences the data integrity measured after suitable signal processing.

Signal integrity, therefore, relates to a change in overall performance of the machine and hence to a change in life, as life is the relationship between performance and time. This may be represented as:

$$\Delta \text{ Life} = f(\text{Signal Integrity})$$

Although end of life is related to the data integrity, the change in life is not directly related,

$$\Delta \text{ Life} \neq f(\text{Data Integrity})$$

It is for this reason that use should be made of the signal integrity as opposed to the data integrity in any testing technique to predict or confirm the life of a transport system. It is interesting to note that the signal integrity of a system can be easily correlated to both the head/tape interface as well as to tape motion control and hence is a parameter that can be continually monitored and related to other aspects of the transport design.

2.4.3 Engineering Strategy

We have already shown that the end of life of a transport system may be related to the data integrity and that a change in life is observed only by evaluating the change in signal integrity of the system prior to any processing electronics. These two relationships may be superimposed as shown in Figure 19. With the ability to predict the rate of change of signal integrity ($\frac{ds}{dt}$) and knowing the level below which compensation is not possible, then it is feasible to determine the point at which data integrity is lost and hence end of life. However, the rate of change of signal integrity is not itself constant and is more probably exponentionally related to time. Therefore, it is essential to define a

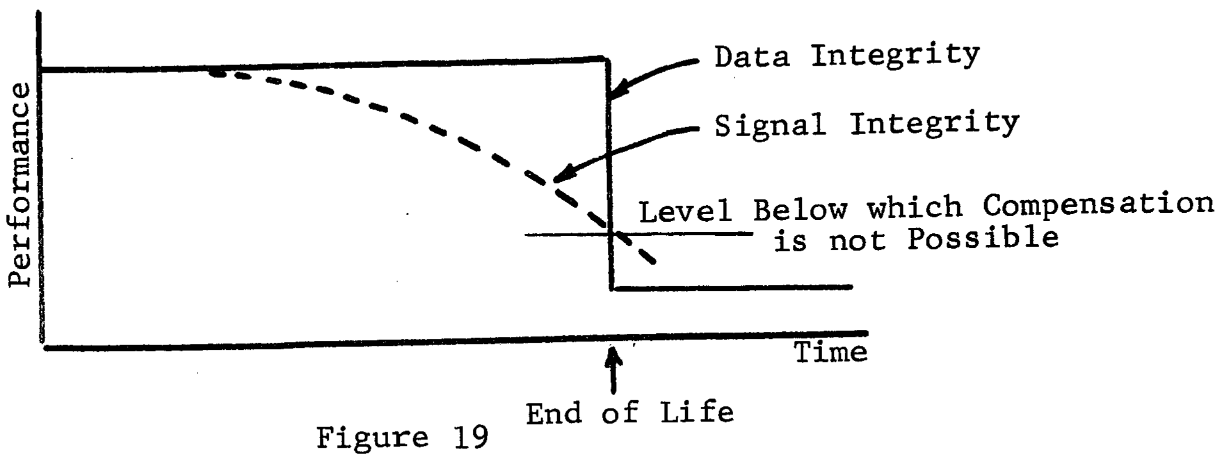

Figure 19

SIGNAL AND DATA INTEGRITY

strategy which will allow the relationship between signal integrity (e.g., performance) and time to be predicted.

Such a strategy requires the establishment of two specific relationships, namely, the change in the systems performance against induced system errors and the change in the errors of the system with time. The former will be called the performance function and the latter the wear function of the system. A combination of these two functions allows a predictable relation to be established between performance and time, that is, a life function.

2.4.3.1 Performance Function

This relates to the transports performance to a change in errors of the system and is illustrated in Figure 20. This relationship simply states that as the magnitude of the errors in the system increase, a corresponding decrease in performance can be expected. It is possible to theoretically predict this relationship using the dynamic model of the transport developed during this design study, however, as important is the fact that this relationship can be evaluated in the laboratory. This is achieved by artificially inducing errors into the system and measuring their influence on the overall signal integrity of the system.

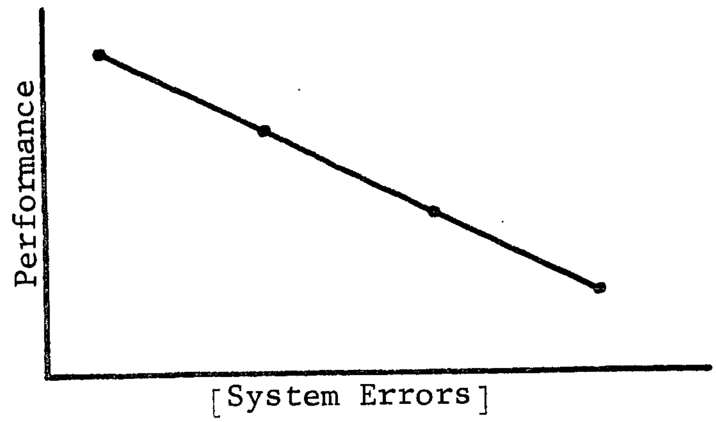

Figure 20

PERFORMANCE FUNCTION CURVE

2.4.3.2 Wear Function

This function relates the rate of change of system errors with time, and is illustrated in Figure 21.

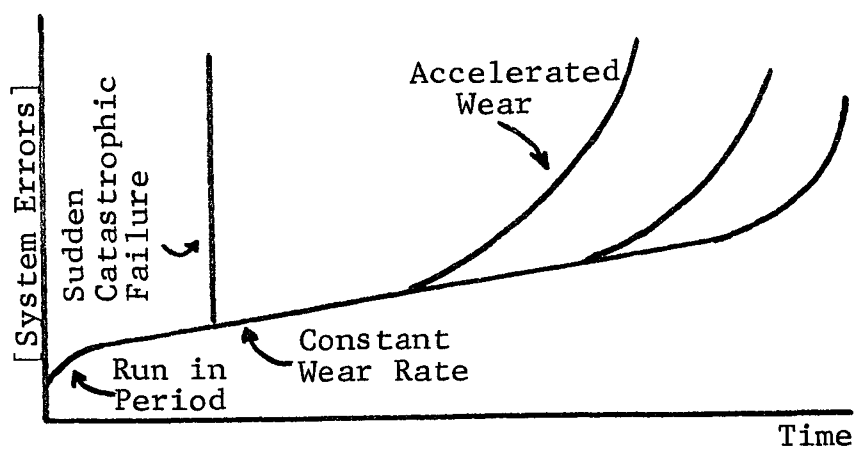

Figure 21

WEAR FUNCTION CURVE

It is effectively a wear life diagram which shows that the rate of wear within the system, once past a point where catastrophic failure may occur, will follow a well defined path which is dependent upon the operating conditions of the system. Wear life diagrams for certain mechanisms are well documented[7]. They show that after an initial run in period a constant wear rate is maintained until a point where accelerated wear takes over owing to some external influence such as lubricant breakdown in the case of antifriction ball bearings.

As this wear function is related to real time it is impossible to construct a precise curve without long term life testing. However, there are several criteria which afford us the ability to predict such a curve with a reasonable degree of confidence. First the concept of modularization coupled with module burn in periods, allows the initial variation owing to the run in period to be overcome, hence establishing the magnitude of the linear portion of the wear function curve. Second, the overall philosophy of design which has been implement throughout this design study together with the removal and or control of all critical elements negates the probability of sudden catastrophic failure occurring during the early life period of the transport. What remains is the need to predict the length of the linear portion of the curve and the establishment of the point in time when accelerated wear occurs. Again, the overall design approach is predicated upon insuring that accelerated wear will not take place during the proposed lifetime. It is for this reason that, throughout the design study, emphasis has been placed on minimizing stresses and loads throughout the system especially those that influence life as in the magnetic tape and rotational components. The need for including a continual feed lubrication system is one example where the added complexity required to implement pulsed lubrication throughout life was considered to be acceptable in order to insure that the bearing system did not experience accelerated wear owing to lack of adequate lubrication.

Given these design criteria together with a wealth of documented material in the literature for specific components; it is possible to construct, with a certain high value of confidence, a wear function curve for the overall transport. Such a curve combined with an evaluated version of the performance function allows the life function curve to be predicted.

2.4.3.3 Life Function

This function relates the rate of change of the transports performance with time. As described earlier, the performance value is meant to represent the signal integrity of the system prior to any electronic compensation, and hence is a parameter than can be evaluated.

The combination of the performance function which relates measured system performance with induced errors and the wear function which indicates the rate of change of actual errors with time allows the life function curve to be constructed

$$\frac{\Delta P}{\Delta |e|} \times \frac{\Delta |e|}{\Delta t} = \frac{\Delta P}{\Delta t} \qquad (20)$$

Such a curve may be represented as shown in Figure 22. This life function is still a predicted relationship but its value is of paramount importance for two specific reasons. First, it allows the above parameters to be more accurately defined with a certain degree of realism and as important, it forms a firm base which, with additional inputs from evaluatory procedures, allows the function to be continually modified to represent a more exacting relationship of performance with time.

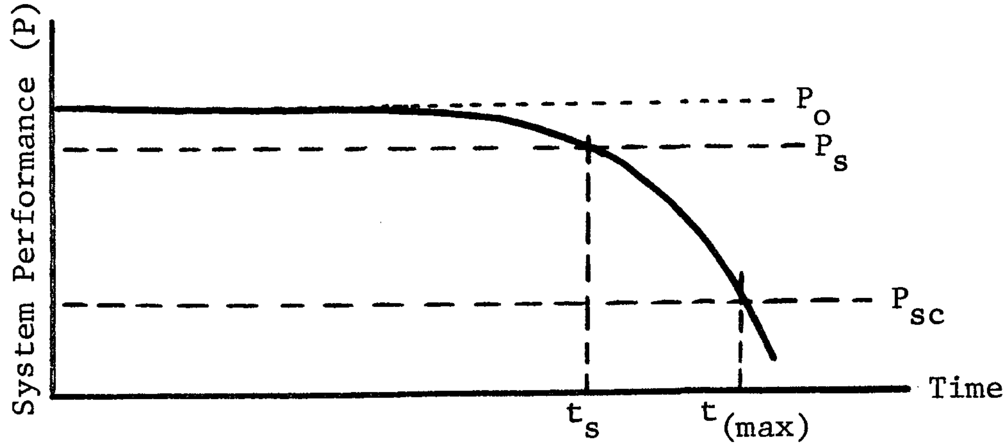

Figure 22

LIFE FUNCTION CURVE

where the following parameters may be defined:

P_o = performance envelope at $t = 0$

P_s = specified performance without compensation

P_{sc} = specified performance with compensation

$t_{(max)}$ = maximum life span of data integrity

t_s = specified life span for design

This modification is explained in greater detail in the following section on implementation and evaluation.

2.4.4 <u>Implementation</u>

It is possible to implement the engineering test strategy by using either partial or full models of the proposed transport. Both are described briefly in this section, however use of a full model has certain advantages and is recommended for a more precise evaluation of the total system.

2.4.4.1 Partial Model

A partial model is meant to represent the division of the overall transport into subelements which may or may not have been modularized. These subelements are then constructed and tested individually as opposed to collectively, to assess their contribution to the overall performance of the machine in terms of signal integrity. As an example the effect of errors in a reel assembly module may be examined theoretically and then experimentally verified by inducing errors into a fabricated reel assembly and measuring the change in response at the recording head (Figure 23).

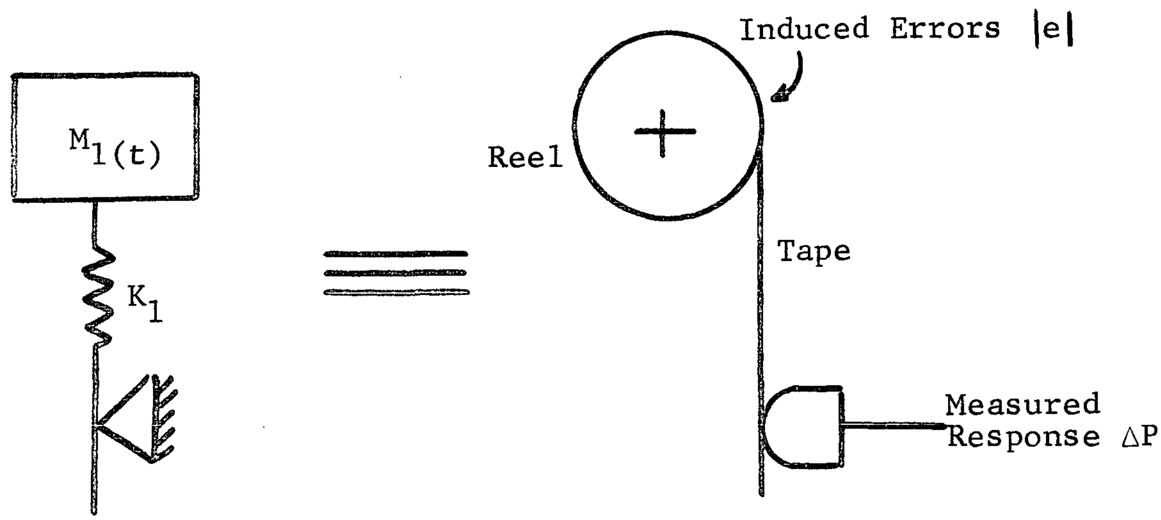

Figure 23

PARTIAL MODEL

More detailed explanation of these models can be found in Section 3.1.1 of this report.

2.4.4.2 Full Model

A full model is meant to represent a complete mechanical version of the transport design. This approach to evaluation and hence determination of the life function curve is recommended as it combines all elements of the transport in a composite form (Figure 24).

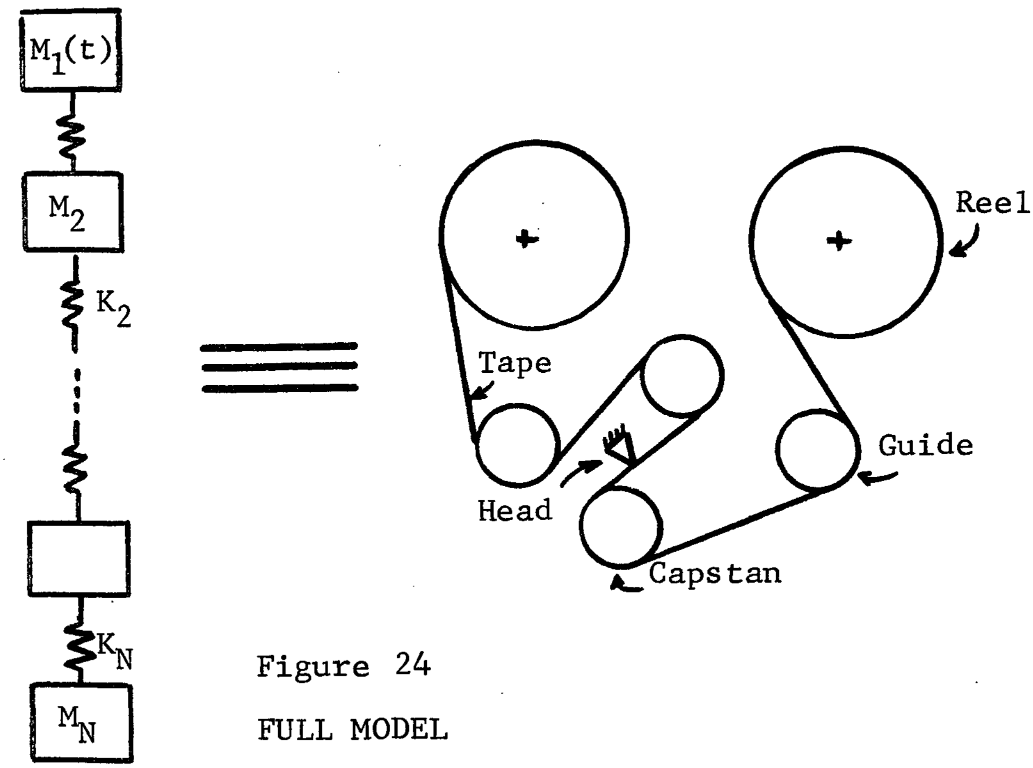

Figure 24

FULL MODEL

2.4.4.3 Evaluation

The evaluation of a full model of the transport allows the predicted life function curve to be continuously up-dated as the evaluation period progresses. The original life function curve combines the predicted wear function with a performance function curve generated from the mathematical model of the tape transport. This performance curve is then adjusted according to the results obtained from actually inducing errors into the system and measuring the effect on the signal integrity of the system (Figure 25). This measured curve is then used to adjust the original life function curve as shown in Figure 26 to obtain a first degree modification.

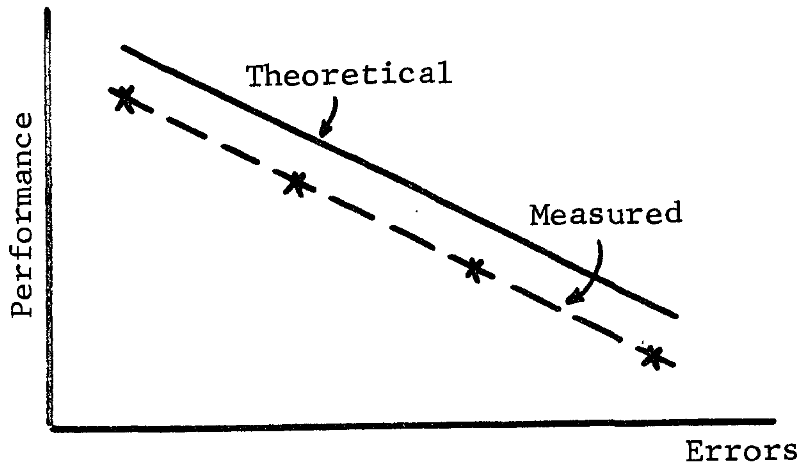

Figure 25

MODIFIED PERFORMANCE FUNCTION

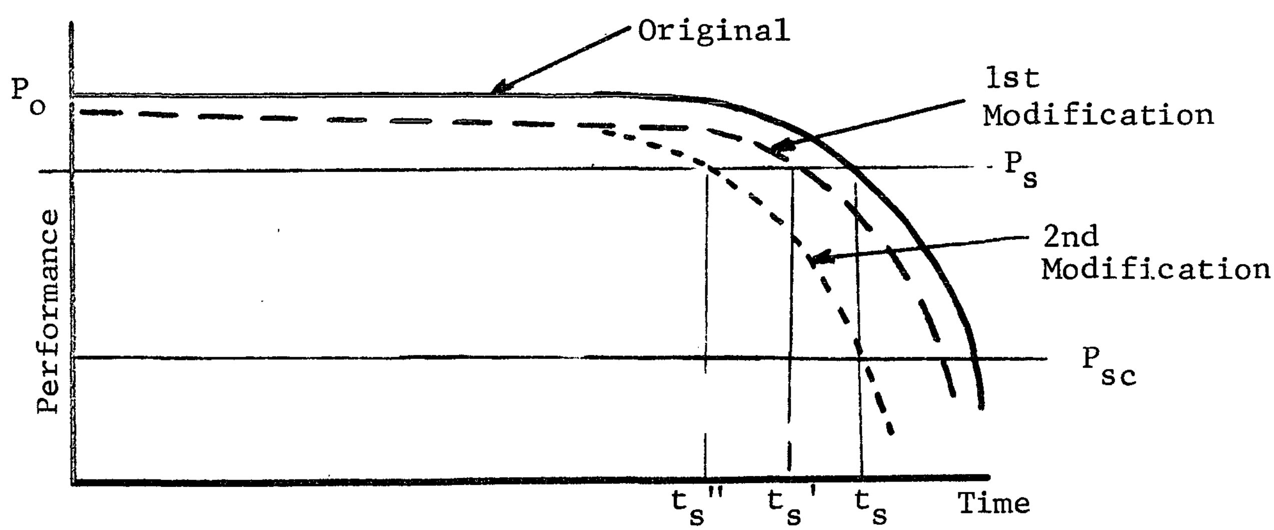

Figure 26

MODIFIED LIFE FUNCTION CURVE

This modified life function curve allows more representative values of the maximum life span and probable specified life span to be determined. The next adjustment results from updating the wear function curve. Such updating can only occur with time, however, an accurate determination of the slope of the linear portion of the curve should be possible over a time period of a few months and, hence, a second and more accurate modification of the life function curve will result.

Using these procedures it will be possible to establish, with a high level of confidence, the usable life of the transport and, hence, confirm the design practices and manufacturing procedures developed during this design study.

3. DESIGN TECHNIQUES AND RESULTS

3.1 Response Analysis

This task was concerned with the performance of the tape transport concept under operating conditions. Wow and flutter characteristics of the transport were determined for system conceptual variations. Forces, torques, and tensions obtained from this task were utilized in the critical component analysis to assess the reliability.

The design information on the dynamic performance of the mechanical system components were obtained from a digital simulation model. The model used in this task consists of an arrangement of lumped springs, mass and dashpots that can be used to simulate the physical behavior (response) of the transport to internal and external disturbances. Mathematical relationships are written between the lumped elements that are arranged to compose the transport. This modular technique allows a concept change by rearranging lumped elements representing the model. The mathematical relationships (equations of motion) that simulate the models dynamic behavior are programmed for solution on the digital computer. The effect of design parameter changes on the performance and reliability can be determined from the numerical solution of these equations of motion.

3.1.1 Modeling

The modeling process is very important in the simulation of the total transport system because the mathematical solution will represent the physical behavior to the degree that the model duplicates the physical features of the transport. The important mechanical characteristics of this system are its mass, elasticity and damping. Lumped elements (non-elastic masses, non-massive springs and non-elastic massive dashpots are used to represent this system. The mathematical descriptions of these lumped elements are shown in Figure 27. In addition, mathematical models are made of the internal and external disturbances such as friction and drag, ball bearing excitation and motor speed fluctions.

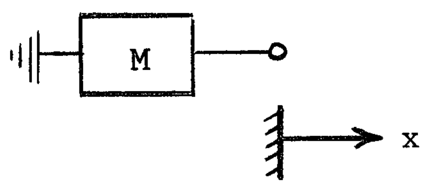

(a) Mass Element

$$M \frac{d^2x}{dt^2} = F_M \tag{21}$$

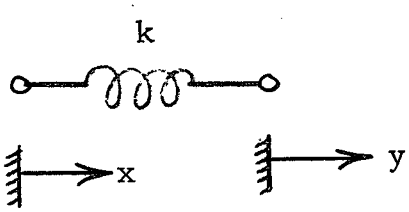

(b) Spring Element

$$k(y - x) = F_s \tag{22}$$

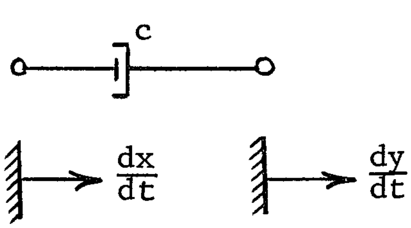

(c) Damping Element

$$c\left(\frac{dy}{dt} - \frac{dx}{dt}\right) = F_d \tag{23}$$

Figure 27

MODEL ELEMENTS

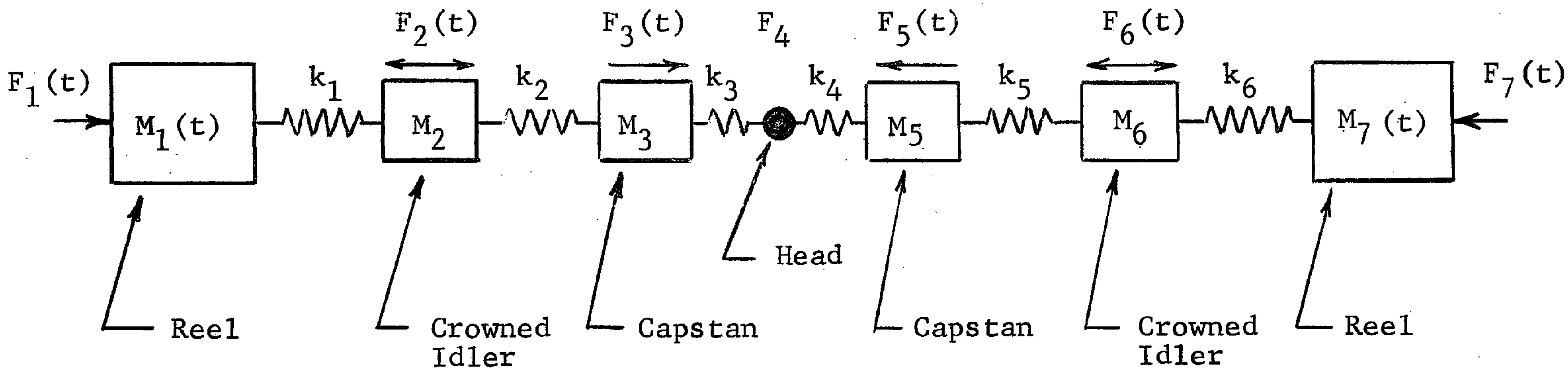

Figure 28

SIMULATION MODEL

The transport concept shown in Figure 13 is now modeled for dynamic analysis. Figure 28 shows a conceptual model of the transport with each subsystem component identified with its appropriate lumped parameter. The subsystems modeled are:

- Reels
- Capstans
- Heads
- Idler Rollers
- Tape

A separately excited DC shunt motor has been modeled for the present analysis. If other type motors are used, they will be modeled as needed. This is an illustration of the integration of the electrical actuation components into the mechanical systems model. Figure 29 shows a schematic diagram of a separately excited shunt motor.

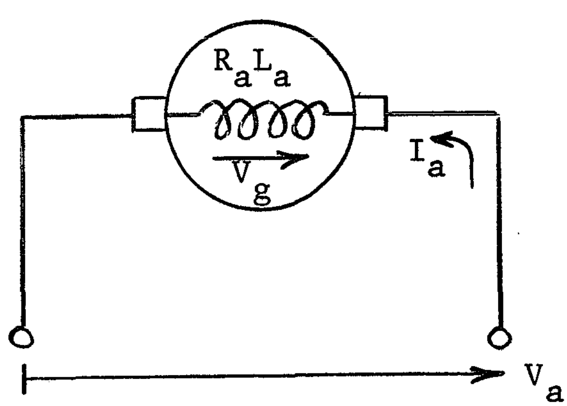

Figure 29

SEPARATELY EXCITED SHUNT MOTOR

The sum of the voltage changes in the armature circuit yields the following equation.

$$V_a = V_g + I_a R_a + L_a \frac{dI_a}{dt} \tag{24}$$

where

V_a = Armature voltage

V_g = Induced voltage

I_a = Armature current

R_a = Armature resistance

L_a = Armature inductance

t = Time

The back emf is related to the motor speed through the following relationship.

$$V_g = K_D \; \phi \; \omega \tag{25}$$

where

K_D = proportionality constant

ϕ = flux

ω = angular velocity

The motor torque, T is related to the armature current I_a through the following relationship

$$T = K_D \, I_a \, \phi \tag{26}$$

These three equations are combined to obtain the following equation relating the torque, speed and armature voltage.

$$V_a = K_D' \omega + \frac{R_a}{K_D'} T + \frac{L_a}{K_D'} \frac{dT}{dt} \qquad (27)$$

Where

$$K_D' = K_D \phi$$

The term $\frac{dT}{dt}$ shows that transient responses are obtained.

3.1.1.1 Reel Model

Figure 30 shows a schematic view of a reel with stored tape. The equation of motion for the reel subassembly is:

$$J \frac{d\omega}{dt} = - f\omega + T_o \sin n\omega t - rF_T + T \qquad (28)$$

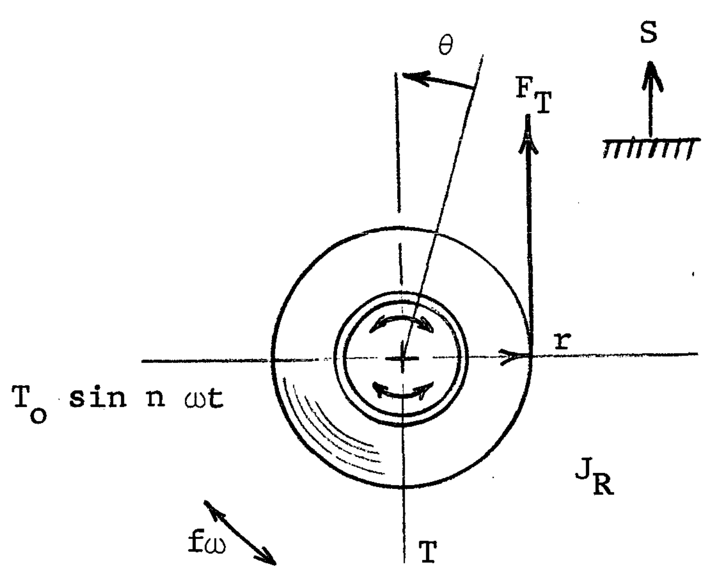

Figure 30

REEL MODEL

Where

f = friction coefficient
T = motor torque
F_T = tape tension
r = tape pack radius
T_o = disturbing torque (bearings)
ω = reel speed
J_R = reel and tape pack moment of inertia
t = time
n = disturbance frequency multiples

The tape pack radius, tape transport length and moment of inertia are functions of time or length of tape transferred, and are described by

$$r = r_o + \frac{u\theta}{2\pi} \text{ (tape addition)} \tag{29}$$

$$r = r_M - \frac{u\theta}{2\pi} \text{ (tape removal)} \tag{30}$$

$$\frac{dr}{dt} = \pm \frac{u\omega}{2\pi} \tag{31}$$

$$S = r\theta \tag{32}$$

$$\dot{S} = \dot{r}\theta + \dot{\theta} r \quad \text{(tape speed)} \tag{33}$$

$$J_R = \rho\frac{\pi}{2} b \, [r^4(t) - r_o^4] + J_H \tag{34}$$

Where

θ = angular coordinate of reel
S = tape transport length
r_o = inner tape pack diameter
u = tape thickness
r_M = maximum tape pack diameter
b = tape width

ρ = tape density

J_H = hub moment of inertia

J_R = hub and tape pack moment of inertia

ω = reel speed

t = time

3.1.1.2 Tape Model

The tape (Figure 31) is modeled as a massless spring with a stiffness,

$$k = \frac{EA}{\ell} \tag{35}$$

where

k = tape spring constant

E = tape modulus of elasticity

ℓ = tape length

A = tape cross-sectional area

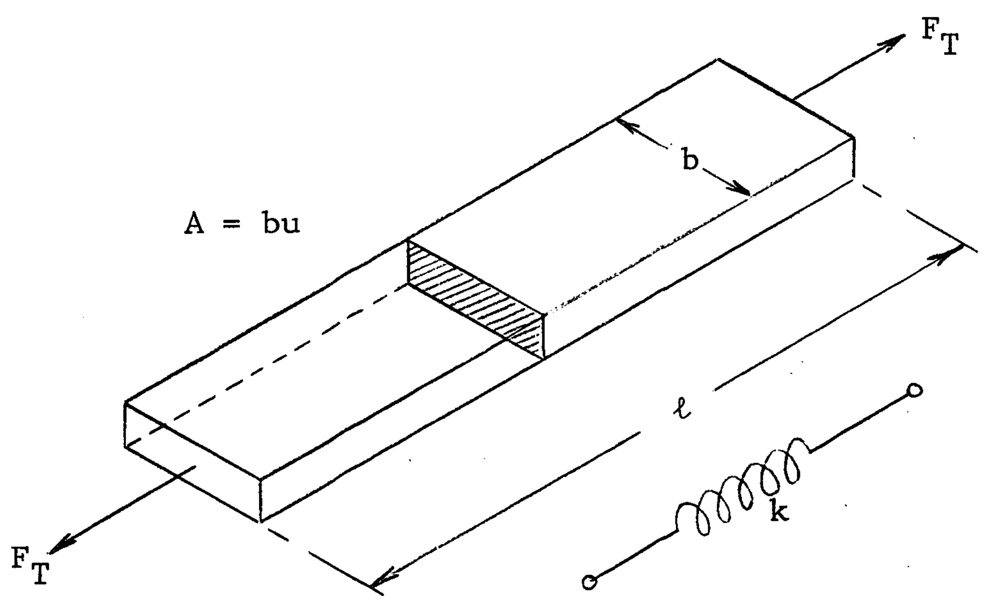

Figure 31 TAPE MODEL

3.1.1.3 Capstan Model

The capstan model is shown in Figure 32. It has a fixed moment of inertia, J_R and a fixed radius, r_c. The equation of motion for the capstan including motor torque, friction and bearing excitation is Equation 13.

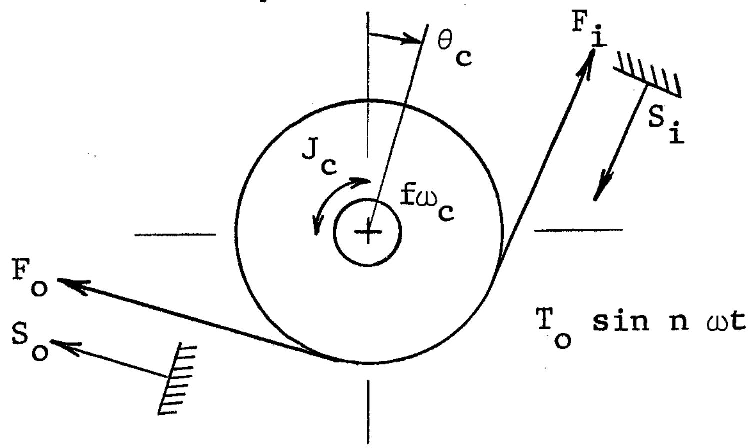

Figure 32
CAPSTAN MODEL

$$-f_c\omega_c + T + F_o r_c + T_c \sin n\omega_c t = J_c \frac{d\omega_c}{dt} \tag{36}$$

Where

θ_c = angular displacement
T_c = disturbance torque
J_c = capstan moment of inertia
f_c = capstan friction coefficient
ω_c = capstan speed
r_c = capstan radius
F_o = output tape tension
F_i = input tape tension
n = disturbance frequency as speed multiple

3.1.1.4 Idler Model

The idler roll model is identical to the capstan except no motor torque is included. Therefore, the idler model is obtained by setting T = 0 in Equation 36.

3.1.1.5 Head Model

The final element in the dynamic model is the head, Figure 33, which exerts a drag on the tape. The equation of motion for the head-tape force balance as shown in Figure 33 is given below.

$$F_i + f_o - f_1(\mathring{S}_H)^{\eta} = F_o \tag{37}$$

where

F_i = input tension

F_o = output tension

f_o = static friction force

f_1, η = dynamic friction coefficients

$\mathring{S}_H$ = tape velocity at head

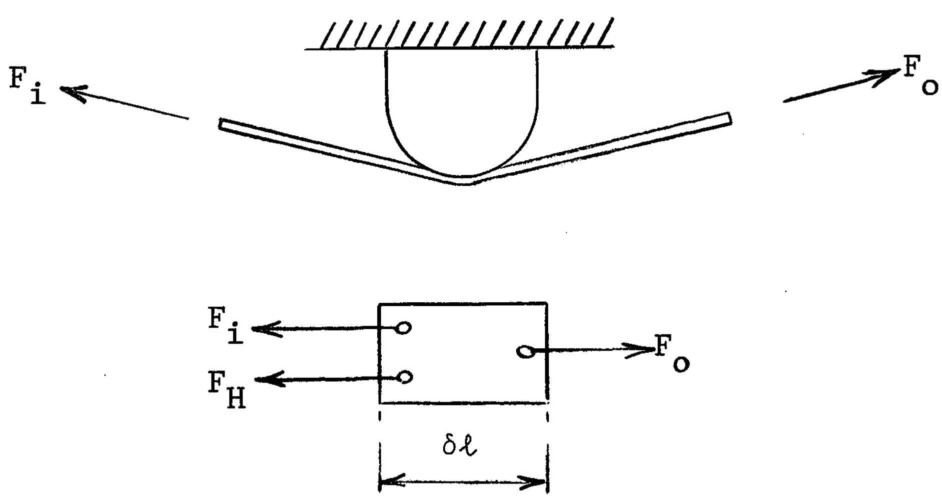

Figure 33

HEAD MODEL

3.1.2 Mathematical Solution

The equations of motion derived in the preceding sections were used to solve the dynamic system response to input disturbances and to determine the transport natural frequencies. Input disturbances due to torque perturbations (bearing error), geometry variations (machining error such as eccentricities, out of roundness etc.) and electrical phenomena such as cogging can be applied to the simulation model. The tape behavior at each component in the transport is calculated as a function of the input disturbances. The analysis was conducted in three parts:

- Natural frequency
- Steady state vibration response
- System response

These analyses are described individually. In each case the equations of motion were derived for the long-life transport concept, then generalized for use in the analysis of any other transport. The natural frequency analysis and steady state vibration response have been programmed for the digital computer. These problem-oriented computer programs are operational. Each analysis is described herein along with some results and a users guide.

3.1.2.1 Natural Frequency

Undamped system natural frequencies are useful in system design to avoid difficulties in the system dynamic performance. The coincidence of disturbance frequencies to natural frequencies yields a potential source of operational difficulties. Either the performance of the transport will be degraded or the tape life could be shortened. Therefore the natural frequency analysis is an indicator of dynamic compatibility of the components in the transport system.

Figure 34 shows the dynamic model for the five-year transport. The equations of motion (38 through 43) are given in terms of

- Tape stiffness $k_i = \frac{EWt}{\ell_i}$
- capstan, idler, reel inertia J_i
- capstan, idler, reel radius r_i
- capstan, idler, reel displacement S_i

where

E = tape Modulus of Elasticity

W = tape width

t = tape thickness

ℓ_i = tape length

t = time

$$\frac{J_1}{r_1^2} \frac{d^2 S_1}{dt^2} + k_1 (S_1 - S_2) = 0 \tag{38}$$

$$\frac{J_1}{r_1^2} \frac{d^2 S_2}{dt^2} + k_1 (S_2 - S_1) + k_2 (S_2 - S_3) = 0 \tag{39}$$

$$\frac{J_3}{r_3^2} \frac{d^2 S_3}{dt^2} + k_2 (S_3 - S_2) + k_3 (S_3 - S_4) = 0 \tag{40}$$

$$\frac{J_4}{r_4^2} \frac{d^2 S_4}{dt^2} + k_3 (S_4 - S_3) + k_4 (S_4 - S_5) = 0 \tag{41}$$

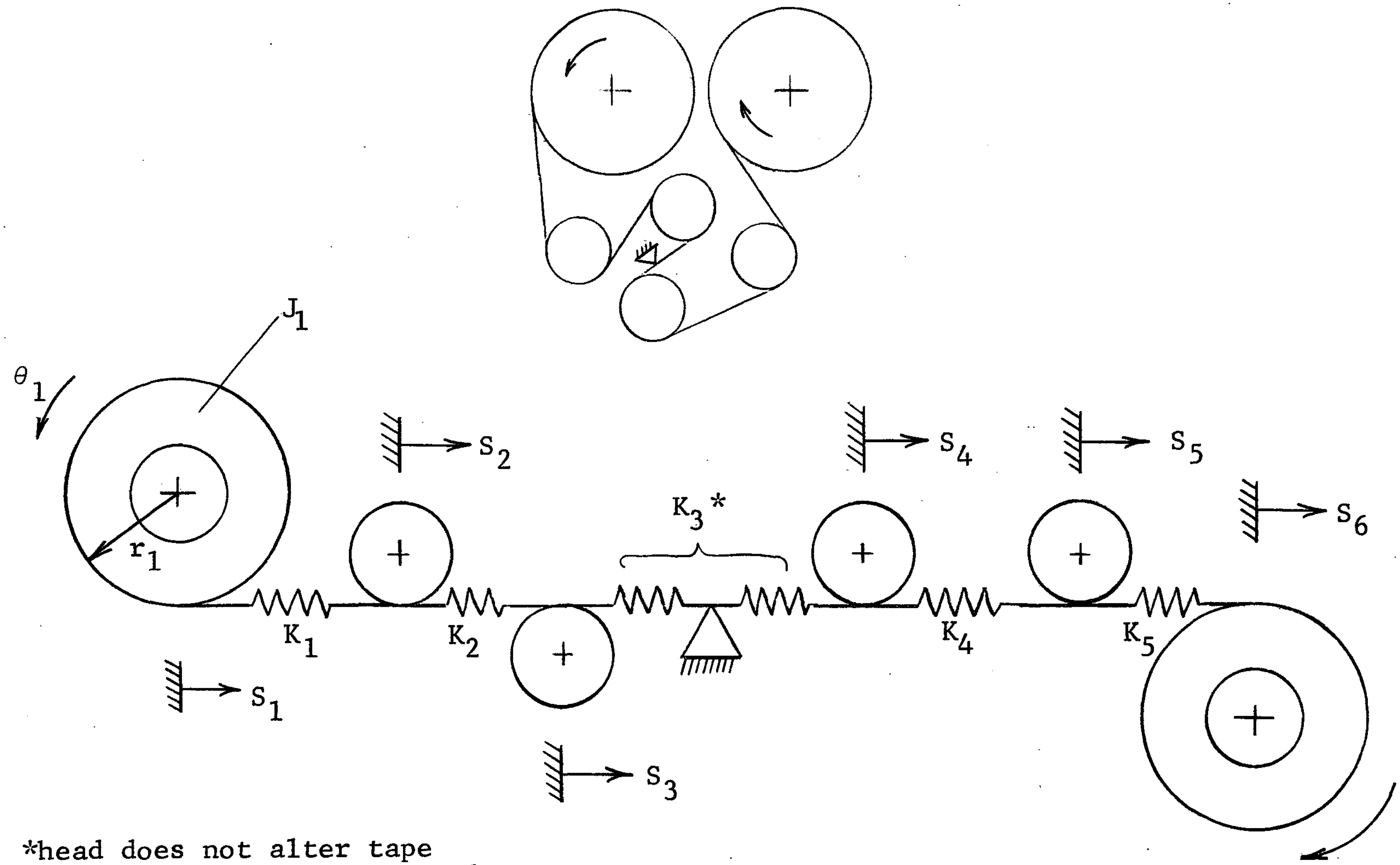

*head does not alter tape stiffness and hence natural frequency

Figure 34

NATURAL FREQUENCY MODEL

$$\frac{J_5}{r_5^2} \frac{d^2 S_5}{dt^2} + k_4 (S_5 - S_4) + k_5 (S_5 - S_6) = 0 \qquad (42)$$

$$\frac{J_6}{r_6^2} \frac{d^2 S_6}{dt^2} + k_5 (S_6 - S_5) = 0 \qquad (43)$$

The Holzer method was used to solve these equations of motion for the system natural frequencies. This method uses an assumed frequency to determine whether the resulting mode shape* satisfies the boundary conditions. (In this case the torque on the reels is zero.) If the trial frequency does not satisfy the boundary conditions, then a new trial frequency is selected. This selection process is made in an orderly manner on the basis of the residual calculated as a result of non-conformance of the mode shape to the boundary condition. Since the mode shape depends on a relative arrangement of the system components, the initial reel displacement is always assumed to be unity. The general recurrence relationship Equation 44, based on a steady state vibratory motion, is used to determine the mode shape as a function of trial frequency ω and system component inertia $\frac{J_i}{r_i^2}$ and tape elasticity k_i.

$$S_n = S_{n-1} - \frac{\omega^2}{k_{n-1}} \sum_{i=1}^{n-1} \frac{J_i}{r_i^2} S_i \qquad (44)$$

*Each system natural frequency has an associated mode shape that defines the relative positions of the components in the system while it is vibrating at the natural frequency.

where

S_n = nth Reel, Idler, Capstan displacement

The indicator which determines whether or not a trial frequency is a natural frequency is the residual function (Equation 45)

$$R = \sum_{i-1}^{n} S_i \frac{J_i}{r_i^2} \omega^2 \tag{45}$$

Natural frequencies are determined in an orderly manner by plotting residual, R, as a function of trial frequency, ω, Figure 35. The intersections of the curve yield the system natural frequencies. It is easy to grasp the amount of calculation necessary to determine each natural frequency. For this reason the natural frequency calculation is performed on the digital

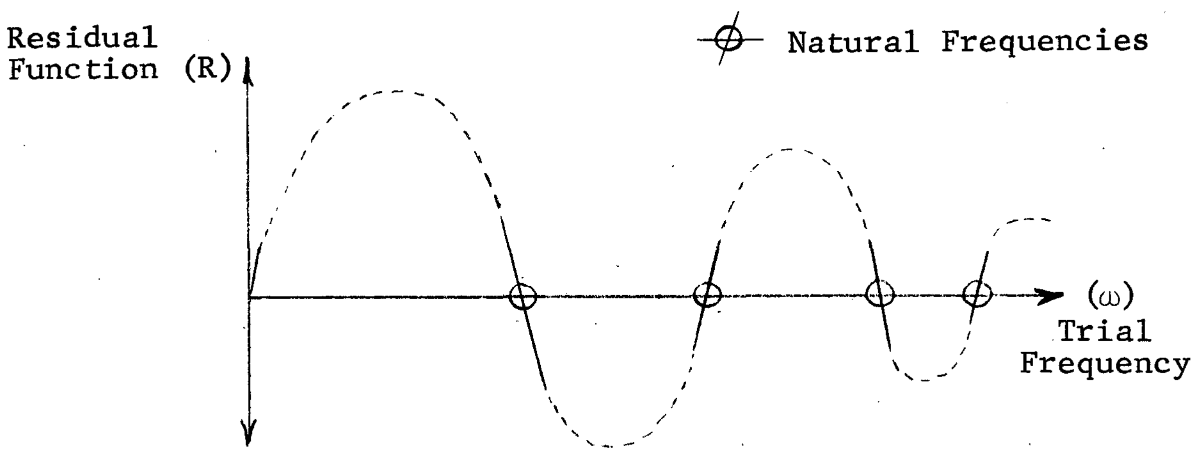

Figure 35

SOLUTION OF SYSTEM NATURAL FREQUENCIES (HOLZER METHOD)

computer. The flow diagram and computer program for the computation are shown in Figures 36 and 37. The computer program is problem oriented and therefore the relevant tape transport is simulated by using alternate input cards for a component and a tape length. The computer program use is described under computer documentation (Section 3.1.3).

3.1.2.2 Steady State Vibration Response

The mathematical model of the tape transport was used to simulate the steady state vibration response (displacements and velocities) of the tape at the transport components. Vibration disturbances generating this response are geometry errors in components size, bearing perturbational torques and any other disturbing forces or displacements. The vibration simulation model is problem oriented and therefore can be used to evaluate varied tape transport concepts. The concept is simulated on the computer by stacking the input cards in the order of concept arrangement.

Components such as reels, idlers and capstans are simulated as masses, the tape can have mass, damping and elasticity and damping is allowed between the components and ground. A general equation of motion (Equation 46) for any transport element was written.

$$\frac{J_n}{r_n}\frac{d^2S_n}{dt^2} + \frac{1}{r_n}(f_n + \beta_n)\frac{dS_n}{dt} + r_n(S_n - S_{n-1})k_{n-1} \qquad (46)$$

$$+ r_n(S_n - S_n + 1)k_n + r_n\left(\frac{dS_n}{dt} - \frac{dS_n}{dt} + 1\right)C_n = T_{ns}\sin N_n \frac{Vt}{r_n}$$

$$+ T_n \cos N_n \frac{Vt}{r_n}$$

where:

S_n = displacement of nth component, in

t = time

r_n = radius of nth component, in

J_n = polar moment of inertia of nth component, in-lb-sec^2

N_n = disturbance frequency

k_n = Spring constant of tape length between, lb/in n and n + 1 component

C_n = damping constant of tape between, lb-$\frac{sec}{in}$ n and n + 1 component.

f_n = damping constant from nth component and ground $\frac{in\text{-}lb\text{-}sec}{rad}$.

$B_n = \frac{K_T K_D}{R}$ = electric motor constants, $\frac{in\text{-}lb\text{-}sec}{rad}$

K_T = Torque sensitivity, lb-in/amp

K_B = Back cmf, volts $\frac{sec}{rad}$

T_{ns}, T_{nc} = Perturbational torque, in-lb

R = armature resistance, ohms

V = tape velocity

Harmonic motion (Equations 47-49) is assumed and a set of 2n algebraic equations that yield S_n as a function of the disturbance parameter result.

$$S_n = A_n \sin \omega_n t + B_n \text{Cos}\ \omega_n t \tag{47}$$

$$\frac{dS_n}{dt} = \omega_n (A_n \cos \omega_n t = B_n \sin \omega_n t) \tag{48}$$

$$\frac{d^2 S_n}{dt^2} = - \omega_n^2 S_n \tag{49}$$

where

$$\omega_n = \frac{VN_n}{r_n} \quad \text{disturbance frequency}$$

The algebraic equations are obtained by substituting Equations 47-49 in the equations of motion and equating sine and cosine terms. A representative set of these equations follow. Equation 50 comes from the sine terms and Equation 51 from the cosine terms.

$$- r_n k_{n-1} A_{n-1} + \left\{ r_n (k_{n-1} - k_n) - \frac{J_n \omega_n^2}{r_n} \right\} A_n \qquad (50)$$

$$- \left\{ \frac{\omega_n}{r_n} (f_n + \beta_n) + r_n C_n \omega_n \right\} B_n - r_n k_n A_{n+1} + r_n C_n \omega_n B_{n+1} = T_{ns}$$

$$- r_n k_{n-1} B_{n-1} + \left\{ r_n C_n \omega_n - \frac{\omega_n}{r_n} (f_n + \beta_n) \right\} A_n \qquad (51)$$

$$+ \left\{ r_n (k_{n-1} + k_n) - \frac{J_n \omega^2}{r_n} \right\} B_n - r_n C_n \omega A_{n+1} - r_n k_n B_{n+1} = T_{nc}$$

The set of simultaneous equations are formed on the computer according to the input data and solved on the computer for each input disturbance (frequency). The results (velocity at the head and other components) for each input disturbance are superimposed to obtain the total wow and flutter. Use of the computer program is described in the section on computation.

3.1.2.3 System Response

The mathematical simulation of the dynamics of the tape transport as it operates has been formulated for computer calculation. The equations of motion for each component as shown in the previous section are generalized in terms of the springs, masses, dampers, and motor constants that make up the transport. The motor voltages and torque perturbations are entered as input functions.

$$\frac{J_n}{r_n}\frac{dg_n}{dt} + \frac{1}{r_n} f_n g_n + r_n(S_n - S_{n-1})k_{n-1} \tag{52}$$

$$+ r_n(S_n - S_{n+1})k_n + r_n(g_n - g_{n+1})C_n = T_{ns}\sin \mu_n \frac{Vt}{r_n}$$

$$+ T_{nc}\cos \mu_n \frac{Vt}{r_n} + T_n$$

$$\frac{L_n}{K_{Tn}}\frac{dT_n}{dt} + \frac{R_n}{K_{Tn}} T_n + K_B \frac{g_n}{r_n} = V_n \tag{53}$$

$$\frac{dS_n}{dt} = g_n \tag{54}$$

where

g_n = tape velocity at components

T_n = component torque

V_n = armature voltage

L_n = armature inductance

J_n = $\frac{P\pi b}{2}(r_n^4(t) - r_o^4) + J\pi$

For idlers and heads equation 53 is not used and the torque term (T_n) in equation 52 is zero. The computer code (not complete at this time) for this dynamic simulation forms the concept through stacking of the cards. A set of n first order differential equations are obtained and solved with a Runge Kutta numerical integration routine.

3.1.3 Computation Program Documentation

Natural frequencies and vibration response of tape transport mechanical components (heads, idler, capstan, reel, and tape) are calculated on this tape transport dynamic simulation model (TTDSM). Natural frequency calculations are performed using the Holzer Method of calculation and the steady state vibration response is obtained through the use of a standard simultaneous equation solver.

The flow diagram for the complete computer program is shown in Figure 36. The computer program itself is shown in Figure 37 on pages 111 to 118. The simulation of a specific model transport is formed by proper sequencing of the data cards as shown in Figure 38. This is followed by the necessary documentation for the cards contained in such a data deck.

The use of this computer program is illustrated as an example for one specific problem on the five year high reliability tape transport. The first example is the derivation of the natural frequencies of the system. The input data for the natural frequency calculation is shown on page 123. The natural frequencies are obtained through a searching technque and therefore, the initial step size (delta) should be larger than 5.0 rad sec^{-1} and the starting frequency must be greater than zero. The searching technique ends either after the set number of frequencies or on the maximum frequency, while the error criterion is used to determine the natural frequency accuracy span. It should be noted that in these examples the tape mass is included and modeled in terms of an equivalent low inertia idler in the center of each system element. The resulting output data is shown in Figure 39 on page 127 where the natural frequency is given in hertz and the mode shape (theta) in radians.

The second illustrated example is that of the steady state vibrational response. The input data for this calculation is given on page 129 to 131. Here the forcing frequency (a single frequency forcing function is allowed per data set) is shown as ST.FREQ., the damping constant on each mechanical component as DRAG COEF, and the forcing function amplitudes (sine and cosine components to obtain proper phasing if required as PERT TORQ. Again the tape mass is modeled in terms of a equivalent low inertia idler in the center of each system element. The output data shown in Figures 40 and 41 on page 133 and 134 tabulates the response (i.e., displacement) at each component in the transport in terms of amplitude and phase angle and also shows the rms vibration velocity of each element of the transport.

FOLDOUT FRAME 1

FOLDOUT FRAME 2

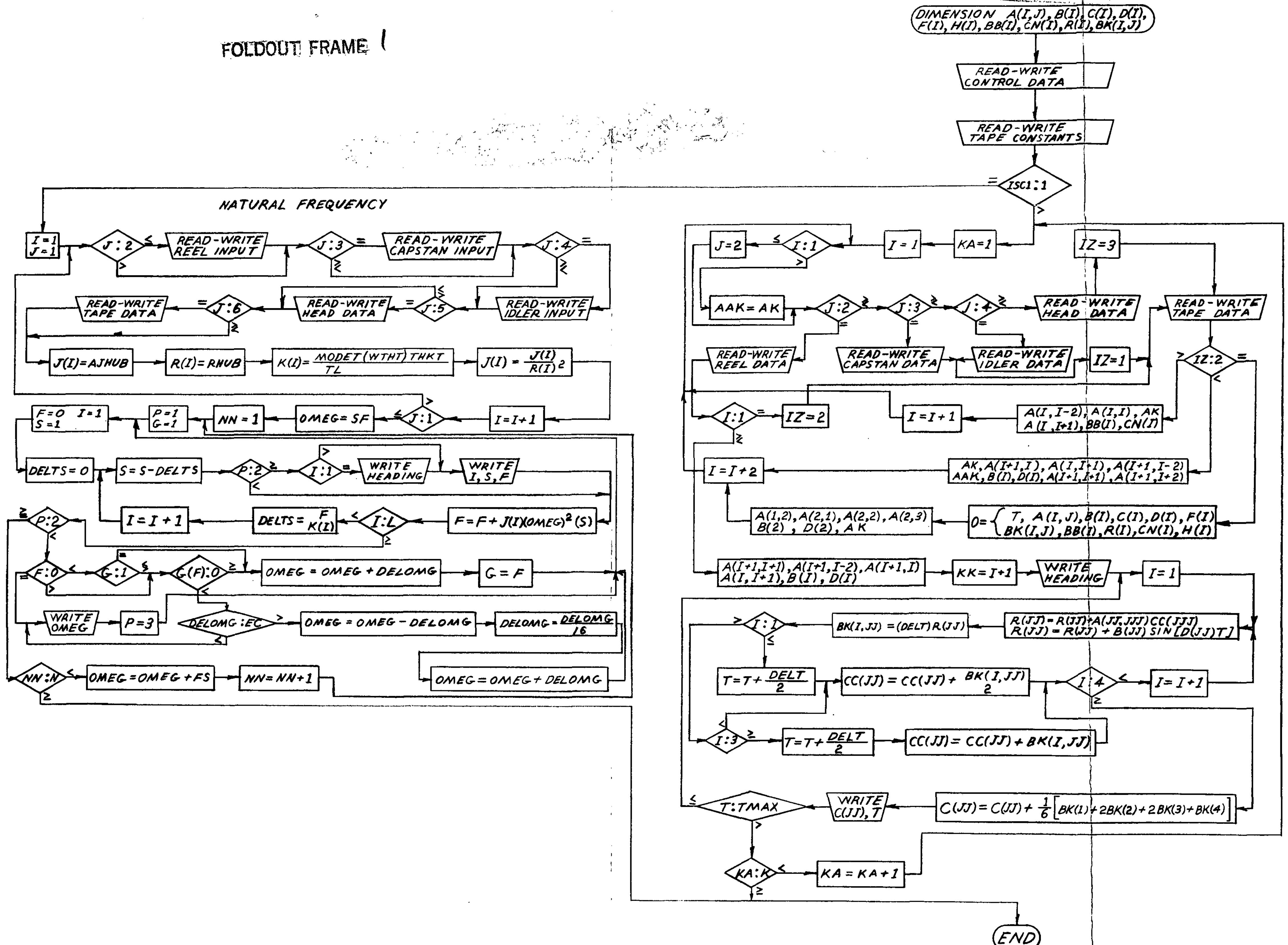

FIGURE 36 TAPE TRANSPORT DYNAMIC SIMULATION MODEL COMPUTER FLOW DIAGRAM

Preceding page blank

TAPE TRANSPORT DYNAMIC SIMULATION MODEL (TTDSM)

```
      DIMENSION A(25,25),B(25),C(25),D(25),TL(25)      ,BB(25),CN(25),R(2
     15),BK(25,25),AJ(25),AK(25),F(25),CC(25),         X(25),IR(25),JC(25
     2),XD(25,25)
      KA = 1
      DO 4 I=1,25,1
      DO 4 JJ=1,25,1
    4 XD(I,JI) = 0.0
    5 DO 761 I=1,25,1
      DO 760 JI=1,25,1
      A(I,JI)= 0.0
  760 BK(I,JI)= 0.0
      B(I) = 0.0
      BB(I) = 0.0
      C(I)= 0.0
      CC(I) = 0.0
      D(I) = 0.0
      IR(I) = 0.0
      JC(I) = 0.0
      F(I) = 0.0
      CN(I) = 0.0
      R(I) = 0.0
      TL(I) = 0.0
      AJ(I) = 0.0
      X(I) = 0.0
  761 AK(I) = 0.0
      REAL MODET
      READ (5,10) DELT,TMAX,AMT,EC,SF,N,K,ISC1,ISC2,FS,FL
   10 FORMAT ( 5E10.5, 4I3, E10.5,E8.3)
      READ (5,20) DENST,MODET,THKT,WTHT,V
   20 FORMAT ( 5E10.5 )
      WRITE (6,30) DELT,TMAX,AMT,EC,SF,N,K,ISC1,ISC2,FS,FL
   30 FORMAT (  19H1CONTROL INPUT DATA//7H DELTA=E10.5,5X6HT MAX=E10.5,5
     1X9HAMT.TAPE=E10.5,5X12HERROR CRIT.=E10.5,5X8HST.FREQ=E10.5/9H NO.F
     2REQ=I3,10X8HNO.SETS=I3,10X4HSC1=I3,17X4HSC2=I3,24X10HFREQ.INT.=E10
     3.5/15H MAX.FREQUENCY=E8.3/)
      WRITE (6,40) DENST,MODET,THKT,WTHT,V
   40 FORMAT (  16H TAPE INPUT DATA/ 9H DENSITY=E10.5,5X9HMOD.ELST=E10.5
     1,5X9HTHK,TAPE=E10.5,5X9HWTH,TAPE=E10.5,5X9HTAPE VEL=E10.5/)
      WRITE (6,50)
   50 FORMAT (  26H TAPE TRANSPORT INPUT DATA /)
      IF ( ISC1 - 2 )  55, 486, 1486
   55 I = 1
      J = 1
   60 JCC = 1
      IF ( J - 2 ) 70, 70, 100
```

Figure 37

TTDSM COMPUTER PROGRAM

```
   70 READ (5,80) J,AJHUB,RHUB,FDRAG,TS,TC,AKD,RA,VA,M,NA
   80 FORMAT (I1,8E9.4,I1,I3)
      WRITE (6,90) J,AJHUB,RHUB,FDRAG,TS,TC,AKD,RA,VA,M,NA
   90 FORMAT(11H REEL,CODE=I1,2X10HINERT.HUB=E9.4,2X6HR,HUB=E9.4,2X10HDR
     1AG COEF=E9.4,2X13HPERT,TORQ(S)=E9.4,2X13HPERT,TORQ(C)=E9.4/6X5HFLU
     2X=E9.4,2X7HRESIST=E9.4,2X6HVOLTS=E9.4,2X6HPT,CD=I1,2X3HNA=I3//)
  100 IF ( J - 3) 140, 110, 140
  110 READ (5,120) J,AJHUB,RHUB,FDRAG,TS,TC,AKD,RA,VA,M,NA
  120 FORMAT (I1,8E9.4,I1,I3)
      WRITE (6,130) J,AJHUB,RHUB,FDRAG,TS,TC,AKD,RA,VA,M,NA
  130 FORMAT  (14H CAPSTAN,CODE=I1,2X10HINERT.HUB=E9.4,2X6HR.HUB=E9.4,2X
     110HDRAG COEF=E9.4,2X13HPERT,TORQ(S)=E9.4,2X13HPERT.TORQ(C)=E9.4/6X
     25HFLUX=E9.4,2X7HRESIST=E9.4,2X6HVOLTS=E9.4,2X6HPT,CD=I1,2X3HNA=I3/
     3/)
      IF ( J - 7 ) 140, 71, 140
   71 READ (5,72) J,BJHUB,GR
   72 FORMAT ( I1,2E9.4 )
      WRITE (6,73) J,BJHUB,GR
   73 FORMAT ( 22H CAPSTAN REDUCER,CODE=I1,10H  INERTIA=E9.4,13H  GEAR R
     1ATIO=E9.4//)
  140 IF ( J - 4) 180, 150, 180
  150 READ (5,160) J,AJHUB ,RHUB,FDRAG,TS,TC,AKD,RA,VA,M,NA
  160 FORMAT ( I1,8E9.4,I1,I3)
      WRITE (6,170) J,AJHUB,RHUB,FDRAG,TS,TC,M,NA
  170 FORMAT (12H IDLER,CODE=I1,2X10HINERT.HUB=E9.4,2X6HR.HUB=E9.4,2X10H
     1DRAG COEF=E9.4,2X13HPERT.TORQ(S)=E9.4,2X13HPERT.TORQ(C)=E9.4/2X6HP
     2T.CD=I1,2X3HNA=I3//)
  180 IF ( J - 5 ) 220, 190, 220
  190 READ (5,200) J,F0,F1,CNN,M
  200 FORMAT ( I1,3E9.4,I1 )
      WRITE (6,210) J,F0,F1,CNN,M
  210 FORMAT (11H HEAD,CODE=I1,2X11HSTAT.FRICT=E9.4,2X10HDYN.FRICT=E9.4,
     12X14HDYN.FRICT.(N)=E9.4,2X6HPT.CD=I1//)
      JCC = 4
      BA = TL(I-1)
  220 IF ( J - 6 ) 260, 230, 260
  230 READ (5,240) J,TLL,M
  240 FORMAT ( I1,E9.4,I1 )
      WRITE (6,250) J,TLL,M
  250 FORMAT (11H TAPE,CODE=I1,2X10HTAPE LGTH=E9.4,2X6HPT.CD=I1//)
      TL(I) = TLL
      IF (JCC - 4 ) 260, 255, 260
  255 TL(I-1)=TL(I)+BA
      AK(I-1) = ( MODET*THKT*WTHT ) / TL(I-1)
      GO TO 60
  260 AJ(I) = AJHUB + ( BJHUB*(GR**2.0))
      BJHUB = 0.0
      GR = 0.0
      R(I) = RHUB
      IF ( J - 1 ) 262,262, 261
  261 AK(I) = ( MODET*THKT*WTHT ) / TL(I)
  262 AJ(I) = AJ(I) / ( R(I)**2.0)
      L = I
      I = I + 1
      IF ( J - 1 ) 270, 270, 60
  270 OMEG = SF
      NN = 1
  280 G = 1.0
      DELOMG = DELT
      IP = 1
```


Figure 37 (Cont.)

```
  290 FA= 0.0
      S = 1.0
      DELTS = 0.0
      I = 1
  300 S = S - DELTS
      IF ( IP - 2 ) 360, 310, 310
  310 IF ( I  - 1 ) 340, 320, 340
  320 WRITE (6,330)
  330 FORMAT ( 30H NATURAL FREQUENCY CALCULATION// 9H  STATION,5X10HTHET
     1A(RAD),5X13HTORQUE(IN-LB)//)
  340 THE = S / R(I)
      WRITE (6,350) I,THE,FA
  350 FORMAT ( 7H          I2,5XE10.4,5XE10.4 )
  360 FA= FA+ AJ(I)*(OMEG**2.0)*S
      IF ( I - L ) 370, 380, 380
  370 DELTS = FA/ AK(I)
      I = I + 1
      GO TO 300
  380 IF ( IP - 2 ) 390, 470, 470
  390 IF ( FA-0.0) 400, 430, 410
  400 IF ( G - 1.0 ) 410, 420, 410
  410 AA = G * FA
      IF ( AA -0.0) 450, 420, 420
  420 OMEG = OMEG + DELOMG
      G = FA
      GO TO 290
  430 AOMEG = OMEG / 6.28318
      WRITE (6,440) NN,AOMEG
  440 FORMAT ( 22H1NATURAL FREQUENCY NO.I3,2H =E10.5,3H HZ//)
      IP = 3
      GO TO 290
  450 IF ( DELOMG - EC ) 430, 460, 460
  460 OMEG = OMEG - DELOMG
      DELOMG = DELOMG / 16.0
      OMEG = OMEG + DELOMG
      GO TO 290
  470 IF ( NN - N ) 4800,481, 481
 4800 IF ( OMEG - FL ) 480, 481, 481
  480 OMEG = OMEG + FS
      NN = NN + 1
      GO TO 280
  481 IF ( KA - K ) 482, 10000, 10000
  482 KA = KA + 1
      GO TO 5
  486 I = 1
  490 IF ( I - 1 ) 495, 495, 500
  495 J = 2
      GO TO 505
  500 AAK = AK(I-2)
  505 IF ( J - 2 ) 540, 510, 540
  510 READ (5,520)J,AJHUB,RHUB,FDRAG,TS,TC,AKD,RA,VA,M,NA
  520 FORMAT (I1,8E9.4,I1,I3)
      WRITE (6,530)J,AJHUB,RHUB,FDRAG,TS,TC,AKD,RA,VA,M,NA
  530 FORMAT(11H REEL,CODE=I1,2X10HINERT,HUB=E9.4,2X6HR,HUB=E9.4,2X10HDR
     1AG COEF=E9.4,2X13HPERT.TORQ(S)=E9.4,2X13HPERT.TORQ(C)=E9.4/6X5HFLU
     2X=E9.4,2X7HRESIST=E9.4,2X6HVOLTS=E9.4,2X6HPT.CD=I1,2X3HNA=I3//)
      IF (I - 1 ) 780, 660, 780
  540 IF ( J - 3) 580, 550, 580
  550 READ (5,560)J,AJHUB,RHUB,FDRAG,TS,TC,AKD,RA,VA,M,NA
  560 FORMAT (I1,8E9.4,I1,I3)
```


Figure 37 (Cont.)

```
      WRITE (6,570)J,AJHUB,RHUB,FDRAG,TS,TC,AKD,RA,VA,M,NA
  570 FORMAT  (14H CAPSTAN,CODE=I1,2X10HINERT.HUB=E9.4,2X6HR.HUB=E9.4,2X
     110HDRAG COEF=E9.4,2X13HPERT.TORQ(S)=E9.4,2X13HPERT.TORQ(C)=E9.4/6X
     25HFLUX=E9.4,2X7HRESIST=E9.4,2X6HVOLTS=E9.4,2X6HPT.CD=I1,2X3HNA=I3/
     3/)
      GO TO 670
  580 IF ( J - 4 ) 630, 590, 630
  590 READ (5,600)J,AJHUB,RHUB,FDRAG,TS,TC,AKD,RA,VA,M,NA
  600 FORMAT ( I1,8E9.4,I1,I3)
      WRITE (6,610)J,AJHUB,RHUB,FDRAG,TS,TC,M,NA
  610 FORMAT (12H IDLER,CODE=I1,2X10HINERT.HUB=E9.4,2X6HR.HUB=E9.4,2X10H
     1DRAG COEF=E9.4,2X13HPERT.TORQ(S)=E9.4,2X13HPERT.TORQ(C)=E9.4/5X6HP
     2T.CD=I1,2X3HNA=I3//)
      GO TO 670
  630 READ (5,640) J,FO,F1,CNN,M
  640 FORMAT ( I1,3E9.4,I1)
      WRITE (6,650) J,FO,F1,CNN,M
  650 FORMAT (11H HEAD,CODE=I1,2X11HSTAT.FRICT=E9.4,2X10HDYN.FRICT=E9.4,
     12X14HDYN.FRICT.(N)=E9.4,2X6HPT.CD=I1//)
      IZ = 3
      GO TO 700
  660 IZ = 2
      GO TO 700
  670 IZ = 1
  700 READ (5,710) J,TLL,M
  710 FORMAT ( I1,E9.4,I1 )
      WRITE (6,720) J,TLL,M
  720 FORMAT (11H TAPE,CODE=I1,2X10HTAPE LGTH=E9.4,2X6HPT.CD=I1//)
      TL(I) = TLL
      IF ( IZ - 2 ) 730, 750, 740
  730 AK(I)=((MODET * THKT* WTHT) / TL(I))
      A(I,I+1) = 1.0
      A(I+1,I-2) = (( AAK)*( RHUB**2.0)) / AJHUB
      A(I+1,I) = (-1.0)*(( RHUB**2.0)/ AJHUB)* ( AAK + AK(I))
      A(I+1,I+1) =((-1.0)/AJHUB) * ( FDRAG + ((AKD**2.0) /RA ))
      A(I+1,I+2) =  ((RHUB**2.0)/AJHUB )*AK(I)
      B(I) = (TS* RHUB)/ AJHUB
      D(I) = (NA* V ) /RHUB
      GO TO 770
  740 AK(I)=((MODET *THKT* WTHT) / TL(I))
      A(I,I-2) = AAK / F1
      A(I,I) =  (AK(I)-AAK ) / F1
      A(I,I+1) =  -AK(I) / F1
      BR(I) = -FO / F1
      CN(I) = CNN
      AAK = AK(I)
      I = I + 1
      GO TO 505
  750 I = 1
      T = 0.0
      AK(I)=((MODET * THKT * WTHT) / TL(I))
      A(1,2) = 1.0
      A(2,1) =  (-1.0)*(( RHUB**2.0) / AJHUB)* AK(I)
      A(2,2) = (-1.0 / AJHUB)* ( FDRAG + (( AKD**2.0 ) / RA))
      A(2,3) = (-1.0)* A(2,1)
      B(2) = ( TS* RHUB) / AJHUB
      D(2) = ( NA* V ) / RHUB
  770 I = I +2
      GO TO 490
  780 A(I,I+1) = 1.0
```

Figure 37 (Cont.)

```
      A(I+1,I-2)=  ( AAK* (RHUB**2.0)) / AJHUB
      A(I+1,I) = (-1.0)* ((RHUB**2.0) / AJHUB ) * AAK
      A(I+1,I+1) = ( -1.0/AJHUB) *  ( FDRAG + (( AKD**2.0) / RA ))
      B(I) = ( TS* RHUB) / AJHUB
      D(I) = ( NA * V ) / RHUB
      KK = I +1
      WRITE (6,785)
  785 FORMAT ( 23H1FORCED RESPONSE OUTPUT//)
  790 I = 1
  795 DO 810 JJ=1,KK,1
      IF ( BB(JJ) - 0.0 ) 796, 7988, 796
  796 IF ( R(JJ) - 0.0 ) 798, 7989, 7988
 7989 ABB = 0.0
      GO TO 799
  798 ABB = -1.0*BB(JJ)
      GO TO 799
 7988 ABB = BB(JJ)
  799 DO 800 JJJ=1,KK,1
  800 R(JJ) = R(JJ) + A(JJ,JJJ)*CC(JJJ)
      R(JJ) = R(JJ) + B(JJ)*( SIN( D(JJ)*T)) + ABB
  810 CONTINUE
      DO 820 JJ=1,KK,1
      BK(I,JJ) = DELT * R(JJ)
  820 CONTINUE
      IF ( I - 1 ) 830, 830, 860
  830 T = T + ( DELT / 2.0 )
  840 DO 850 JJ=1,KK,1
  850 CC(JJ) = CC(JJ) + ( BK(I,JJ) / 2.0 )
      GO TO 890
  860 IF ( I - 3 ) 840,870,900
  870 T = T + ( DELT / 2.0 )
      CC(JJ) = CC(JJ) + BK(I,JJ)
  890 I = I + 1
      GO TO 795
  900 DO 940 JJ=1,KK,1
      I = 1
  910 C(JJ) = C(JJ) + (1.0 /6.0)*(  BK(I,JJ) +(2.0*BK(I+1,JJ))+(2.0*BK(I
     1+2,JJ)) + BK(I+3,JJ))
      IF ( JJ- 1 ) 920, 920, 931
  920 WRITE (6,930) T,C(JJ)
  930 FORMAT ( 6H TIME=E10.4,5X9HRESPONSE=E10.4//)
      GO TO 940
  931 WRITE (6,932) JJ,C(JJ)
  932 FORMAT ( 4H JJ=I3,2X6HC(JJ)=E10.4)
  940 CONTINUE
      IF ( T - TMAX ) 790, 790, 1000
 1000 IF ( KA - K ) 1010, 10000, 10000
 1010 KA = KA + 1
      GO TO 5
 1486 I = 1
 1490 IF ( I - 1 ) 1495, 1495, 1500
 1495 J = 2
      GO TO 1505
 1500 AAK = AK(I-2)
      CCH = CH
 1505 IF ( J - 2 ) 1540, 1510, 1540
 1510 READ (5,1520)J,AJHUB,RHUB,FDRAG,TS,TC,AKD,RA,VA,M,NA
 1520 FORMAT (I1,8E9.4,I1,I3)
      WRITE (6,1530)J,AJHUB,RHUB,FDRAG,TS,TC,AKD,RA,VA,M,NA
 1530 FORMAT(11H REEL,CODE=I1,2X10HINERT,HUB=E9.4,2X6HR,HUB=E9.4,2X10HDR
```

Figure 37 (Cont.)

```
     1AG COEF=E9.4,2X13HPERT.TORQ(S)=E9.4,2X13HPERT.TORQ(C)=E9.4/6X5HFLU
     1X=E9.4,2X7HRESIST=E9.4,2X6HVOLTS=E9.4,2X6HPT.CD=I1,2X3HNA=I3//)
      IF (I - 1 ) 1780, 1660, 1780
 1540 IF ( J - 3) 1580, 1550, 1580
 1550 READ (5,1560)J,AJHUB,RHUB,FDRAG,TS,TC,AKD,RA,VA,M,NA
 1560 FORMAT (I1,8E9.4,I1,I3)
      WRITE (6,1570)J,AJHUB,RHUB,FDRAG,TS,TC,AKD,RA,VA,M,NA
 1570 FORMAT  (14H CAPSTAN,CODE=I1,2X10HINERT.HUB=E9.4,2X6HR.HUB=E9.4,2X
     110HDRAG COEF=E9.4,2X13HPERT.TORQ(S)=E9.4,2X13HPERT.TORQ(C)=E9.4/6X
     25HFLUX=E9.4,2X7HRESIST=E9.4,2X6HVOLTS=E9.4,2X6HPT.CD=I1,2X3HNA=I3/
     3/)
      IF ( J - 7 ) 1670, 1571, 1670
 1571 READ (5,1572) J,BJHUB,GR,BFDRAG,BAKD,BRA
 1572 FORMAT ( I1,5E9.4 )
      WRITE (6,1573) J,BJHUB,GR,BFDRAG,BAKD,BRA
 1573 FORMAT ( 22H CAPSTAN REDUCER,CODE=I1,10H  INERTIA=E9.4,13H  GEAR R
     1ATIO=E9.4,12H  DRAG COEF=E9.4,7H  FLUX=E9.4,13H  RESISTANCE=E9.4//
     2)
      BSF = SF * GR
      GR = 0.0
      GO TO 1670
 1580 IF ( J - 4 ) 1630, 1590, 1630
 1590 READ (5,1600)J,AJHUB,RHUB,FDRAG,TS,TC,AKD,RA,VA,M,NA
 1600 FORMAT ( I1,8E9.4,I1,I3)
      WRITE (6,1610)J,AJHUB,RHUB,FDRAG,TS,TC,M,NA
 1610 FORMAT (12H IDLER,CODE=I1,2X10HINERT.HUB=E9.4,2X6HR.HUB=E9.4,2X10H
     1DRAG COEF=E9.4,2X13HPERT.TORQ(S)=E9.4,2X13HPERT.TORQ(C)=E9.4/5X6HP
     2T.CD=I1,2X3HNA=I3//)
      GO TO 1670
 1630 READ (5,1640)J,F0,F1,CNN,M
 1640 FORMAT ( I1,3E9.4,I1)
      WRITE (6,1650)J,F0,F1,CNN,M
 1650 FORMAT (11H HEAD,CODE=I1,2X11HSTAT.FRICT=E9.4,2X10HDYN.FRICT=E9.4,
     12X14HDYN.FRICT.(N)=E9.4,2X6HPT.CD=I1//)
      IZ = 3
      GO TO 1700
 1660 IZ = 2
      GO TO 1700
 1670 IZ = 1
 1700 READ (5,1710)J,TLL,M,CH
 1710 FORMAT ( I1,E9.4,I1,E9.4)
      WRITE (6,1720)J,TLL,M,CH
 1720 FORMAT (11H TAPE,CODE=I1,2X10HTAPE LGTH=E9.4,2X6HPT.CD=I1,2X11HHEA
     1D COEF.=E9.4//)
      IF ( J - 5 ) 1725, 1721, 1725
 1721 TTL = TLL
      GO TO 1630
 1725 TLL = TLL + TTL
      TTL = 0.0
      IF ( IZ - 2 ) 1730, 1750, 1730
 1750 AK(I) = (( MODET* THKT* WTHT) / TLL)
      A(1,1) = ( RHUB*AK(I))-((AJHUB* ( SF**2.0)) /RHUB)
      BETA = (( AKD**2.0) / RA)
      A(1,2) = ((-SF/RHUB) * ( FDRAG+BETA ))-( RHUB*CH* SF)
      A(1,3) = (-AK(I)* RHUB)
      A(2,1) = -A(1,2)
      A(2,2) = A(1,1)
      A(2,4) =  A(1,3)
      B(1) = TS
      B(2) = TC
```

Figure 37 (Cont.)

```
      A(1,4) = ( RHUB*CH* SF)
      A(2,3) = -A(1,4)
      I = I + 2
      GO TO 1490
 1730 AK(I) = (( MODET*THKT* WTHT) / TLL)
      A(I,I) = RHUB*(AAK+AK(I))-(( AJHUB*(SF**2.0)) / RHUB)-((BJHUB*(BSF
     1**2.0))/RHUB)
      BJHUB = 0.0
      A(I+1,I+1) = A(I,I)
      A(I,I-2) = -RHUB*AAK
      A(I,I-1) = RHUB*CCH*SF
      BETA = (( AKD**2.0) / RA)
      BBETA = (( BAKD**2.0) / BRA)
      A(I,I+1)= (-1.0)*((SF/RHUB)*(FDRAG+BETA ) +(RHUB*(CH+CCH)*SF) +
     1(( BSF**2.0) / RHUB) * ( BFDRAG + BBETA))
      BSF = 0.0
      BAKD = 0,0
      BRA = 0.0
      BBETA = 0.0
      BFDRAG = 0.0
      A(I,I+2) = -RHUB*AK(I)
      A(I,I+3) = RHUB*CH*SF
      A(I+1,I) = -A(I,I+1)
      A(I+1,I-2) = -A(I,I-1)
      A(I+1,I-1) = A(I,I-2)
      A(I+1,I+2) = -A(I,I+3)
      A(I+1,I+3) = A(I,I+2)
      B(I) = TS
      B(I+1) = TC
      I = I + 2
      GO TO 1490
 1780 A(I,I-2) = -RHUB*AAK
      A(I,I-1) = RHUB*CCH*SF
      A(I,I) = (RHUB*AAK) - ((AJHUB* (SF**2.0)) / RHUB)
      BETA = (( AKD**2.0) / RA)
      A(I,I+1) = (-1.0)*((( FDRAG + BETA) /RHUB) +CCH)*SF
      A(I+1,I-2) = -A(I,I-1)
      A(I+1,I-1) = A(I,I-2)
      A(I+1,I) = -A(I,I+1)
      A(I+1,I+1) = A(I,I)
      B(I) = TS
      B(I+1) = TC
      KK = I + 1
      NMAX = 25
      ESP1 = 1,0
      N = KK
      DO 1971 JJ=1,KK,1
 1971 A(JJ,KK+1) = B(JJ)
      CALL LSIMEQ(A,NMAX,IR,JC,N,ESP1,X,IERR1)
      WRITE (6,1975) KA
 1975 FORMAT ( 8H1SET NO.I3,16H RESPONSE OUTPUT    //)
      DO 1810 JJ=1,KK,2
      ARES = ((  X(JJ)**2.0) + (  X(JJ+1)**2.0))**0,5
      PHA = ATAN(   X(JJ) /   X(JJ+1))
      WRITE (6,1800) JJ,X(JJ)
 1800 FORMAT ( 12H ELEMENT NO.I3,5X9HRESPONSE=E10.5,1X6HINCHES)
      JZ = JJ+1
      WRITE (6,1801) JZ,X(JZ),ARES,PHA
 1801 FORMAT ( 12H ELEMENT NO.I3,5X9HRESPONSE=E10.5,1X6HINCHES,5X19HRESP
     1ONSE AMPLITUDE=E10.5,1X6HINCHES,5X6HPHASE=F9.4,1X4HRAD./)
```

Figure 37 (Cont.)

```
          XD(KA,JJ) = SF * ARES
     1810 CONTINUE
          IF ( KA - K ) 1820, 1830, 1830
     1820 KA = KA + 1
          GO TO 5
     1830 WRITE (6,1831)
     1831 FORMAT ( 29H1TOTAL FORCED RESPONSE OUTPUT //)
          DO 1860 JJ=1,KK,2
          DO 1850 KA=1,K,1
     1850 AVEL = AVEL + XD(KA,JJ)**2.0
          VEL = ( AVEL**0.5)
          JZ = JJ+1
          WRITE (6,1851) JJ,JZ,VEL
     1851 FORMAT (   9H ELEMENT(I2,1H-I2,1H),5X9HVELOCITY=E10.5,9H IN./SEC./)
          AVEL = 0.0
          VEL = 0.0
     1860 CONTINUE
    10000 END

 END OF UCC 1108 FORTRAN V COMPILATION.      0 *DIAGNOSTIC* MESSAGE(S)
```

Figure 37 (Cont.)

TTDSM: Tape Transport Dynamic Simulation Model

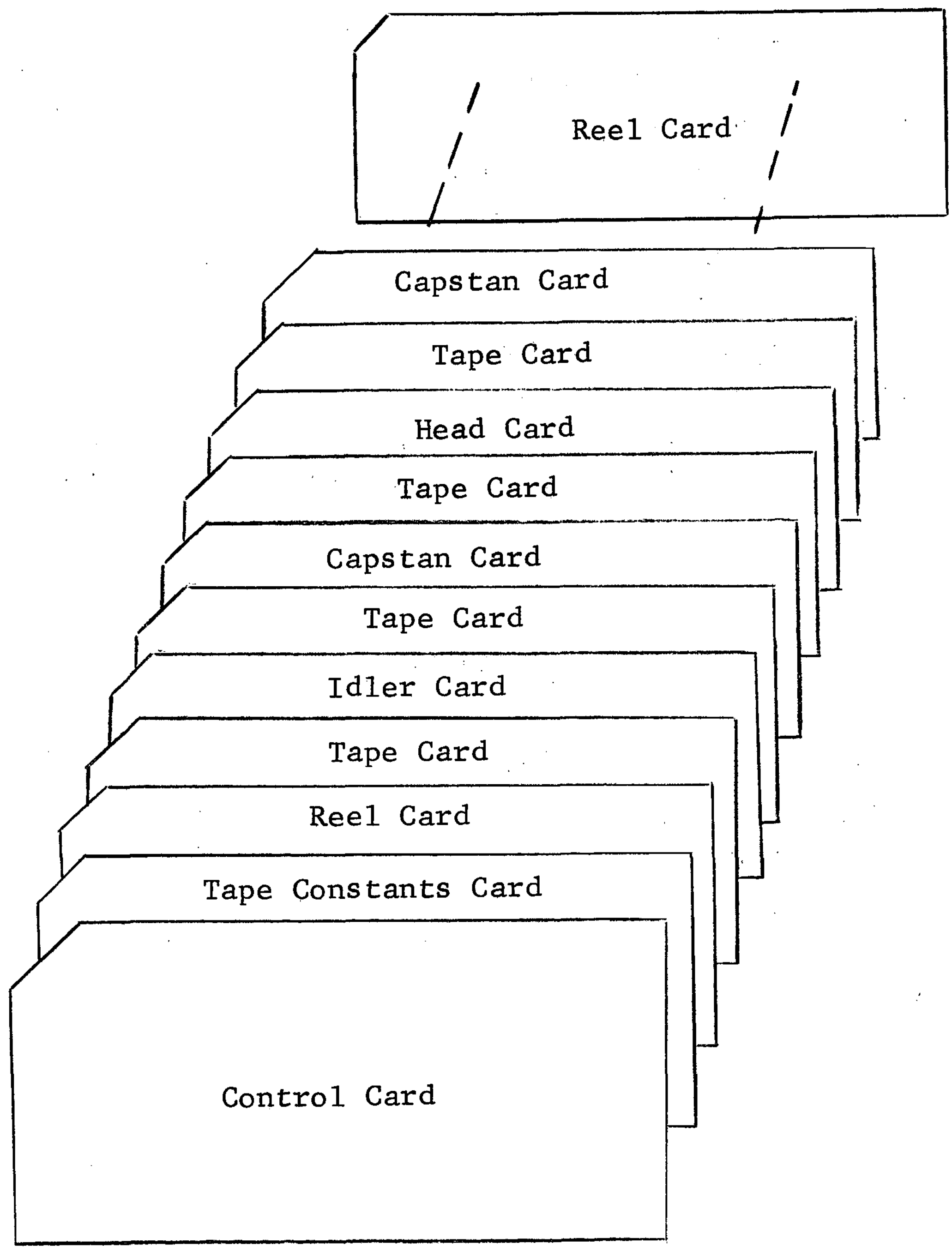

Figure 38

TTDSM INPUT DATA

CONTROL CARD

Code	Nomenclature	Field	Format	Units
DELT	Frequency Step Size	1-10	E10.5	Rad/sec
	Blank	11-20		
	Blank	21-30		Feet
EC	Error Criterion	31-40	E10.5	Rad/sec
SF	Starting Frequency	41-50	E10.5	Rad/sec
N	Number of Frequency	51-53	I3	
K	Number of Data Sets	54-56	I3	
ISC1	Switch 1	57-59	I3	Note 1
	Blank	60-62		
FS	Frequency Interval	63-72	E10.5	Rad/sec
FL	Maximum Frequency	73-80	E8.3	Rad/sec

Note 1: ISC1 = 1 for natural frequency calculation
ISC1 = 3 for linear forced response calculation

TAPE CONSTANTS CARD

Code	Nomenclature	Field	Format	Units
DENST	Tape Density	1-10	E10.5	lb/in
MODET	Modulus of Elasticity	11-20	E10.5	lb/in
THKT	Thickness	21-30	E10.5	in
WTHT	Width	31-40	E10.5	in
V	Tape Velocity	41-50	E10.5	in/sec

REEL, CAPSTAN, AND IDLER CARDS

Code	Nomenclature	Field	Format	Units
J	Next Element*	1	I1	
AJHUB	Inertia	2-10	E9.4	lb/in/sec
RHUB	Radius	11-19	E9.4	in
FDRAG	Drag Coefficient	20-28	E9.4	lb/in/sec
TS	Torque Perturbation (sine)	29-37	E9.4	in/lb
TC	Torque Perturbation (cosine)	38-46	E9.4	in/lb
AKD**	Flux	47-55	E9.4	
RA**	Resistance	56-64	E9.4	Ohms
VA**	Voltage	65-73	E9.4	Volts
M	Linear Subroutine Code	74	I1	
NA	Perturbation Ratio	75-77	I3	

---

*Next Element Code. Each of the following input cards requires a "next element" code to inform the computer of what type of data is to be read from the following card. The following integers are entered in the first data field column "J".

Enter J=1 to end reading

Enter J=2 if next element is a reel

Enter J=3 if next element is a capstan

Enter J=4 if next element is an idler

Enter J=5 if next element is a head

Enter J=6 if next element is a tape

Enter J=7 if next element is a reducer

The program assumes that the first card after the control and tape constant cards will be a reel.

**Equal to +0.0000 + 00 for idlers

$$\text{Flux} = \sqrt{K_T\ K_B}$$

where: K_T = torque senstivity $\left(\frac{\text{in-oz}}{\text{amp}}\right)$

K_B = back EMF $\left(\frac{\text{volts-sec}}{\text{rad}}\right)$

TAPE CARD

Code	Nomenclature	Field	Format	Units
J	Next Element	1	I1	
TLL	Tape Length	2-10	E9.4	in
M	Linear Subroutine Code	11	I1	
CH	Head Constant	12-20	E9.4	lb/sec/in

HEAD CARD

Code	Nomenclature	Field	Format	Units
J	Next Element	1	I1	
FO	Static Friction	2-10	E9.4	lb
F1	Dynamic Friction	11-19	E9.4	lb/sec/in
CNN	Dynamic Friction (μ)	20-28	E9.4	
M	Linear Subroutine Code	29	I1	

LOW SPEED CAPSTAN REDUCER

Code	Nomenclature	Field	Format	Units
J	Next Element	1	I1	
BJHUB	Inertia	2-10	E9.4	lb/in/sec
GR	Gear Ratio	11-19	E9.4	C:1
BFDRAG	Drag Coefficient	20-28	E9.4	in/lb/sec
BKD	Flux	29-37	E9.4	
BRA	Resistance	38-46	E9.4	Ohms

FOLDOUT FRAME 1

FOLDOUT FRAME #2

CONTROL INPUT DATA

DELTA= .50000+01 T MAX= .70000-00 AMT.TAPE= .12000+04 ERROR CRIT.= .10000+01 ST.FREQ= .50000+01
NO.FREQ= 10 NO.SETS= 1 SC1= 1 SC2= 0 FREQ.INT.= .00000
MAX.FREQUENCY= .400+04

TAPE INPUT DATA
DENSITY= .50000-01 MOD.ELST= .65000+06 THK.TAPE= .10000-02 WTH.TAPE= .50000-00 TAPE VEL= .15000+01

TAPE TRANSPORT INPUT DATA

REEL,CODE=6 INERT.HUB= .8141-02 R.HUB= .2532+01 DRAG COEF= .3820-02 PERT.TORQ(S)= .1130-02 PERT.TORQ(C)= .0000
FLUX= .5880+01 RESIST= .6000+02 VOLTS= .0000 PT.CD=1 NA= 1

TAPE,CODE=4 TAPE LGTH= .1688+01 PT.CD=1

IDLER,CODE=6 INERT.HUB= .2183-06 R.HUB= .1000+01 DRAG COEF= .0000 PERT.TORQ(S)= .0000 PERT.TORQ(C)= .0000
PT.CD=1 NA= 1

TAPE,CODE=4 TAPE LGTH= .1688+01 PT.CD=1

IDLER,CODE=6 INERT.HUB= .8530-04 R.HUB= .7500-00 DRAG COEF= .6960-03 PERT.TORQ(S)= .0000 PERT.TORQ(C)= .0000
PT.CD=1 NA= 1

TAPE,CODE=4 TAPE LGTH= .2000+01 PT.CD=1

IDLER,CODE=6 INERT.HUB= .2590-06 R.HUB= .1000+01 DRAG COEF= .0000 PERT.TORQ(S)= .0000 PERT.TORQ(C)= .0000
PT.CD=1 NA= 1

TAPE,CODE=3 TAPE LGTH= .2000+01 PT.CD=1

CAPSTAN,CODE=6 INERT.HUB= .9140-04 R.HUB= .6250-00 DRAG COEF= .5800-03 PERT.TORQ(S)= .0000 PERT.TORQ(C)= .0000
FLUX= .1040+01 RESIST= .4000+02 VOLTS= .0000 PT.CD=1 NA= 1

TAPE,CODE=4 TAPE LGTH= .1600+01 PT.CD=1

IDLER,CODE=6 INERT.HUB= .2075-06 R.HUB= .1000+01 DRAG COEF= .2000-02 PERT.TORQ(S)= .0000 PERT.TORQ(C)= .0000
PT.CD=1 NA= 1

TAPE,CODE=3 TAPE LGTH= .1600+01 PT.CD=1

CAPSTAN,CODE=7 INERT.HUB= .2771-03 R.HUB= .6250-00 DRAG COEF= .5800-03 PERT.TORQ(S)= .0000 PERT.TORQ(C)= .0000
FLUX= .0000 RESIST= .0000 VOLTS= .0000 PT.CD=1 NA= 1

CAPSTAN REDUCER,CODE=6 INERTIA= .2014-03 GEAR RATIO= .6000+01

FOLDOUT FRAME 1

FOLDOUT FRAME 2

```
TAPE,CODE=4  TAPE LGTH= .2000+01  PT.CD=1

IDLER,CODE=6  INERT.HUB= .2590-06  R.HUB= .1000+01  DRAG COEF= .0000     PERT.TORQ(S)= .0000     PERT.TORQ(C)= .0000
 PT.CD=1  NA=  1

TAPE,CODE=4  TAPE LGTH= .2000+01  PT.CD=1

IDLER,CODE=6  INERT.HUB= .8530-04  R.HUB= .7500-00  DRAG COEF= .6960-03  PERT.TORQ(S)= .0000     PERT.TORQ(C)= .0000
 PT.CD=1  NA=  1

TAPE,CODE=4  TAPE LGTH= .1688+01  PT.CD=1

IDLER,CODE=6  INERT.HUB= .2181-06  R.HUB= .1000+01  DRAG COEF= .0000     PERT.TORQ(S)= .0000     PERT.TORQ(C)= .0000
 PT.CD=1  NA=  1

TAPE,CODE=2  TAPE LGTH= .1688+01  PT.CD=1

REEL,CODE=1  INERT.HUB= .8141-02  R.HUB= .2532+01  DRAG COEF= .3820-02  PERT.TORQ(S)= .1130-02  PERT.TORQ(C)= .0000
     FLUX= .5880+01  RESIST= .6000+02  VOLTS= .0000     PT.CD=1  NA=  1
```

Preceding page blank

Preceding page blank

NATURAL FREQUENCY NO. 1 = .24669+02 HZ

NATURAL FREQUENCY CALCULATION

STATION	THETA(RAD)	TORQUE(IN-LB)
1	.3949-00	.0000
2	.8415-00	.3051+02
3	.9108-00	.3051+02
4	.4800-00	.3300+02
5	.4430-00	.3300+02
6	.1067+00	.3456+02
7	-.1014+00	.3456+02
8	-.9544-01	.5206+01
9	-.1700-00	.5205+01
10	-.1521-00	.4741+01
11	-.6979-01	.4740+01

NATURAL FREQUENCY NO. 2 = .30339+02 HZ

NATURAL FREQUENCY CALCULATION

STATION	THETA(RAD)	TORQUE(IN-LB)
1	.3949-00	.0000
2	.7603-00	.4614+02
3	.6942-00	.4615+02
4	.2190-00	.4902+02
5	-.1323-00	.4902+02
6	-.3205-00	.4832+02
7	-.8934-00	.4832+02
8	.1551+01	-.3427+03
9	.4879+01	-.3427+03
10	.5335+01	-.3225+03
11	.2768+01	-.3225+03

NATURAL FREQUENCY NO. 3 = .11633+03 HZ

NATURAL FREQUENCY CALCULATION

STATION	THETA(RAD)	TORQUE(IN-LB)
1	.3949-00	.0000
2	-.2524+01	.6784+03
3	-.8061+01	.6781+03
4	-.7205+01	.1883+03
5	-.1337+02	.1873+03
6	-.4136+01	-.8575+03
7	.1399-00	-.8579+03
8	-.1722-00	.4219+02
9	-.5756-00	.4216+02
10	-.4690-00	.7191+01
11	-.1999-00	.7136+01

Figure 39

NATURAL FREQUENCY OUTPUT DATA

NATURAL FREQUENCY NO. 4 = .17537+03 HZ

NATURAL FREQUENCY CALCULATION

STATION	THETA(RAD)	TORQUE(IN-LB)
1	.3949-00	.0000
2	-.7008+01	.1542+04
3	-.2001+02	.1540+04
4	-.7480+01	-.1223+04
5	.9541-01	-.1225+04
6	.6008+01	-.1208+04
7	.1912+02	-.1207+04
8	-.1701+04	.2784+06
9	-.4548+04	.2778+06
10	-.1592+04	-.3501+06
11	.9031+02	-.3506+06

NATURAL FREQUENCY NO. 5 = .19322+03 HZ

NATURAL FREQUENCY CALCULATION

STATION	THETA(RAD)	TORQUE(IN-LB)
1	.3949-00	.0000
2	-.8721+01	.1872+04
3	-.2457+02	.1869+04
4	-.4581+01	-.2250+04
5	.1484+02	-.2252+04
6	.4612+01	.9472+03
7	-.9254-01	.9487+03
8	.4214+01	-.6942+03
9	.1130+02	-.6926+03
10	.2233+01	.1202+04
11	-.1585+01	.1203+04

NATURAL FREQUENCY NO. 6 = .56391+04 HZ

NATURAL FREQUENCY CALCULATION

STATION	THETA(RAD)	TORQUE(IN-LB)
1	.3949-00	.0000
2	-.8279+04	.1594+07
3	-.6366+04	-.6746+06
4	.5593+07	-.9097+09
5	-.1653+03	.9089+09
6	-.4325+07	.8785+09
7	-.4966+07	-.2481+09
8	.4620+12	-.7508+14
9	-.5332+09	.7515+14
10	.4671+10	-.9764+12
11	.1224+10	.3026+12

Figure 39 (Cont.)

NATURAL FREQUENCY OUTPUT DATA

FOLDOUT FRAME /

FOLDOUT FRAME 2

CONTROL INPUT DATA

```
DELTA= .50000+01      T MAX= .70000-00      AMT.TAPE= .12000+04      ERROR CRIT.= .10000+01      ST.FREQ= .59300-00
NO.FREQ=  1           NO.SETS= 14           SC1=  3                  SC2=  0                         FREQ.INT.= .00000
MAX.FREQUENCY= .200+04
```

TAPE INPUT DATA

```
DENSITY= .50000-01      MOD.ELST= .65000+06      THK.TAPE= .10000-02      WTH.TAPE= .50000-00      TAPE VEL= .15000+01
```

TAPE TRANSPORT INPUT DATA

```
REEL.CODE=6  INERT.HUB= .8141-02  R.HUB= .2532+01  DRAG COEF= .3820-02  PERT.TORQ(S)= .6330-03  PERT.TORQ(C)= .0000
     FLUX= .5880+01  RESIST= .6000+02  VOLTS= .0000     PT.CD=1  NA=  1

TAPE.CODE=4  TAPE LGTH= .1688+01  PT.CD=1  HEAD COEF.= .0000

IDLER.CODE=6  INERT.HUB= .2183-06  R.HUB= .1000+01  DRAG COEF= .0000     PERT.TORQ(S)= .0000     PERT.TORQ(C)= .0000
    PT.CD=1  NA=  1

TAPE.CODE=4  TAPE LGTH= .1688+01  PT.CD=1  HEAD COEF.= .0000

IDLER.CODE=6  INERT.HUB= .8530-04  R.HUB= .7500-00  DRAG COEF= .6960-03  PERT.TORQ(S)= .0000     PERT.TORQ(C)= .0000
    PT.CD=1  NA=  1

TAPE.CODE=4  TAPE LGTH= .2000+01  PT.CD=1  HEAD COEF.= .0000

IDLER.CODE=6  INERT.HUB= .2590-06  R.HUB= .1000+01  DRAG COEF= .0000     PERT.TORQ(S)= .0000     PERT.TORQ(C)= .0000
    PT.CD=1  NA=  1

TAPE.CODE=3  TAPE LGTH= .2000+01  PT.CD=1  HEAD COEF.= .0000

CAPSTAN.CODE=6  INERT.HUB= .9140-04  R.HUB= .6250-00  DRAG COEF= .5800-03  PERT.TORQ(S)= .0000     PERT.TORQ(C)= .0000
     FLUX= .1040+01  RESIST= .4000+02  VOLTS= .0000     PT.CD=1  NA=  1

TAPE.CODE=4  TAPE LGTH= .1600+01  PT.CD=1  HEAD COEF.= .0000

IDLER.CODE=6  INERT.HUB= .2075-06  R.HUB= .1000+01  DRAG COEF= .2000-02  PERT.TORQ(S)= .0000     PERT.TORQ(C)= .0000
    PT.CD=1  NA=  1

TAPE.CODE=3  TAPE LGTH= .1600+01  PT.CD=1  HEAD COEF.= .0000

CAPSTAN.CODE=7  INERT.HUB= .2771-03  R.HUB= .6250-00  DRAG COEF= .5800-03  PERT.TORQ(S)= .0000     PERT.TORQ(C)= .0000
     FLUX= .0000     RESIST= .0000     VOLTS= .0000     PT.CD=1  NA=  1

CAPSTAN REDUCER.CODE=6  INERTIA= .2014-03  GEAR RATIO= .6000+01  DRAG COEF= .9660-04  FLUX= .1040+01  RESISTANCE= .4000+02
```

FOLDOUT FRAME 1

FOLDOUT FRAME 2

```
TAPE,CODE=4  TAPE LGTH= .2000+01  PT.CD=1  HEAD COEF.= ,0000

IDLER,CODE=6  INERT,HUB= .2590-06  R.HUB= ,1000+01  DRAG COEF= ,0000     PERT,TORQ(S)= ,0000     PERT,TORQ(C)= ,0000
    PT.CD=1  NA=  1

TAPE,CODE=4  TAPE LGTH= .2000+01  PT.CD=1  HEAD COEF.= ,0000

IDLER,CODE=6  INERT,HUB= .8530-04  R.HUB= .7500-00  DRAG COEF= ,6960-03  PERT.TORQ(S)= ,0000     PERT,TORQ(C)= ,0000
    PT.CD=1  NA=  1

TAPE,CODE=4  TAPE LGTH= .1688+01  PT.CD=1  HEAD COEF.= ,0000

IDLER,CODE=6  INERT,HUB= .2181-06  R.HUB= .1000+01  DRAG COEF= ,0000     PERT.TORQ(S)= ,0000     PERT,TORQ(C)= ,0000
    PT.CD=1  NA=  1

TAPE,CODE=2  TAPE LGTH= .1688+01  PT.CD=1  HEAD COEF.= ,0000

REEL,CODE=1  INERT,HUB= .8141-02  R.HUB= .2532+01  DRAG COEF= .3820-02  PERT.TORQ(S)= .6330-03  PERT.TORQ(C)= .0000
     FLUX= ,5880+01  RESIST= ,6000+02  VOLTS= ,0000     PT.CD=1  NA=  1
```

Preceding page blank

Preceding page blank

```
SET NO.  6 RESPONSE OUTPUT

ELEMENT NO.  1     RESPONSE= ,26910-05 INCHES
ELEMENT NO.  2     RESPONSE=-,48438-03 INCHES RESPONSE AMPLITUDE= .48439-03 INCHES   PHASE=   -,0056 RAD.

ELEMENT NO.  3     RESPONSE= ,15275-05 INCHES
ELEMENT NO.  4     RESPONSE=-,48438-03 INCHES RESPONSE AMPLITUDE= .48438-03 INCHES   PHASE=   -,0032 RAD.

ELEMENT NO.  5     RESPONSE= ,36401-06 INCHES
ELEMENT NO.  6     RESPONSE=-,48438-03 INCHES RESPONSE AMPLITUDE= .48438-03 INCHES   PHASE=   -,0008 RAD.

ELEMENT NO.  7     RESPONSE=-,10123-05 INCHES
ELEMENT NO.  8     RESPONSE=-,48437-03 INCHES RESPONSE AMPLITUDE= .48437-03 INCHES   PHASE=    ,0021 RAD.

ELEMENT NO.  9     RESPONSE=-,23887-05 INCHES
ELEMENT NO. 10     RESPONSE=-,48437-03 INCHES RESPONSE AMPLITUDE= .48438-03 INCHES   PHASE=    ,0049 RAD.

ELEMENT NO. 11     RESPONSE=-,33898-05 INCHES
ELEMENT NO. 12     RESPONSE=-,48437-03 INCHES RESPONSE AMPLITUDE= .48438-03 INCHES   PHASE=    ,0070 RAD.

ELEMENT NO. 13     RESPONSE=-,43881-05 INCHES
ELEMENT NO. 14     RESPONSE=-,48437-03 INCHES RESPONSE AMPLITUDE= .48439-03 INCHES   PHASE=    ,0091 RAD.

ELEMENT NO. 15     RESPONSE=-,30117-05 INCHES
ELEMENT NO. 16     RESPONSE=-,48437-03 INCHES RESPONSE AMPLITUDE= .48438-03 INCHES   PHASE=    ,0062 RAD.

ELEMENT NO. 17     RESPONSE=-,16354-05 INCHES
ELEMENT NO. 18     RESPONSE=-,48437-03 INCHES RESPONSE AMPLITUDE= .48437-03 INCHES   PHASE=    ,0034 RAD.

ELEMENT NO. 19     RESPONSE=-,47188-06 INCHES
ELEMENT NO. 20     RESPONSE=-,48437-03 INCHES RESPONSE AMPLITUDE= .48437-03 INCHES   PHASE=    ,0010 RAD.

ELEMENT NO. 21     RESPONSE= ,69160-06 INCHES
ELEMENT NO. 22     RESPONSE=-,48437-03 INCHES RESPONSE AMPLITUDE= .48437-03 INCHES   PHASE=   -,0014 RAD.
```

Figure 40

VIBRATION RESPONSE OUTPUT DATA (AMPLITUDES AND PHASE)

```
TOTAL FORCED RESPONSE OUTPUT

ELEMENT( 1- 2)     VELOCITY= .19276-02 IN./SEC.
ELEMENT( 3- 4)     VELOCITY= .19242-02 IN./SEC.
ELEMENT( 5- 6)     VELOCITY= .19221-02 IN./SEC.
ELEMENT( 7- 8)     VELOCITY= .18727-02 IN./SEC.
ELEMENT( 9-10)     VELOCITY= .18399-02 IN./SEC.
ELEMENT(11-12)     VELOCITY= .17939-02 IN./SEC.
ELEMENT(13-14)     VELOCITY= .17785-02 IN./SEC.
ELEMENT(15-16)     VELOCITY= .17864-02 IN./SEC.
ELEMENT(17-18)     VELOCITY= .18106-02 IN./SEC.
ELEMENT(19-20)     VELOCITY= .18114-02 IN./SEC.
ELEMENT(21-22)     VELOCITY= .18134-02 IN./SEC.

DATA CARDS ENCOUNTERED BY SYSTEM - IGNORED
END
```

Figure 41

VIBRATION RESPONSE OUTPUT DATA (RMS VELOCITIES)

3.2 Double Cone Guide Roller Transient Analysis

The guiding action of a crowned roller, was studied by determining the tape response to a given input disturbance as it passes over the roller. The position of a tape on a double cone guide roller for a harmonic off center position at the input roller (Figure 42) is investigated. This non-linear analysis provides design data on the attenuation of input disturbances, e_i, to the tape. The calculated transfer function yields the tape response, e_o. Table 11 gives the nomenclature for the analysis and problem description.

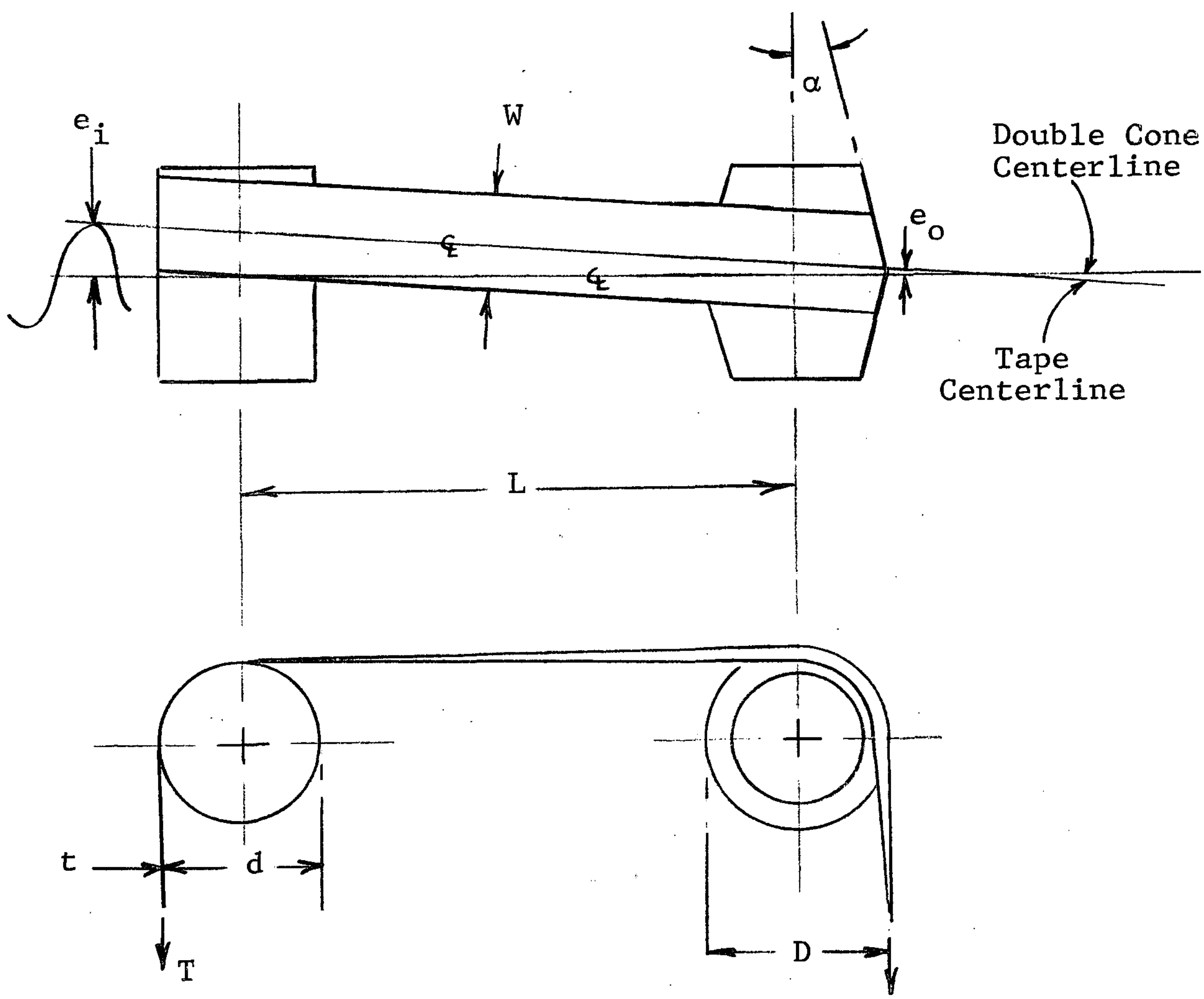

Figure 42

DOUBLE CONE GUIDE ROLLER SYSTEM

Table 11

GUIDE ROLLER TRANSIENT ANALYSIS NOMENCLATURE

C	constant
d	diameter of cylinder roller
D	maximum diameter of double cone roller
e_o	distance tape is off-center at double cone roller
e_i	distance tape is off-center on cylindrical roller
E	modulus of elasticity of tape
K	torsional spring stiffness at junction of tape and double cone roller
L	length between rollers
M	moment in tape
P	dimensionless geometry factor
Q	dimensionless tension
R	dimensionless moment
r	tape reaction
s	arc length
s_o	original tape length
S	dimensionless torsional spring stiffness
t	tape thickness
T	tape tension
U	dimensionless output eccentricity
V	dimensionless input eccentricity
W	tape width
W_c	Tape Contact width
y	coordinate to point along width of tape measured from double cone roller center
y'_L	slope of tape at cone roller
Z	dimensionless tape width
α	cone angle for roller
ε	strain in tape
ε_c	strain in tape due to cone
ε_o	strain constant

Table 11

GUIDE ROLLER TRANSIENT ANALYSIS NOMENCLATURE

μ	Poisson's ratio for tape
σ	stress in tape
ω	system response

3.2.1 Modeling

It is assumed that the tape can be modeled as a beam fixed at the point where the tape leaves the cylindrical roller and pinned at its junction with the double cone-roller. The effects of local slippage between the tape and the roller are modeled with a torsion spring, (Figure 43). However, it is assumed that the frictional forces between the roller and the tape are sufficient to prevent any gross relative motion.

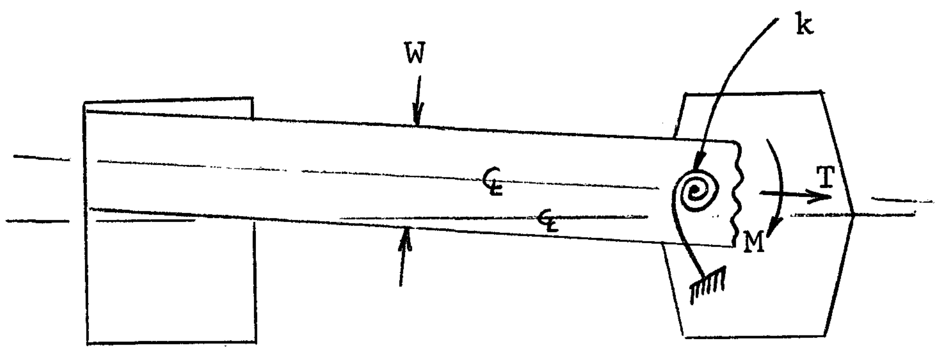

Figure 43

TAPE TORSIONAL RESTRAINT

A torsion spring, k, also provides a simulation of the resistance to tape rotation as it enters the double cone roller. The loading on the beam is given by the stress distribution across the tape at its junction with the double cone roller. This loading was determined from the tape tension in its free state and the strain distribution in the tape as it passes around the double cone roller.

3.2.2 Analysis

The strain distribution across the tape due to roller geometry and global tape tension is given by the following expressions

$$\varepsilon = \varepsilon_o + C\,|y| \tag{55}$$

Where ε_o represents the tape tension and $C\,|y|$ represents the strain to roller geometry.

For some wrap angle around the cone, $\Delta\theta$, the arc length at position Y is

$$s = (D/2 - |y|\,\alpha)\,\Delta\theta \tag{56}$$

where the cone angle, α is assumed to be small. Figure 44 shows the geometry of the roller. The original length of the tape along this arc is approximately

$$s_o = (D/2)\,\Delta\theta \tag{57}$$

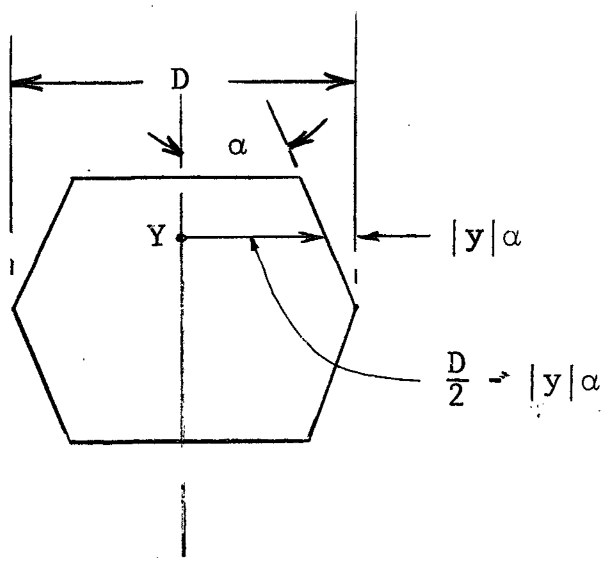

Figure 44

ROLLER GEOMETRY

The strain due to the cone is

$$\varepsilon_o = (s - s_o)/s_o = -2\ |y|\ \alpha/D \tag{58}$$

From this expression the constant C becomes

$$C = -2\alpha/D \tag{59}$$

Therefore

$$\varepsilon = \varepsilon_o - 2\alpha\ |y|\ /D \tag{60}$$

Using Hooke's law, the stress in the tape is proportional to the strain ε, therefore

$$\sigma = E\varepsilon = E\ (\varepsilon_o - 2\alpha\ |y|\ /D) \tag{61}$$

The total tension in the tape when it is displaced an amount, e, off the center of the coned roller will be

$$T = \int_{-(\frac{W}{2} - \varepsilon_o)}^{\frac{W}{2} + e_o} \sigma t dy = \int_{-(\frac{W}{2} - e_o)}^{\frac{W}{2} + e_o} E\ (\varepsilon_o - 2\alpha\ |y|\ /D)\ tdy$$

$$= \int_{-\frac{W}{2} - e_o}^{o} E\left[\varepsilon_o - 2\alpha\ (-y)/D\right]\ tdy + \int_{o}^{\frac{W}{2} + e_o} E(\varepsilon_o - 2\alpha\ y/D)\ tdy$$

$$= Et \left[\varepsilon_o\, y + \alpha y^2 /D\right]_{-(\frac{W}{2} - e_o)}^{o} + Et \left[\varepsilon_o y - \alpha\, y^2/D\right]_{o}^{\frac{W}{2} + e_o}$$

$$= Et \left[\varepsilon_o \left(\frac{W}{2} - e_o\right) - \alpha\left(\frac{W}{2} - e_o\right)^2/D + \varepsilon_o\left(\frac{W}{2} + e_o\right) - \alpha\left(\frac{W}{2} + e_o\right)^2/D\right]$$

Collecting terms yields,

$$T = Et\ (\varepsilon_o W - \alpha W^2/2D - 2\alpha\, e_o{}^2/D) \tag{62}$$

In the evaluation of the integral of the absolute value of y it was assumed that $e_o \leq W/2$. Thus it can be seen that the tension, T, in the tape at its entry to the roller is a function of: a constant strain ε_o; the roller geometry α and D; the tape geometry W and t; the tape physical property E; and the tape output exit position e_o.

The tape stress distribution also results in a moment about the center line of the tape given by

$$M = \int_{-(\frac{W}{2} - e_o)}^{\frac{W}{2} + e_o} (y - e_o)\sigma t dy = \int_{-(\frac{W}{2} - e_o)}^{\frac{W}{2} + e_o} (y - e_o)\ E\ (\varepsilon_o - 2\alpha|y|\ /D)\ tdy$$

$$= \int_{-(\frac{W}{2} - e_o)}^{o} (y - e_o)\ E\left[\varepsilon_o - 2\alpha\ (-y)\ /D\right]\ tdy + \int_{o}^{\frac{W}{2} + e_o} (y-e_o)E(\varepsilon_o-2\alpha y/D)\ tdy$$

$$= Et \int_{-(\frac{W}{2} - e_o)}^{o} \left[(- e_o \varepsilon_o) + y(\varepsilon_o - 2e_o\alpha/D) + y^2(2\alpha/D)\right] dy$$

$$+ Et \int_{o}^{\frac{W}{2} + e_o} \left[(-e_o\varepsilon_o) + y\ (\varepsilon_o + 2\ e_o\ \alpha/D) + y^2\ (-2\alpha/D)\right] dy$$

$$M = Et \left[(e_o\varepsilon_o)\ (y) + (y^2/2)\ (\varepsilon_o - 2e_o\alpha/D + y^3/3)\ (2\alpha/D\right]_{-(\frac{W}{2} - e_o)}^{o}$$

$$+ Et \left[(-e_o\varepsilon_o)\ (y) + (y^2/2)\ (\varepsilon_o + 2e_o\alpha/D + (y^3/3)\ (-2\alpha/D)\right]_{o}^{(\frac{W}{2} + e_o)}$$

$$= Et \left\{(-e_o\varepsilon_o)\ (\tfrac{W}{2} - e_o) + \left[-(\tfrac{W}{2} - e_o)^2\ /2\right] (\varepsilon_o - 2e_o\alpha/D)\right.$$

$$+ \left[(\tfrac{W}{2} - e_o)^3\ /3\right] (2\alpha/D) + (-e_o\varepsilon_o)\ (\tfrac{W}{2} + e_o)$$

$$\left. + \left[(\tfrac{W}{2} + e_o)^2\ /2\right] (\varepsilon_o + 2e_o\alpha D) + (\tfrac{W}{2} + e_o)^3\ /3\quad (-2\alpha/D\right\}$$

Finally, collecting terms yields

$$M = (Ee_o\ t\alpha/6D)\quad (4e_o{}^2 - 3W^2) \tag{63}$$

Again in the development of this equation, it was assumed that $e_o \leq W/2$. The moment, M, is then a function of: the tape modulus of elasticity E; the tape geometry t and W the roller geometry α and D; and the roller exit displacement e_o. There, fore, both the tension and the tape moment are nonlinear functions of the tape exit displacement.

Figure 45 shows the beam used to simulate the behavior of the tape between rollers. K is a local torsional spring used to simulate local slippage at the point where the tape initially contacts the roller.

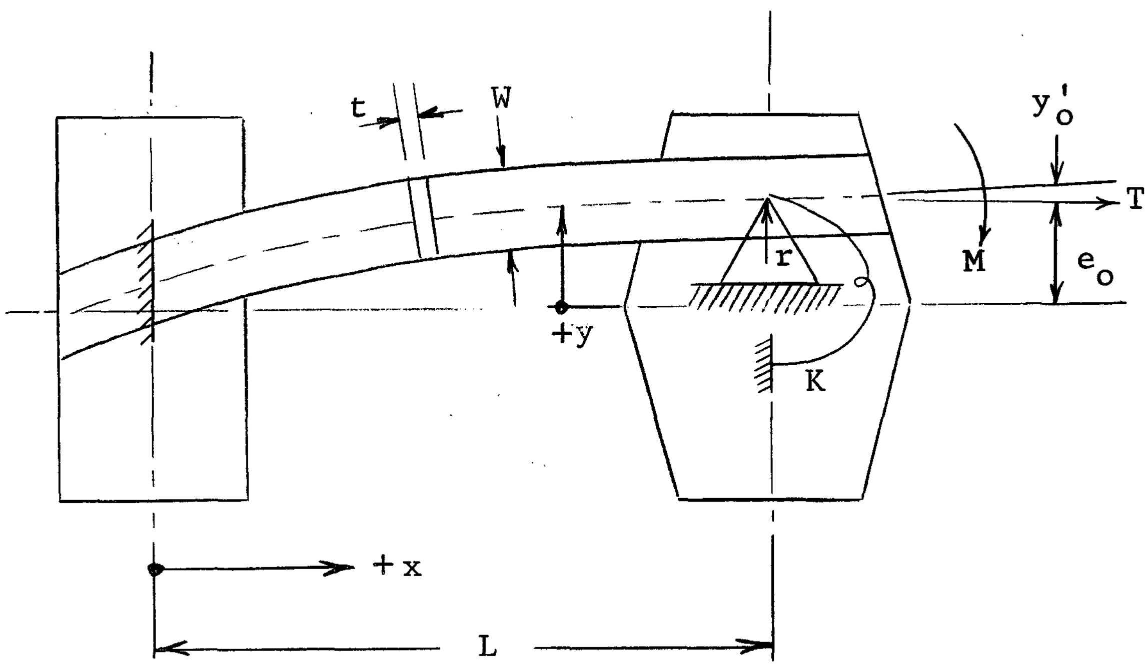

Figure 45

BEAM MODEL OF TAPE

The total moment, M_T, at any position in this beam is given by

$$M_T = EIy'' - r\ (L - x) - M - T\ (e_o - y) - Ky_o' \qquad (64)$$

or

$$EIy'' - Ty = r\ (L - x) - M + Ky'$$

$$EIy'' - Ty = r\ (L - x) - M - T\ e_o - Ky_o' \qquad (65)$$

The solution to this differential equation yields the displacement of the tape at any position as a function of its properties and end conditions.

$$y = C_1 \cosh (\sqrt{T/EI}\ x) + C_2 \sinh (\sqrt{T/EI}\ x) + \frac{r}{T} (L - x) - \frac{M + T e_o + K y_o'}{T} \tag{66}$$

Taking derivatives

$$y' = C_1 \sqrt{T/EI} \sinh (\sqrt{T/EI}\ x) + C_2 \sqrt{T/EI} \cosh (\sqrt{T/EI}\ x) - \frac{r}{T} \tag{67}$$

$$y'' = C_1 \ (T/EI \ \cosh (\sqrt{T/EI}\ x) + C_2 (T/EI) \sinh (\sqrt{T/EI}\ x) \tag{68}$$

At $x = 0$, $y = e_i$, therefore

$$e_i = C_1 + \frac{rL}{T} - \frac{M + T e_o + K y_o'}{T} \tag{69}$$

At $x = 0$, $y' = y_i'$, therefore

$$y_i' = C_2 \sqrt{T/EI} - \frac{r}{T} \tag{70}$$

At $x = L$, $y = e_o$, therefore

$$e_o = C_1 \cosh (\sqrt{T/EI}\ L) + C_2 \sinh (\sqrt{T/EI}\ L) - \frac{M + T e_o + K y'_o}{T} \tag{71}$$

At $x = L$, $y' = y_o''$ is given by

$$y'_o = C_1 \sqrt{T/EI} \sinh (\sqrt{T/EI}\ L) + C_2 \sqrt{T/EI} \cosh (\sqrt{T/EI}\ L) - \frac{r}{T} \tag{72}$$

Equations 69 through 72 can be rewritten

$$C_1\ [1] + C_2\ [0] + r\left[\frac{L}{T}\right] + y'_o\left[-\frac{K}{T}\right] = e_i + e_o + \frac{M}{T} \tag{73}$$

$$C_1\ [0] + C_2\left[\sqrt{\frac{T}{EI}}\right] + r\left[-\frac{1}{T}\right] + y'_o\ [0] = y'_i \tag{74}$$

$$C_1\left[\cosh\left(\sqrt{\frac{T}{EI}}\,L\right)\right] + C_2\left[\sinh\left(\sqrt{\frac{T}{EI}}\,L\right)\right] + r\ [0] + y'_o\left[-\frac{K}{T}\right]$$
$$= 2\ e_o + \frac{M}{T} \tag{75}$$

$$C_1\left[\sqrt{\frac{T}{EI}}\sinh\left(\sqrt{\frac{T}{EI}}\,L\right)\right] + C_2\left[\sqrt{\frac{T}{EI}}\cosh\left(\sqrt{\frac{T}{EI}}\,L\right)\right] + r\left[-\frac{1}{T}\right]$$
$$+ y'_o\ [-1] = 0 \tag{76}$$

Solving the above set of simultaneous equations for the coefficient C_1 and C_2, yields the following slope equation

$$y'_o = \left\{\left(\sqrt{\frac{T}{EI}}\,L\right)^2\left(2\,\frac{e_o}{L} + \frac{M}{TL}\right)\sinh\left(\sqrt{\frac{T}{EI}}\,L\right) + \left(\sqrt{\frac{T}{EI}}\,L\right)^2\left(\frac{e_i}{L}\right.\right.$$
$$\left.+\frac{3e_o}{L} + \frac{2M}{TL}\right)\left[1-\cosh\left(\sqrt{\frac{T}{EI}}\,L\right)\right] + y'_i\left[\sqrt{\frac{T}{EI}}\,L\right.$$
$$\left.\left.-\sinh\left(\sqrt{\frac{T}{EI}}\,L\right)\right]\right\} \Bigg/ \left\{\left(\sqrt{\frac{T}{EI}}\,L\right)^2\frac{K}{TL}\sinh\left(\sqrt{\frac{T}{EI}}\,L\right)\right.$$
$$-2\sqrt{\frac{T}{EI}}\,L\,\frac{K}{TL}\ 1-\cosh\left(\sqrt{\frac{T}{EI}}\,L\right) + \sqrt{\frac{T}{EI}}\,L\cosh\left(\sqrt{\frac{T}{EI}}\,L\right)$$
$$\left.-\sinh\left(\sqrt{\frac{T}{EI}}\,L\right)\right\} \tag{77}$$

The following nondimensional parameters are defined to simplify the calculation procedure.

$$P = \frac{\alpha t L^4}{DI} \qquad \text{ratio of roller geometry to tape geometry} \tag{78}$$

$$Q = L\sqrt{\frac{T}{EI}} \qquad \text{ratio of tape tension to tape lateral stiffness} \tag{79}$$

$$R = \frac{ML}{EI} \qquad \text{ratio of roller movement to tape lateral stiffness} \tag{80}$$

$$S = \frac{KL}{EI} \qquad \text{ratio of roller torsional stiffness to tape lateral stiffness} \tag{81}$$

$$U = \frac{e_o}{L} \qquad \text{ratio of response to free tape length} \tag{82}$$

$$V = \frac{e_i}{L} \qquad \text{ratio of input disturbance to free tape length} \tag{83}$$

$$Z = \frac{W}{L} \qquad \text{ratio of tape width to free tape length} \tag{84}$$

Substituting these relationships into equation 77 yields

$$y'_o = \left\{Q^2 \left(2U + \frac{R}{Q^2}\right) \sinh (Q) + Q\left(V + 3U + \frac{2R}{Q^2}\right) \left[1 - \cosh (Q)\right] + y'_i \left[Q - \sinh (Q)\right]\right\} \div \left\{S \sinh (Q) - \left(\frac{2S}{Q}\right) \left[1 - \cosh (Q)\right] + Q \cosh (Q) - \sinh (Q)\right\} \tag{85}$$

Substituting equation 63 into 80

$$R = \frac{Ee_o t\alpha L}{} \; \frac{(4e_o^{\,2} - 3W^2)}{6\ DEI} = \frac{\alpha t L^4}{6DI} \; \frac{e_o}{L} \; (\frac{4e_o^{\,2}}{L^2} - 3W^2)$$

$$R = \frac{PU}{6} (4U^2 - 3Z^2) \tag{86}$$

Since the full width of the tape may not be in contact with the double cone roller, this width (and thus Z) must be computed. The tape will be in contact as long as its stress, σ, is positive. For this to be true the total strain zero or equation 61 becomes

$$\frac{\varepsilon_o - 2\alpha \; (\frac{W_c}{2} + e_o)}{D} = 0 \tag{87}$$

Then

$$\varepsilon_o = \frac{-2\alpha \; (\frac{W_c}{2} - e_o)}{D} \tag{88}$$

where W_c = tape contract width

Substituting this into equation 62, the tension for a contact width W_c is obtained.

$$T = \left[\frac{Et \; 2\alpha W_c \; (\frac{W_c}{2} - e_o)}{D} - \frac{\alpha W_c^{\,2}}{2D} - \frac{2\alpha e_o^{\,2}}{D} \right]$$

$$\frac{TL^2}{EI} = Q^2 = \frac{\alpha t L^4}{EI} \left[\frac{W_c^{\,2}}{2L^2} + \frac{2W_c e_o}{L^2} - \frac{2e_o^{\,2}}{L^2} \right]$$

$$Q^2 = \frac{P}{2} (Z_c^{\,2} + 4ZU - 4U^2) \tag{89}$$

Solving this equation for Z_c

$$Z_c = \sqrt{\frac{4V \; 16U^2 - 4 \left(\frac{- 4U^2 - 2Q^2}{P} \right)}{2}}$$

$$Z_c = - 2U + \sqrt{\frac{8U^2 + 2Q^2}{P}} \qquad (90)$$

Here the positive sign for the radical was chosen since Z_c is the width to length ratio.

3.2.3 Computational Procedure

Equations 85 , 86 , and 90 are used to obtain the response of the system for given values of the dimensionless geometry factory P, the dimensionless tape width, the dimensionless tension Q, the dimensionless torsional spring stiffness and given values for the input eccentricity V. The input eccentricity is given by

$$V = Vm \sin (B A) \qquad (91)$$

Where Vm is the dimensionless amplitude of the input disturbance, B is the dimensionless frequency ($2\pi L/\lambda$), the dimensionless tape position parameter A is the length of tape passing around input roller divided by L and λ is the wave length of the input disturbance.

Then

$$Y'_i = B \; Vm \cos (B A) \qquad (92)$$

Figure 46 is a flow diagram for a computer program to carry out the calculations described above. The program is designed to compute response for the continuous sinusoidal input of equation 91 or for a single sinusoidal pulse (one-half wave).

The program described first reads in the relevant data and prints the data out along with a heading. A and U are set to their initial values of zero. Then the dimensionless width is checked for full contact using equation 90. If full contact does not exist the value for full contact is used instead of the actual width in succeeding calculations. The dimensionless movement R is then calculated according to equation 86. The input tape eccentricity and slope are calculated in accordance with the continuous or pulse input depending on the sign of the input magnitude (equations 91 and 92). Then equation 85 is used to calculate the output slope Y'_0. After printing out A, V, U, and Z (displacement, input eccentricity, output eccentricity, and contact width) a length of tape DA is passed over the rollers by incrementing A by an amount DA. As the tape rolls into the coned roller U, the dimensionless response, is reduced by an amount Y'_0 DA, since no slippage on the rollers is assumed. The program then checks A to determine if the length desired has passed over the rollers. If it has, the calculations are complete; if not, the contact width is again calculated and the program proceeds from that point as described before.

The computer flow diagram and computer program follow as Figures 46 and 47, respectively.

3.2.3.1 Computer Program Use

The computer program for the transient analysis of the double cone guide roller can be used to evaluated specific guidance designs or it can be used to generate general design data. The use of this computer program involves selection of pertinent input data. To illustrate its use, a preliminary analysis of the guidance system used in the functional layout, Figure 2, of the five year recorder was made.

Double coned roller Diameter,	$D = 1.5$ in.
Double coned roller Angle,	$\chi = 1.75$ deg.
Tape thickness,	$t = .001$ in.
Distance between rollers,	$L = 4.675$ in.
Tape tension,	$T = 6$ oz.
Tape modulus,	$E = 800{,}000$ psi
Tape width,	$W = .5$ in.
Input disturbance,	$e_i = 0.14$ in.
Torsional stiffness ratio,	$S = KL/EI = 10$
Disturbance wave length,	$\lambda = 18.85$ in./cycle
Length of tape handled,	$\ell = 1500$ in.

The dimensionless variables are now formed.

$$P = \frac{\alpha t L^4}{DI} = 1000$$

$$Q = L\sqrt{\frac{T}{EI}} = 1.0$$

$$S = \frac{KL}{EI} = 3.0$$

$$VM = \frac{e_i}{L} = .003$$

$$Z = \frac{W}{L} = .107$$

The calculation step size, D, is selected and appears on the computer input/out data. The constant, C, is equal to $2\pi/\lambda$. The computer input data is shown in Figure 48 as it appears on the data card. Figure 49 shows the input/output data for the selected tape handling analysis. The input data is given to the computer and is printed out prior to the output data. The four output data columns are

$X = vt$	length of tape passing over the double-coned roller as a function of tape velocity and elapsed time.
$V = \frac{e_i}{L}$	dimensionless input disturbance as a function of x.
$U = \frac{e_o}{L}$	dimensionless output response as a function of x.
$Z = \frac{W_o}{L}$	dimensionless tape contact width as function of x.

The guidance system performance is assessed by computing the percentage disturbance transmission past the double coned roller.

$$\text{Disturbance Transmission (DT)} = \frac{\text{peak output response}}{\text{peak input disturbance}} \times 100\%$$

For the foregoing problem,

$$DT = \frac{.0074}{.003} \times 100\% = 24.3\% \tag{93}$$

Finally,

Figure 50 shows a plot of the input/output data generated on this computer program. It indicates the response attenuation of the input disturbance with a phase lag of about 90 degrees.

FOLDOUT FRAME 1

FOLDOUT FRAME 2

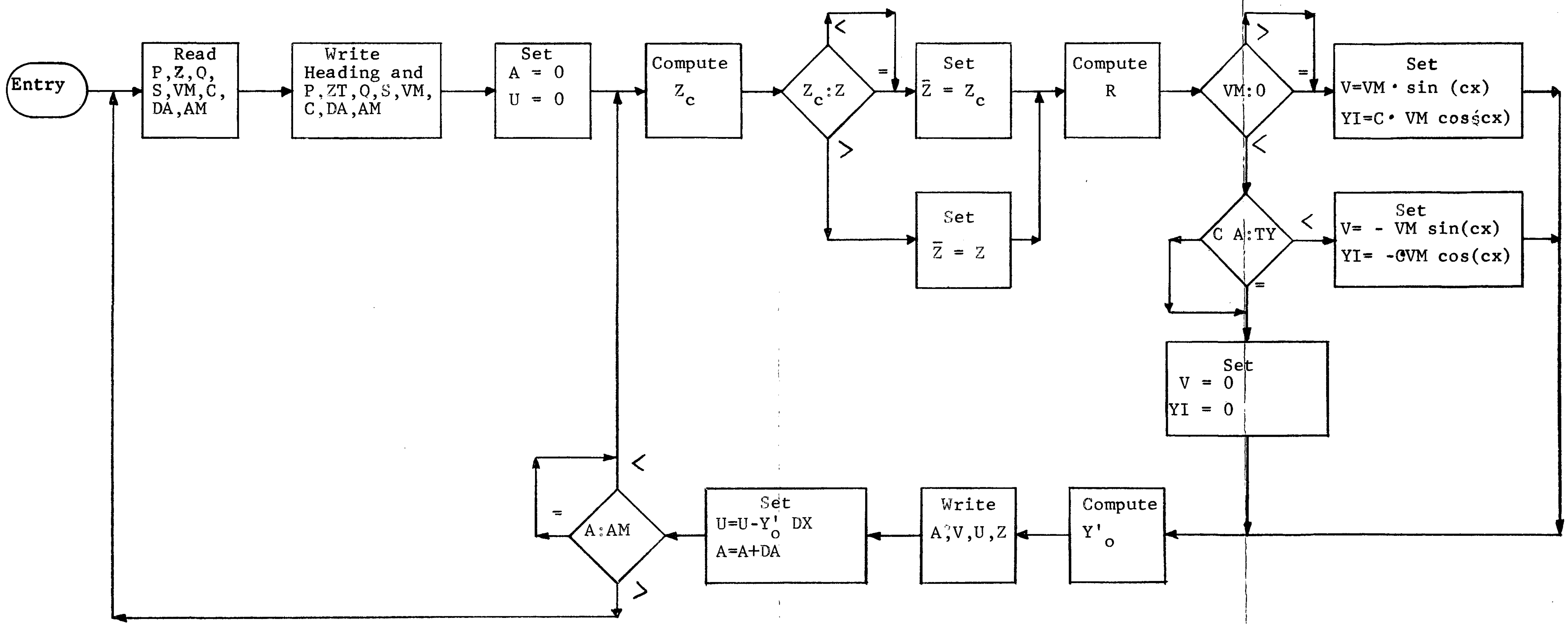

Figure 46

DOUBLE CONE TRANSIENT ANALYSIS COMPUTER FLOW DIAGRAM

PRECEDING PAGE BLANK NOT FILMED

```
    1 READ (5,2) P,ZT,Q,S,VM,C,DX,XM
    2 FORMAT (10F8.0)
      WRITE (6,3) P,ZT,Q,S,VM,C,DX,XM
    3 FORMAT (44H1DOUBLE CONE GUIDE ROLLER TRANSIENT ANALYSIS////11H INP
     1UT DATA//3H P=E13.4,5X2HZ=E13.4,5X2HQ=E13.4,5X2HS=E13.4/3H V=E13.4
     2,5X2HC=E13.4,4X3HDX=E13.4,4X3HXM=E13.4///12H OUTPUT DATA//9X1HX,12
     3X1HV,12X1HU,12X1HZ/)
      X=0.
      U=0.
    4 ZP=-2.*U+SQRT(8.*U*U+2.*Q*Q/(P))
      IF (ZP-ZT) 5,5,6
    5 Z=ZP
      GO TO 7
    6 Z=ZT
    7 R=(P*U/6.)*(4.*U*U-3.*Z*Z)
      CH=EXP(Q)
      SH=(CH-1./CH)/2.
      CH=(CH+1./CH)/2.
      IF (VM) 9,8,8
    8 V=VM*SIN(C*X)
      YI=C*VM*COS(C*X)
      GO TO 12
    9 IF (C*X-3.1415927) 10,11,11
   10 V=-VM*SIN(C*X)
      YI=-C*VM*COS(C*X)
      GO TO 12
   11 V=0.
      YI=0.
   12 YP=(Q*Q*(2.*U+R/Q**2)*SH+Q*(V+3.*U+2.*R/Q**2)*(1.-CH)+YI*(Q-SH))/(
     1S*SH-(2.*S/Q)*(1.-CH)+Q*CH-SH)
      WRITE (6,13) X,V,U,Z
   13 FORMAT (4E13.4)
      U=U-YP*DX
      X=X+DX
      IF (X-XM) 4,4,1
      END

END OF UCC 1108 FORTRAN V COMPILATION.      0 *DIAGNOSTIC* MESSAGE(S)
```

Figure 47

DOUBLE CONE TRANSIENT ANALYSIS COMPUTER PROGRAM

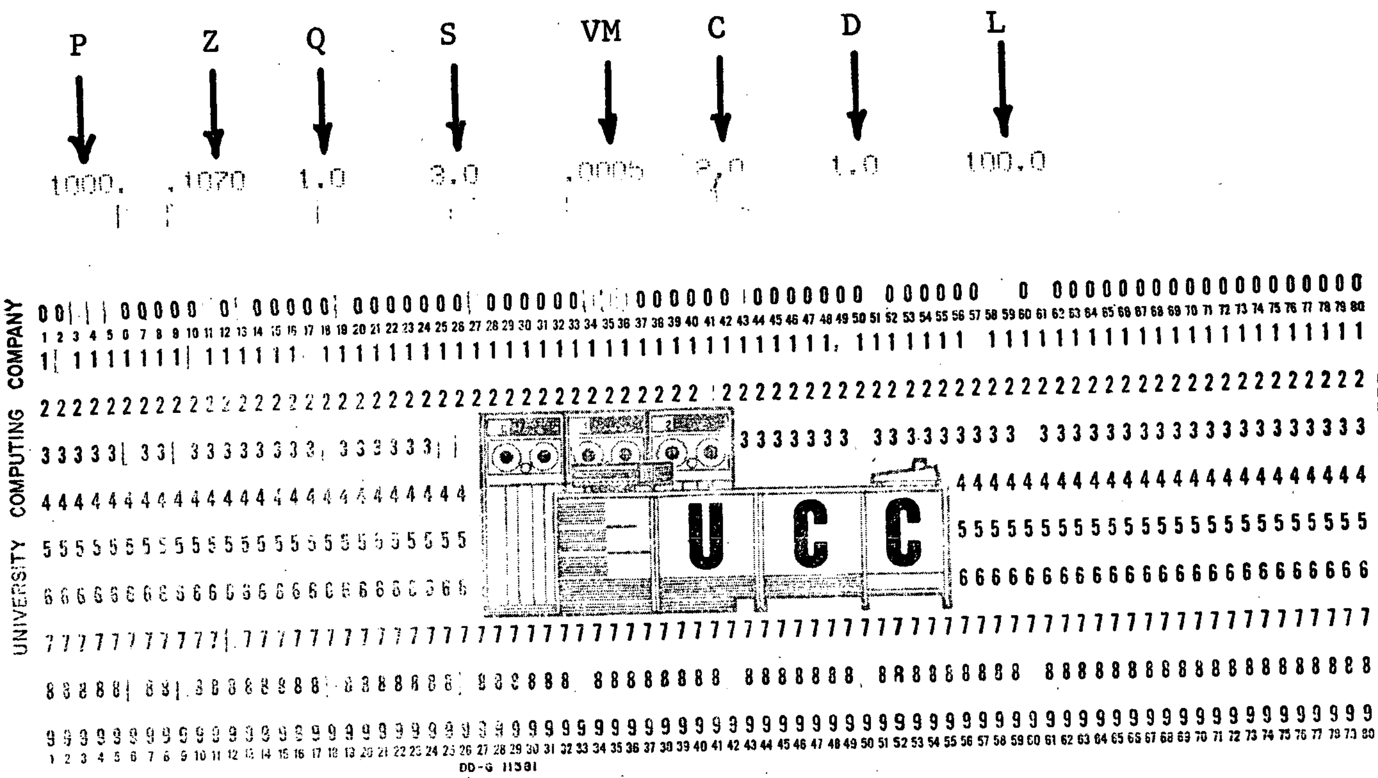

Figure 48

DOUBLE CONE TRANSIENT ANALYSIS INPUT DATA CARD

DOUBLE CONE GUIDE ROLLER TRANSIENT ANALYSIS

INPUT DATA

P=	.2720+03	Z=	.1660-00	Q=	.5200-00	S=	.3000+01
V=	.1660-02	C=	.3330-00	DX=	.2500-00	XM=	.3000+03

OUTPUT DATA

X	V	U	Z
.0000	.0000	.0000	.4459-01
.2500-00	.1380-03	.1002-05	.4459-01
.5000-00	.2751-03	.2753-05	.4458-01
.7500-00	.4103-03	.5236-05	.4458-01
.1000+01	.5426-03	.8429-05	.4457-01
.1250+01	.6712-03	.1231-04	.4457-01
.1500+01	.7951-03	.1684-04	.4456-01
.1750+01	.9135-03	.2198-04	.4455-01
.2000+01	.1026-02	.2771-04	.4453-01
.2250+01	.1131-02	.3397-04	.4452-01
.2500+01	.1228-02	.4071-04	.4451-01
.2750+01	.1316-02	.4789-04	.4449-01
.3000+01	.1396-02	.5546-04	.4448-01
.3250+01	.1466-02	.6334-04	.4446-01
.3500+01	.1526-02	.7149-04	.4445-01
.3750+01	.1575-02	.7985-04	.4443-01
.4000+01	.1613-02	.8836-04	.4441-01
.4250+01	.1640-02	.9694-04	.4440-01
.4500+01	.1656-02	.1055-03	.4438-01
.4750+01	.1660-02	.1141-03	.4436-01
.5000+01	.1653-02	.1225-03	.4435-01
.5250+01	.1634-02	.1308-03	.4433-01
.5500+01	.1604-02	.1389-03	.4431-01
.5750+01	.1563-02	.1466-03	.4430-01
.6000+01	.1511-02	.1540-03	.4428-01
.6250+01	.1448-02	.1610-03	.4427-01
.6500+01	.1376-02	.1675-03	.4426-01
.6750+01	.1294-02	.1736-03	.4425-01
.7000+01	.1203-02	.1790-03	.4423-01
.7250+01	.1104-02	.1839-03	.4422-01
.7500+01	.9968-03	.1882-03	.4422-01
.7750+01	.8830-03	.1918-03	.4421-01
.8000+01	.7630-03	.1947-03	.4420-01
.8250+01	.6378-03	.1968-03	.4420-01
.8500+01	.5081-03	.1983-03	.4420-01
.8750+01	.3750-03	.1990-03	.4420-01
.9000+01	.2392-03	.1989-03	.4420-01
.9250+01	.1018-03	.1981-03	.4420-01
.9500+01	-.3636-04	.1965-03	.4420-01
.9750+01	-.1742-03	.1942-03	.4420-01
.1000+02	-.3109-03	.1911-03	.4421-01
.1025+02	-.4454-03	.1873-03	.4422-01
.1050+02	-.5769-03	.1829-03	.4423-01
.1075+02	-.7043-03	.1777-03	.4424-01
.1100+02	-.8268-03	.1719-03	.4425-01
.1125+02	-.9437-03	.1655-03	.4426-01

Figure 49

DOUBLE CONE TRANSIENT ANALYSIS-EXAMPLE OF INPUT/OUTPUT DATA

FOLDOUT FRAME 1

PRECEDING PAGE BLANK NOT FILMED

FOLDOUT FRAME 2

DOUBLE CONED ROLLER GUIDANCE PERFORMANCE
CONE ANGLE = 1.75 DEG.
DIA. = 1.5 IN., L = 4.675 IN.
TAPE TENSION = 6 OZ.

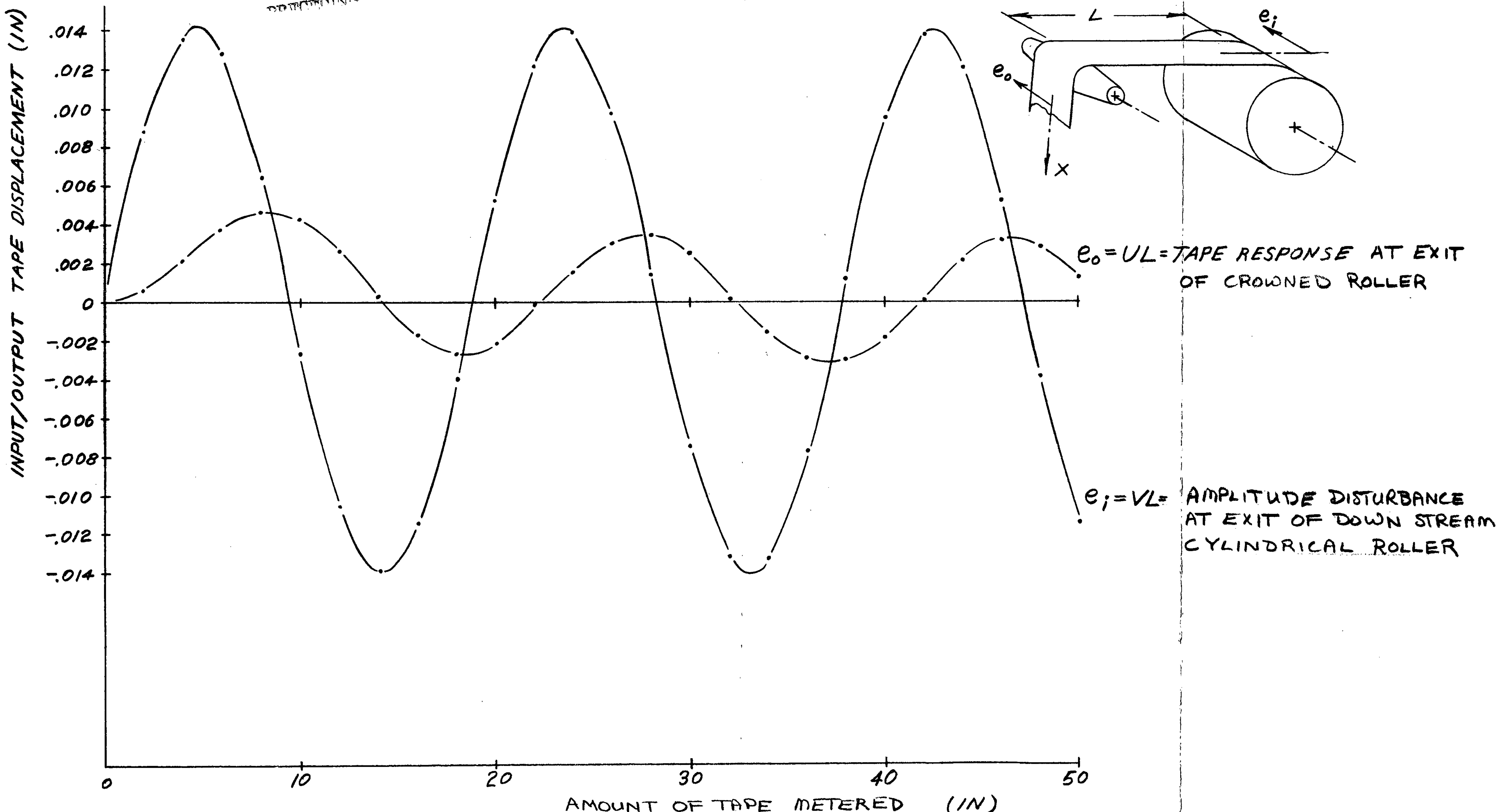

Figure 50 DOUBLE CONE ROLLER GUIDANCE PERFORMANCE

3.3 Tape Pack Design Analysis

3.3.1 Modeling

The major cause of damage in a tape pack arises from spoking. It can be eliminated through the design of tape packs without negative tangential stressed tape loops. The stress distribution in a roll of magnetic tape which has been wound at constant tension on a thick walled cylindrical reel is computed with the aid of a digital computer. The computational procedure is outlined below.

1. Start with one layer of tape on the reel.
2. Compute the stress in this layer due to the tension.
3. Add another layer of tape.
4. Compute the stress in this layer due to the tension.
5. Compute the stresses in the tape layers below this outer layer due to the pressure from the outer layer.
6. Add these computed stresses to the previous stresses in the various layers to obtain their total stresses.
7. Return to 3 and repeat until the total number of layers desired are taken into account.

The stress equations for a thick walled cylinder were utilized in this analysis. This assumption was used in an earlier analysis by G.K.I.[8] The tape geometry, tape physical properties, the geometry of the tape pack, the hub geometry, and the hub material properties can be varied in this procedure.

3.3.2 Computation Procedure

The nomenclature and formulas necessary for this analysis are given on the following page. Flow diagrams (Figures 51 and 52) for a computer program and a computer program to carry out the procedure also are given. The input to the program is explained in the nomenclature while the output is self-explanatory.

Table 12

TAPE PACK DESIGN NOMENCLATURE*

TR	input	thickness of reel
WR	input	width of reel
ER	input	modulus of elasticity of reel
RR	input	outer radius of reel
TT	input	thickness of tape
WT	input	width of tape
ET	input	modulus of elasticity of tape
PT	input	Poisson's ratio for tape
T	input	tape tension
IT	input	total number of tape wraps**
I	defined in flow diagram	counter
IQ	defined in flow diagram	counter
R	defined in flow diagram	radius to tape layer J
A	defined in flow diagram	inner radius of tape

*Derivation of equations are given in most standard strength of materials text books. For example, see Timoshenko's Strength of Material, Part II, Van Nostrand Company, Princeton, New Jersey, 1958.

**IT must be less than 5000 for the program in accordance with the flow diagram.

Table 12 (Cont.)

TAPE PACK DESIGN NOMENCLATURE

B	defined in flow diagram	outer radius of tape
P	$\frac{T}{(WT \cdot B)}$	pressure due to outer wrap of tape
PR	$\left(\frac{P}{ET}\right)\left[\frac{2B^2}{(B^2-A^2)}\right] \div \left\{\frac{A \cdot WT}{(ER \cdot TR \cdot WR)} + \frac{(B^2+A^2)}{\left[ET(B^2-A^2)\right]} + \frac{PT}{ET}\right\}$	pressure between reel and tape
S(J)	defined in flow diagram	stress in tape layer J
J	defined in flow diagram	counter
DSJ	$\left(\frac{PR \cdot A^2}{R^2}\right)(B^2+R^2) \div (B^2-A^2) - \left(\frac{P \cdot B^2}{R^2}\right)\frac{(A^2+R^2)}{(B^2-A^2)}$	stress in layer J due to P and PR

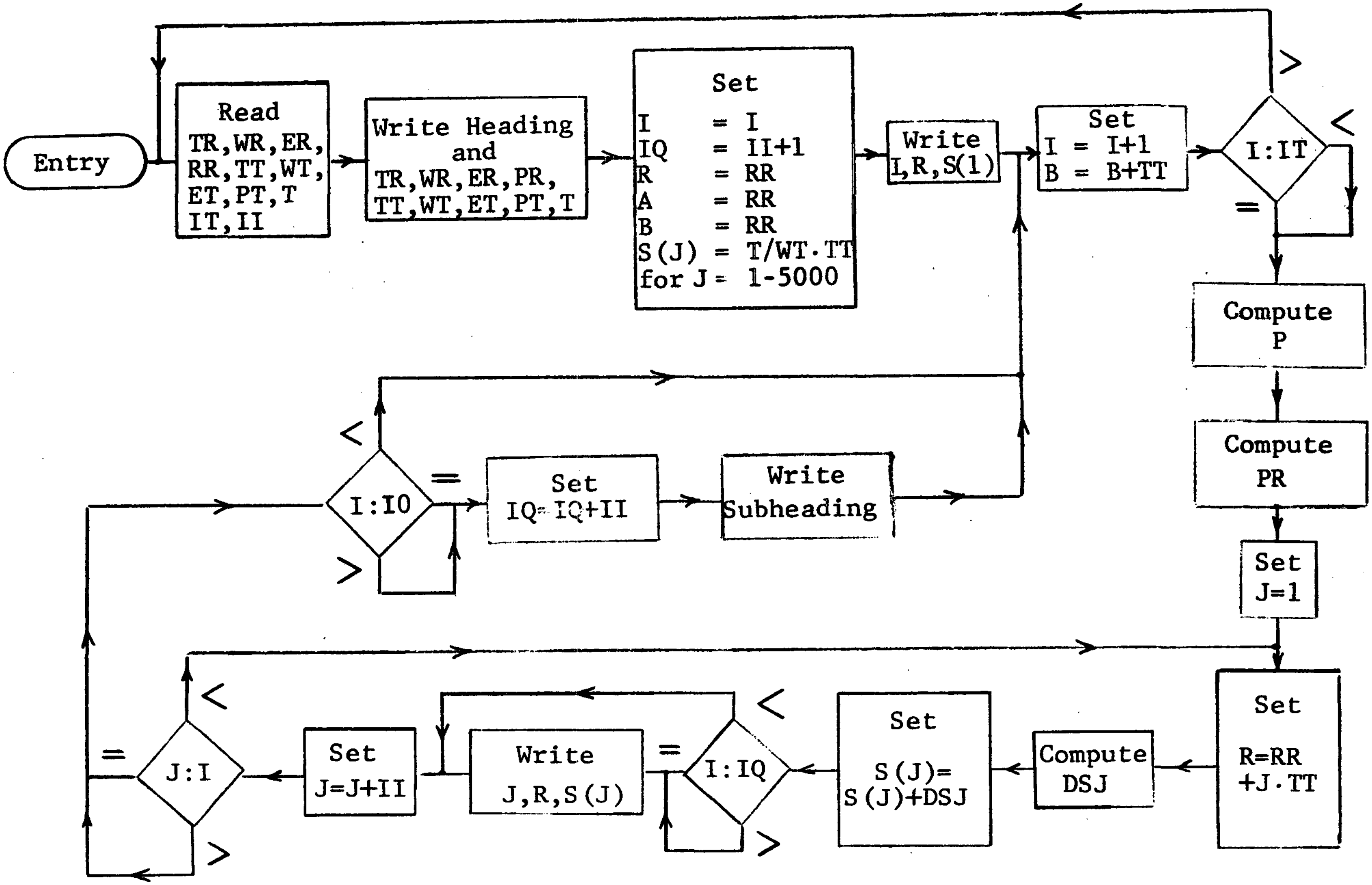

Figure 51

TAPE PACK ANALYSIS COMPUTER FLOW DIAGRAM

```
      DIMENSION S(5000)
    1 READ (5,2) TR,WR,ER,RR,TT,WT,ET,PT,T,IT,II,RP
    2 FORMAT (2F5.0,F10.0,3F5.0,F10.0,2F5.0,2I5,F5.0)
      RR=RR/2.
      WRITE (6,3) TR,WR,ER,RR,RP,TT,WT,ET,PT,T
    3 FORMAT (19H1TAPE PACK STRESSES///6X2HTR,10X2HWR,10X2HER,10X2HRR,10
     1X2HRP/5E12.4//6X2HTT,10X2HWT,10X2HET,10X2HPT,10X1HT/5E12.4/)
      I=1
      IQ=II+1
      R=RR
      A=RR
      B=RR
      DO 4 J=1,5000
    4 S(J)=T/(WT*TT)
      TL=.52359878*B
      WRITE (6,5) I,R,S(1)
    5 FORMAT (/6H WRAPS,4X6HRADIUS,6X6HSTRESS/I6,2E12.4//6H WRAPS,4X6HRA
     1DIUS,6X6HSTRESS)
    6 I=I+1
      B=B+TT
      TL=TL+.52359878*B
      IF (I-IT) 7,7,1
    7 P=T/(WT*B)
      PR=(P/ET)*(2.*B*B/(B*B-A*A))/((WT/(WR*ER))*((2.*A*(A-TR)+TR*TR)/(T
     1R*(2.*A-TR))+RP)+(B*B+A*A)/(ET*(B*B-A*A))+PT/ET)
      J=1
    8 AJ=J
      R=RR+AJ*TT
      DSJ=(PR*A*A/(R*R))*(B*B+R*R)/(B*B-A*A)-(P*B*B/(R*R))*(A*A+R*R)/(B*
     1B-A*A)
      S(J)=S(J)+DSJ
      IF (I-IQ) 11,9,9
    9 WRITE (6,10) J,R,S(J)
   10 FORMAT (I6,2E12.4)
   11 J=J+II
      IF (J-I) 8,12,12
   12 IF (I-IQ) 6,13,13
   13 IQ=IQ+II
      WRITE (6,14) I,TL
   14 FORMAT (//1H ,I6,10H WRAPS OR ,F5.0,49H FEET OF TAPE WERE USED FOR
     1 THE PRECEDING RESULTS//6H WRAPS,4X6HRADIUS,6X6HSTRESS)
      GO TO 6
      END

END OF UCC 1108 FORTRAN V COMPILATION,      0 *DIAGNOSTIC* MESSAGE(S)
```

Figure 52

TAPE PACK ANALYSIS COMPUTER PROGRAM

Figure 53 shows the minimum tape pack stress for a varied amount of tape as a function of winding tension for a 1/2 in. thick, 2 in. dia. aluminum hub.

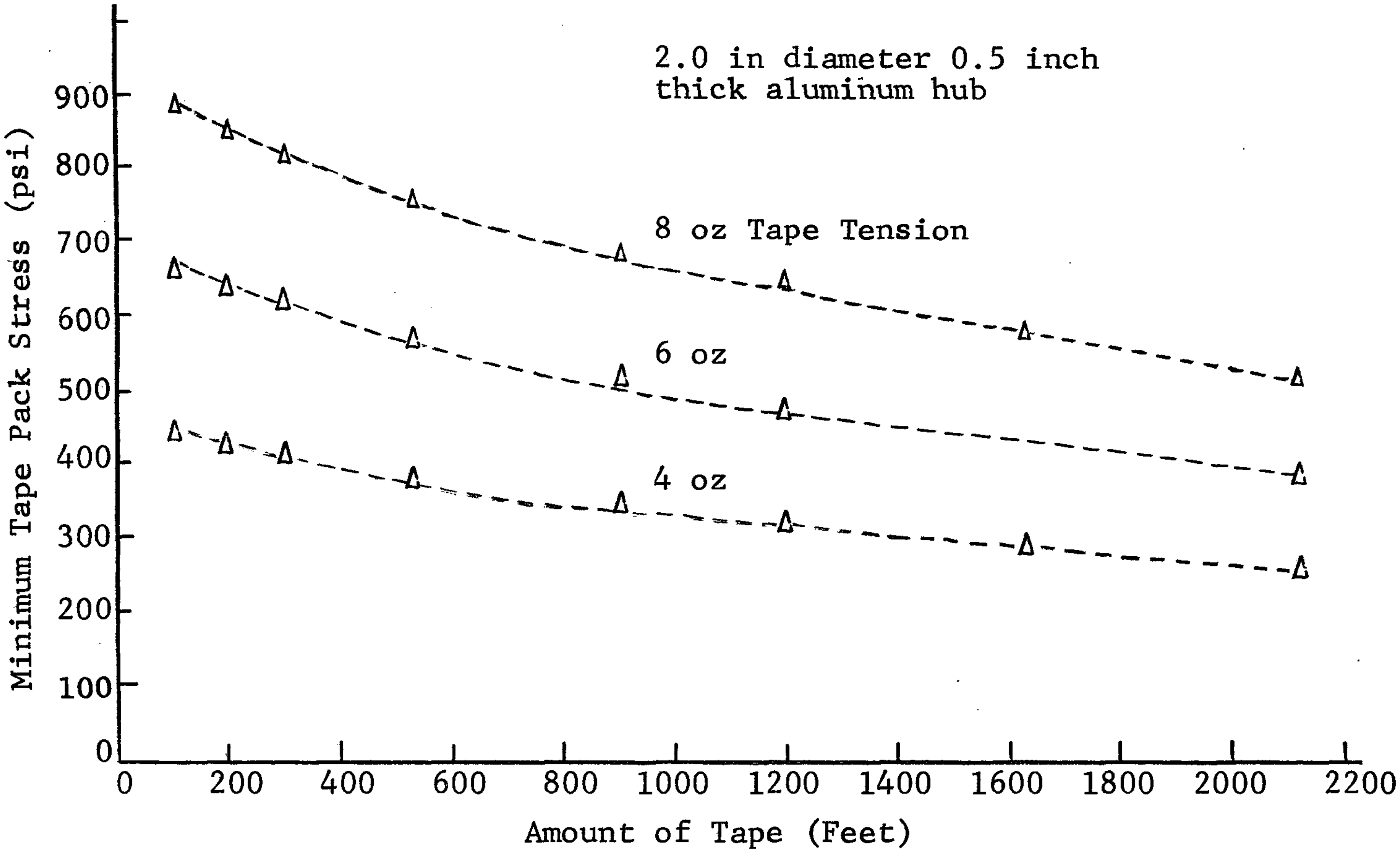

Figure 53

MINIMUM TAPE PACK STRESS AS A FUNCTION OF TAPE PACK
SIZE FOR VARIED WINDING TENSION

3.4 Tape Stress in a Double Coned Roller

3.4.1 Modeling

This analysis is performed to determine the stress in a magnetic tape as it passes over a double coned roller with a cone angle, α, a major radius, $\frac{D}{2}$ and a total wrap angle, θ. As the tape passes around the roller, longitudinal fibers near the center of the tape are elongated more than those near the edge. For the purposes of practical tape transports, the tape is assumed to pass around a straight roller to a double coned roller and onto a second straight roller, (Figure 54). The straight rollers are assumed to be at equal distances, L, from the double cone roller. The tape system is symmetric about the verticle through the double cone roller and therefore the analysis is simplified by investigating half of the total system. The roller radius for small values of α at any position y, Figure 54 is given by

$$r = \frac{D}{2} - y\alpha \tag{94}$$

The length of tape in contact with the roller at any position y is given by

$$L_T = \theta r = \left(\frac{D}{2} - y\alpha \right)\theta \tag{95}$$

At the outside edge of the tape

$$L_{TE} = \theta \left(\frac{D}{2} - \frac{W\alpha}{2} \right) \tag{96}$$

where

W is the tape width

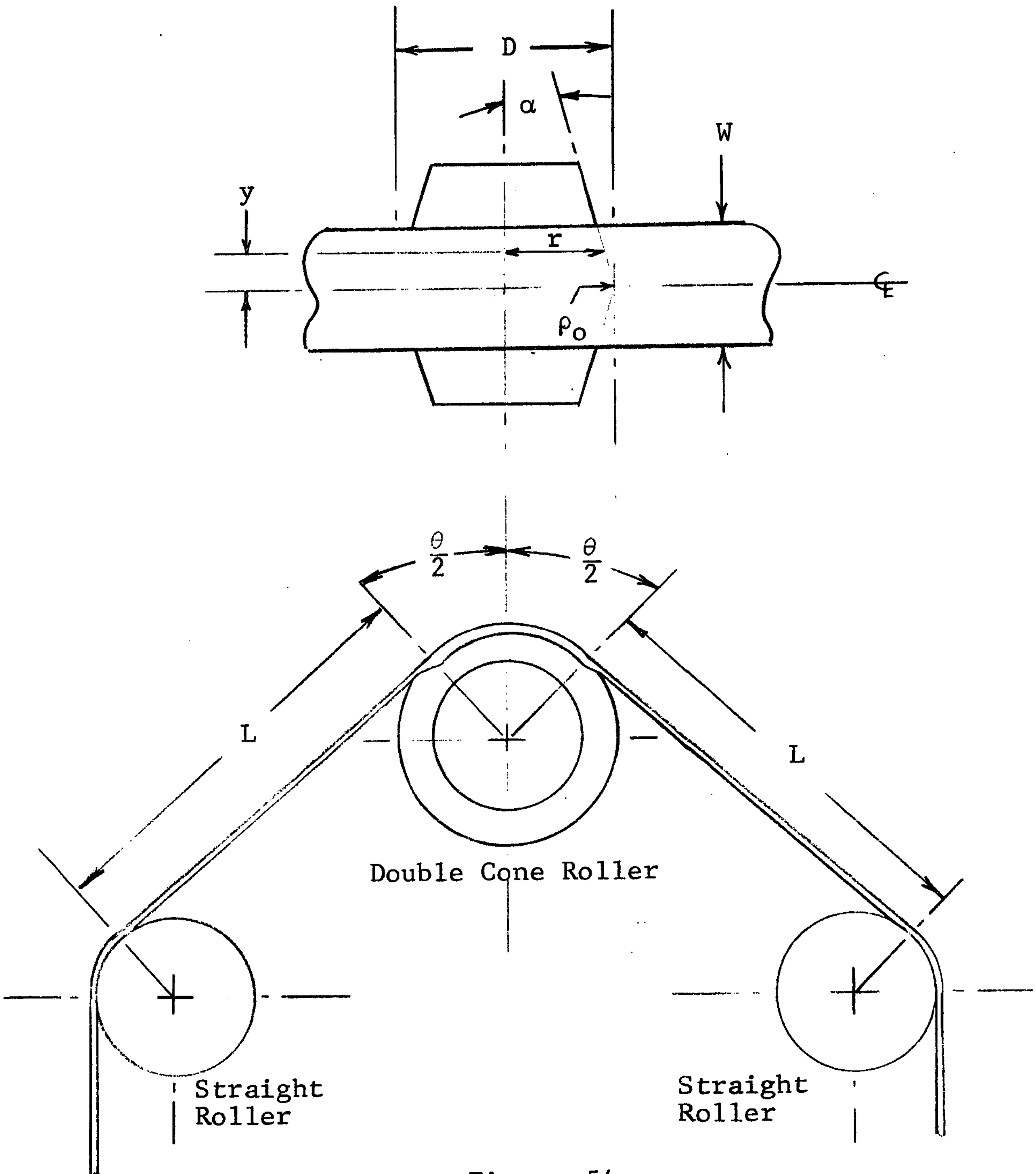

Figure 54

TAPE ROLLER SYSTEM

C4

The difference in the tape length at any position y is

$$\delta = L_T - L_{TE} = \theta\, \alpha (\frac{W}{2} - y) \tag{97}$$

If a first order approximation is used (no Poisson effect) the strain distribution is

$$\varepsilon = \frac{\delta}{L_{TE}} = \frac{2E\alpha (\frac{W}{2} - y)}{D - W\alpha} \tag{98}$$

The stress distribution is

$$\sigma_L = E\varepsilon = \frac{2E\alpha (\frac{W}{2} - y)}{D - W\alpha} \tag{99}$$

For Layer 1

$$\sigma_{L1} = \frac{2E_1\alpha (\frac{W}{2} - y)}{D - W\alpha} \tag{100}$$

For Layer 2

$$\sigma_{L2} = \frac{2E_2\alpha (\frac{W}{2} - y)}{D - W\alpha} \tag{101}$$

The local tension associated with a specific contact width is determined by equating the summation of stresses across the tape to the tape tension.

$$T_R = 2\int_o^{\frac{W_o}{2}} (\sigma_{L1}t_1 + \sigma_{L2}t_2)\, dy \tag{102}$$

where W_o is the total tape width in contact.

This relationship becomes

$$T_R = \frac{\alpha}{2}\left(\frac{E_1t_1 + E_2t_2}{D - W_o\alpha}\right)W_o^{\,2} \tag{103}$$

or an explicit relationship for W_o is

$$W_o = \frac{T_R}{E_1t_1 + E_2t_2}\left[-1 + \sqrt{1 + \frac{2D}{T_R\alpha}(E_1t_1 + E_2t_2)}\right] \tag{104}$$

or approximately

$$W_o \sim \sqrt{\frac{2DT_R}{\alpha}\frac{1}{E_1t_1 + E_2t_2}} \tag{105}$$

The stress, due to excess tension, after total tape width contact is achieved is given by

$$\sigma_1 = \left[\frac{T - T_c}{W}\right]\frac{E_1}{t_1E_1 + t_2E_2} \tag{106}$$

$$\sigma_2 = \left[\frac{T - T_c}{W}\right]\frac{E_2}{E_1t_1 + E_2t_2} \tag{107}$$

T_c is the tension for full tape width contact, W

The stresses along the tape length due to bending around the roller are

$$\sigma_{BA} = \frac{E_1\bar{Y}}{1 - \mu_1^{\,2}}\left(\frac{2}{D} + \frac{\mu_1}{\rho_o}\right) \tag{108}$$

where

ρ_o = radius of curvature of roller apex

$\bar{Y}$ = centroid of the equivalent cross-section

μ_1 = Poisson's ratio inside tape layer

μ_2 = Poisson's ratio outside tape layer and

$$\bar{Y} = \frac{\left[t_1^{\,2} + \frac{E_2}{E_1}\ t_2^{\,2} + 2\,\frac{E_2}{E_1}\ t_1 t_2\right]}{2(t_1 + \frac{E_2}{E_1}\ t_2)}$$

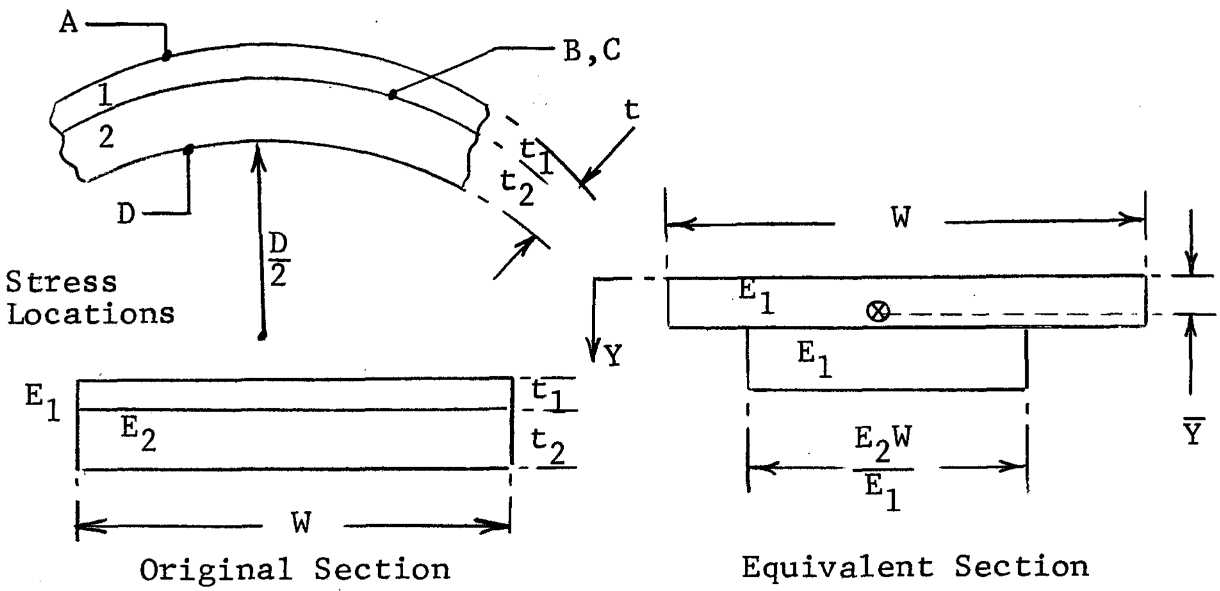

Figure 55

EQUIVALENT CROSS-SECTIONS

$$\sigma_{BB} = E_1\ \frac{(\bar{Y} - t_1)}{1 - \mu_1^{\,2}}\ \left(\frac{2}{D} + \frac{\mu_1}{\rho_o}\right) \tag{109}$$

$$\sigma_{BC} = E_2\ \frac{(\bar{Y} - t_1)}{1 - \mu_2^{\,2}}\ \left(\frac{2}{D} + \frac{\mu_2}{\rho_o}\right) \tag{110}$$

$$\sigma_{BD} = E_2\ \frac{(\bar{Y} - t_1 - t_2)}{1 - \mu_2^{\,2}}\ \left(\frac{2}{D} + \frac{\mu_2}{\rho_o}\right) \tag{111}$$

The stress in the direction of the tape width due to bending around the roller are

$$\sigma_{WA} = \frac{E_1 \bar{\bar{Y}}}{1 - \mu_1^2} \left(\frac{1}{\rho_o} + \frac{2\mu_1}{D} \right) \tag{112}$$

$$\sigma_{WB} = \frac{E_1 (\bar{\bar{Y}} - t_1)}{1 - \mu_2^2} \left(\frac{1}{\rho_o} + \frac{2\mu_1}{D} \right) \tag{113}$$

$$\sigma_{WD} = E_2 \frac{(\bar{\bar{Y}} - t_1)}{1 - \mu_2^2} \left(\frac{1}{\rho_o} + \frac{2\mu_2}{D} \right) \tag{114}$$

$$\sigma_{WD} = E_2 \frac{(\bar{\bar{Y}} - t_1 - t_2)}{1 - \mu_2^2} \left(\frac{1}{\rho_o} + \frac{2\mu_2}{D} \right) \tag{115}$$

The total stress in the direction of tape motion are:

$$\sigma_{LA} = \sigma_{L1} + \sigma_1 + \sigma_{BA} \tag{116}$$

$$\sigma_{LB} = \sigma_{L1} + \sigma_1 + \sigma_{BB} \tag{117}$$

$$\sigma_{LC} = \sigma_{L2} + \sigma_2 + \sigma_{BC} \tag{118}$$

$$\sigma_{LD} = \sigma_{L2} + \sigma_2 + \sigma_{BD} \tag{119}$$

3.4.2 Computational Procedure

The preceding tape stresses and their respective contact widths were programmed for analysis on the digital computer. A description of the computer input data is shown in Figure 56 and the computer program in Figure 57. A sample of the output data generated from this analysis is shown in Figure 58 where principal stresses are given for both the oxide layer and mylar layer at each of two parts, that is, on the outer surface and on the inner surface. The direction of the principal stresses are also specified as along the length, width, and thickness. As is usual, positive stresses are tensile and negative stresses are compressive. The actual width of tape in contact with the roller is also printed out as contact width.

Code	Nomenclature	Field	Format	Units
I	Orientation 1 = oxide out 0 = oxide in	1	I1	—
D	Roller major diameter	2-10	F9.0	in
TT	Total tape tension	11-20	F10.0	oz
W	Tape width	21-30	F10.0	in
R	Roller apex curvature	31-40	F10.0	in
ALP	Cone tape angle	41-50	F10.0	rad
TO	Oxide thickness	1-10	F10.0	in
TM	Mylar thickness	11-20	F10.0	in
EO	Elastic modulus of oxide	21-30	F10.0	psi
EM	Elastic modulus of Mylar	31-40	F10.0	psi
PO	Poisson's ratio, oxide	41-50	F10.0	—
PM	Poisson's ratio, Mylar	51-60	F10.0	—

Figure 56

TAPE STRESSES OVER DOUBLE CONE ROLLER INPUT DATA

```
    1 READ(5,2) I,D,TT,W,R,ALP
    2 FORMAT (I1,F9.0,5F10.0)
      READ (5,3) TO,TM,EO,EM,PO,PM
    3 FORMAT (6F10.0)
      IF(I) 4,4,5
    4 E1=EO
      E2=EM
      P1=PO
      P2=PM
      T1=TO
      T2=TM
      TW=TT/W
      GO TO 6
    5 E1=EM
      E2=EO
      P1=PM
      P2=PO
      T1=TM
      T2=TO
      TW=TT/W
    6 CONTINUE
      CW=W
      T1L=T1
      T2L=T2
      EL=E2*(1.-P1*P1)/(E1*(1.-P2*P2))
      TE=T1L*E1+T2L*E2
      Y=(T1L*T1L+EL*T2L*T2L+2.*EL*T1L*T2L)/(2.*(T1L+EL*T2L))
      SBA=(E1*Y/(1.-P1*P1))*(2./D+P1/R)
      SBB=(E1*(Y-T1L)/(1.-P1*P1))*(2./D+P1/R)
      SBC=(E2*(Y-T1L)/(1.-P2*P2))*(2./D+P2/R)
      SBD=(E2*(Y-T1L-T2L)/(1.-P2*P2))*(2./D+P2/R)
      RHO=D/2.
      ABC=(RHO-CW*ALP)
      Q1=(E1*ALP*CW)/(ABC)
      Q2=(E2*ALP*CW)/(ABC)
      TR=((ALP/2.)*TE*CW*CW)/(RHO-CW*ALP)
      TWL=TW/16.-TR/CW
      IF (TWL) 30,31,31
   30 CW=(TT/TE)*(-1.+(1.+(2.*RHO*TE)/(TT*ALP))**.5)
      ABC=(RHO-CW*ALP)
      Q1=(E1*ALP*CW)/(ABC)
      Q2=(E2*ALP*CW)/(ABC)
   31 S1=TWL*E1/TE
      S2=TWL*E2/TE
      SLA=SBA+Q1+S1
      SLB=SBB+Q1+S1
      SLC=SBC+Q2+S2
      SLD=SBD+Q2+S2
      SWA=(E1*Y/(1.-P1*P1))*(1./R+2.*P1/D)
      SWB=(E1*(Y-T1L)/(1.-P1*P1))*(1./R+2.*P1/D)
```

Figure 57

COMPUTER PROGRAM FOR STRESS ANALYSIS
(DOUBLE CONE ROLLER)

```
      SWC=(E2*(Y-T1L)/(1.-P2*P2))*(1./R+2.*P2/D)
      SWD=(E2*(Y-T1L-T2L)/(1.-P2*P2))*(1./R+2.*P2/D)
      STA=0.0
      STB=0.0
      STC=0.0
      STD=0.0
      T=TW*W
      TR=TR*16.
      IF (I) 7,7,8
    7 SOSL = SLA
      SOST = STA
      SOSW = SWA
      SOCL = SLB
      SOCT = STB
      SOCW = SWB
      SMSL = SLD
      SMST = STD
      SMSW = SWD
      SMCL = SLC
      SMCT = STC
      SMCW = SWC
       GO TO 20
    8 SOSL = SLD
      SOST = STD
      SOSW = SWD
      SOCL = SLC
      SOCT = STC
      SOCW = SWC
      SMSL = SLA
      SMST = STA
      SMSW = SWA
      SMCL = SLB
      SMCT = STB
      SMCW = SWB
   20 CONTINUE
      WRITE (6,9)
    90FORMAT (1H1,10X, 54HPRINCIPAL STRESSES IN TAPE PASSING OVER DB-CNE
     1D ROLLER ////)
      WRITE (6,10)
   10 FORMAT (5X,19HPHYSICAL PARAMETERS //)
      WRITE (6,14)TT,W,D,R,CW
   140FORMAT ( 8X,30HTAPE TENSION                       ,F10.2,2X,3HOZ.,/
     1         8X,30HTAPE WIDTH                         ,F10.3,2X,3HIN.,/
     2         8X,30HROLLER DIAMETER                    ,F10.3,2X,3HIN.,/
     3         8X,30HCROWN RADIUS                       ,F10.2,2X,3HIN.,/
     4         8X,30HCONTACT WIDTH                      ,F10.2,2X,3HIN.//)
      WRITE (6,11)
   11 FORMAT (5X,15HTAPE PROPERTIES //)
      WRITE (6,15)TO,TM,EO,EM,PO,PM
   150FORMAT ( 8X,30HOXIDE THICKNESS                    ,F10.5,2X,3HIN.,/
```

Figure 57 (Cont.)

COMPUTER PROGRAM FOR STRESS ANALYSIS
(DOUBLE CONE ROLLER)

```
     1           8X,30HMYLAR THICKNESS                  ,F10.5,2X,3HIN.,/
     2           8X,30HOXIDE ELASTIC MODULUS            ,F10.0,2X,3HPSI,/
     3           8X,30HMYLAR ELASTIC MODULUS            ,F10.0,2X,3HPSI,/
     4           8X,30HPOISSON'S RATIO (OXIDE)          ,F10.2,2X,3H   ,/
     5           8X,30HPOISSON'S RATIO (MYLAR)          ,F10.2,2X,3H   ,//)
       IF (I) 25,25,26
    25 WRITE (6,12)
    12 FORMAT(5X,43HOXIDE STRESSES,PSI (OXIDE AWAY FROM ROLLER)//)
       GO TO 23
    26 WRITE (6,22)
    22 FORMAT (5X,41HOXIDE STRESSES,PSI (OXIDE AGAINST ROLLER)//)
    23 CONTINUE
       WRITE (6,16) SOSL,SOST,SOSW,SOCL,SOCT,SOCW
    160FORMAT ( 8X,30HSURFACE,LENGTH DIRECTION          ,F10.0,2X,3HPSI,/
     1           8X,30HSURFACE,THICKNESS DIRECTION       ,F10.0,2X,3HPSI,/
     2           8X,30HSURFACE,WIDTH DIRECTION           ,F10.0,2X,3HPSI,/
     3           8X,30HCENTER,LENGTH DIRECTION           ,F10.0,2X,3HPSI,/
     4           8X,30HCENTER,THICKNESS DIRECTION        ,F10.0,2X,3HPSI,/
     5           8X,30HCENTER,WIDTH DIRECTION            ,F10.0,2X,3HPSI,//)
       WRITE (6,13)
    13 FORMAT (5X,18HMYLAR STRESSES,PSI //)
       WRITE (6,17) SMSL,SMST,SMSW,SMCL,SMCT,SMCW
    170FORMAT ( 8X,30HSURFACE,LENGTH DIRECTION          ,F10.0,2X,3HPSI,/
     1           8X,30HSURFACE,THICKNESS DIRECTION       ,F10.0,2X,3HPSI,/
     2           8X,30HSURFACE,WIDTH DIRECTION           ,F10.0,2X,3HPSI,/
     3           8X,30HCENTER,LENGTH DIRECTION           ,F10.0,2X,3HPSI,/
     4           8X,30HCENTER,THICKNESS DIRECTION        ,F10.0,2X,3HPSI,/
     5           8X,30HCENTER,WIDTH DIRECTION            ,F10.0,2X,3HPSI,//)
       GO TO 1
       END

 END OF UCC 1108 FORTRAN V COMPILATION.     0 *DIAGNOSTIC* MESSAGE(S)
```

Figure 57 (Cont.)

COMPUTER PROGRAM FOR STRESS ANALYSIS
(DOUBLE CONE ROLLER)

PRINCIPAL STRESSES IN TAPE PASSING OVER DB-CNED ROLLER 2°

PHYSICAL PARAMETERS

TAPE TENSION	4.00	OZ.
TAPE WIDTH	.500	IN.
ROLLER DIAMETER	1.500	IN.
CROWN RADIUS	1.00	IN.
CONTACT WIDTH	.19	IN.

TAPE PROPERTIES

OXIDE THICKNESS	.00020	IN.
MYLAR THICKNESS	.00092	IN.
OXIDE ELASTIC MODULUS	100000.	PSI
MYLAR ELASTIC MODULUS	650000.	PSI
POISSON'S RATIO (OXIDE)	.40	
POISSON'S RATIO (MYLAR)	.40	

OXIDE STRESSES,PSI (OXIDE AWAY FROM ROLLER)

SURFACE,LENGTH DIRECTION	568.	PSI
SURFACE,THICKNESS DIRECTION	0.	PSI
SURFACE,WIDTH DIRECTION	117.	PSI
CENTER,LENGTH DIRECTION	527.	PSI
CENTER,THICKNESS DIRECTION	0.	PSI
CENTER,WIDTH DIRECTION	81.	PSI

MYLAR STRESSES,PSI

SURFACE,LENGTH DIRECTION	2189.	PSI
SURFACE,THICKNESS DIRECTION	0.	PSI
SURFACE,WIDTH DIRECTION	-567.	PSI
CENTER,LENGTH DIRECTION	3423.	PSI
CENTER,THICKNESS DIRECTION	0.	PSI
CENTER,WIDTH DIRECTION	524.	PSI

Figure 58

PRINCIPAL STRESSES IN TAPE PASSING OVER DOUBLE CONE ROLLER

PRINCIPAL STRESSES IN TAPE PASSING OVER DB-CNED ROLLER -3°

PHYSICAL PARAMETERS

TAPE TENSION	4.00	OZ.
TAPE WIDTH	.500	IN.
ROLLER DIAMETER	1.500	IN.
CROWN RADIUS	1.00	IN.
CONTACT WIDTH	.15	IN.

TAPE PROPERTIES

OXIDE THICKNESS	.00020	IN.
MYLAR THICKNESS	.00092	IN.
OXIDE ELASTIC MODULUS	100000.	PSI
MYLAR ELASTIC MODULUS	650000.	PSI
POISSON'S RATIO (OXIDE)	.40	
POISSON'S RATIO (MYLAR)	.40	

OXIDE STRESSES,PSI (OXIDE AWAY FROM ROLLER)

SURFACE,LENGTH DIRECTION	665.	PSI
SURFACE,THICKNESS DIRECTION	0.	PSI
SURFACE,WIDTH DIRECTION	117.	PSI
CENTER,LENGTH DIRECTION	624.	PSI
CENTER,THICKNESS DIRECTION	0.	PSI
CENTER,WIDTH DIRECTION	81.	PSI

MYLAR STRESSES,PSI

SURFACE,LENGTH DIRECTION	2820.	PSI
SURFACE,THICKNESS DIRECTION	0.	PSI
SURFACE,WIDTH DIRECTION	-567.	PSI
CENTER,LENGTH DIRECTION	4054.	PSI
CENTER,THICKNESS DIRECTION	0.	PSI
CENTER,WIDTH DIRECTION	524.	PSI

Figure 58 (Cont.)

PRINCIPAL STRESSES IN TAPE PASSING OVER DOUBLE CONE ROLLER

PRINCIPAL STRESSES IN TAPE PASSING OVER DB-CNED ROLLER 3°

PHYSICAL PARAMETERS

TAPE TENSION	6.00	OZ.
TAPE WIDTH	.500	IN.
ROLLER DIAMETER	1.500	IN.
CROWN RADIUS	1.00	IN.
CONTACT WIDTH	.19	IN.

TAPE PROPERTIES

OXIDE THICKNESS	.00020	IN.
MYLAR THICKNESS	.00092	IN.
OXIDE ELASTIC MODULUS	100000.	PSI
MYLAR ELASTIC MODULUS	650000.	PSI
POISSON'S RATIO (OXIDE)	.40	
POISSON'S RATIO (MYLAR)	.40	

OXIDE STRESSES,PSI (OXIDE AWAY FROM ROLLER)

SURFACE,LENGTH DIRECTION	785.	PSI
SURFACE,THICKNESS DIRECTION	0.	PSI
SURFACE,WIDTH DIRECTION	117.	PSI
CENTER,LENGTH DIRECTION	744.	PSI
CENTER,THICKNESS DIRECTION	0.	PSI
CENTER,WIDTH DIRECTION	81.	PSI

MYLAR STRESSES,PSI

SURFACE,LENGTH DIRECTION	3601.	PSI
SURFACE,THICKNESS DIRECTION	0.	PSI
SURFACE,WIDTH DIRECTION	-567.	PSI
CENTER,LENGTH DIRECTION	4835.	PSI
CENTER,THICKNESS DIRECTION	0.	PSI
CENTER,WIDTH DIRECTION	524.	PSI

Figure 58 (Cont.)

PRINCIPAL STRESSES IN TAPE PASSING
OVER DOUBLE CONE ROLLER

PRINCIPAL STRESSES IN TAPE PASSING OVER DB-CNED ROLLER 3°

PHYSICAL PARAMETERS

TAPE TENSION	8.00	OZ.
TAPE WIDTH	.500	IN.
ROLLER DIAMETER	1.500	IN.
CROWN RADIUS	1.00	IN.
CONTACT WIDTH	.21	IN.

TAPE PROPERTIES

OXIDE THICKNESS	.00020	IN.
MYLAR THICKNESS	.00092	IN.
OXIDE ELASTIC MODULUS	100000.	PSI
MYLAR ELASTIC MODULUS	650000.	PSI
POISSON'S RATIO (OXIDE)	.40	
POISSON'S RATIO (MYLAR)	.40	

OXIDE STRESSES,PSI (OXIDE AWAY FROM ROLLER)

SURFACE,LENGTH DIRECTION	886.	PSI
SURFACE,THICKNESS DIRECTION	0.	PSI
SURFACE,WIDTH DIRECTION	117.	PSI
CENTER,LENGTH DIRECTION	845.	PSI
CENTER,THICKNESS DIRECTION	0.	PSI
CENTER,WIDTH DIRECTION	81.	PSI

MYLAR STRESSES,PSI

SURFACE,LENGTH DIRECTION	4259.	PSI
SURFACE,THICKNESS DIRECTION	0.	PSI
SURFACE,WIDTH DIRECTION	-567.	PSI
CENTER,LENGTH DIRECTION	5493.	PSI
CENTER,THICKNESS DIRECTION	0.	PSI
CENTER,WIDTH DIRECTION	524.	PSI

Figure 58 (Cont.)

PRINCIPAL STRESSES IN TAPE PASSING
OVER DOUBLE CONE ROLLER

PRINCIPAL STRESSES IN TAPE PASSING OVER DB-CNED ROLLER 3°

PHYSICAL PARAMETERS

TAPE TENSION	10.00	OZ.
TAPE WIDTH	.500	IN.
ROLLER DIAMETER	1.500	IN.
CROWN RADIUS	1.00	IN.
CONTACT WIDTH	.24	IN.

TAPE PROPERTIES

OXIDE THICKNESS	.00020	IN.
MYLAR THICKNESS	.00092	IN.
OXIDE ELASTIC MODULUS	100000.	PSI
MYLAR ELASTIC MODULUS	650000.	PSI
POISSON'S RATIO (OXIDE)	.40	
POISSON'S RATIO (MYLAR)	.40	

OXIDE STRESSES, PSI (OXIDE AWAY FROM ROLLER)

SURFACE, LENGTH DIRECTION	976.	PSI
SURFACE, THICKNESS DIRECTION	0.	PSI
SURFACE, WIDTH DIRECTION	117.	PSI
CENTER, LENGTH DIRECTION	934.	PSI
CENTER, THICKNESS DIRECTION	0.	PSI
CENTER, WIDTH DIRECTION	81.	PSI

MYLAR STRESSES, PSI

SURFACE, LENGTH DIRECTION	4840.	PSI
SURFACE, THICKNESS DIRECTION	0.	PSI
SURFACE, WIDTH DIRECTION	-567.	PSI
CENTER, LENGTH DIRECTION	6074.	PSI
CENTER, THICKNESS DIRECTION	0.	PSI
CENTER, WIDTH DIRECTION	524.	PSI

Figure 58 (Cont.)

PRINCIPAL STRESSES IN TAPE PASSING OVER DOUBLE CONE ROLLER

3.5 Bearings and Lubrication

A general review of bearing technology has identified the anti-friction ball bearing as an excellent candidate for the five-year transport. Utilizing conservative design procedures, for both the bearing and its lubricant system, will produce a highly reliable bearing system, if meticulous cleanliness procedures and cautious assembly practice are followed during the fabrication and check-out phases. The application of rolling bearings to the five-year transport is further enhanced over other bearing techniques, e.g., the aerostatic bearing, because it is easily incorporated into the transport structure with only minimal penalties in power consumption. Relative to this latter point, the ball bearing requires an order of magnitude (a factor of 20) less power than its equivalent aerostatic (pressurized air) bearing.

Traditionally, instrument ball bearings have been used in satellite recorders because they require the lowest power levels. Instrument ball bearings differ from the standard contact type ball bearing in that the curvature between balls and races is greater. Standard load carrying bearings have a curvature ratio of approximately 52% while instrument bearings are about 57%. The larger degree of curvature, see Figure 59, (increasing percentage) leads to higher contact stress, but also to lower torque resistance. For the goals of the five-year transport, this type of trade away from reliability cannot be made so automatically. To achieve the reliability levels required here, major design areas dominating the use of ball bearings are:

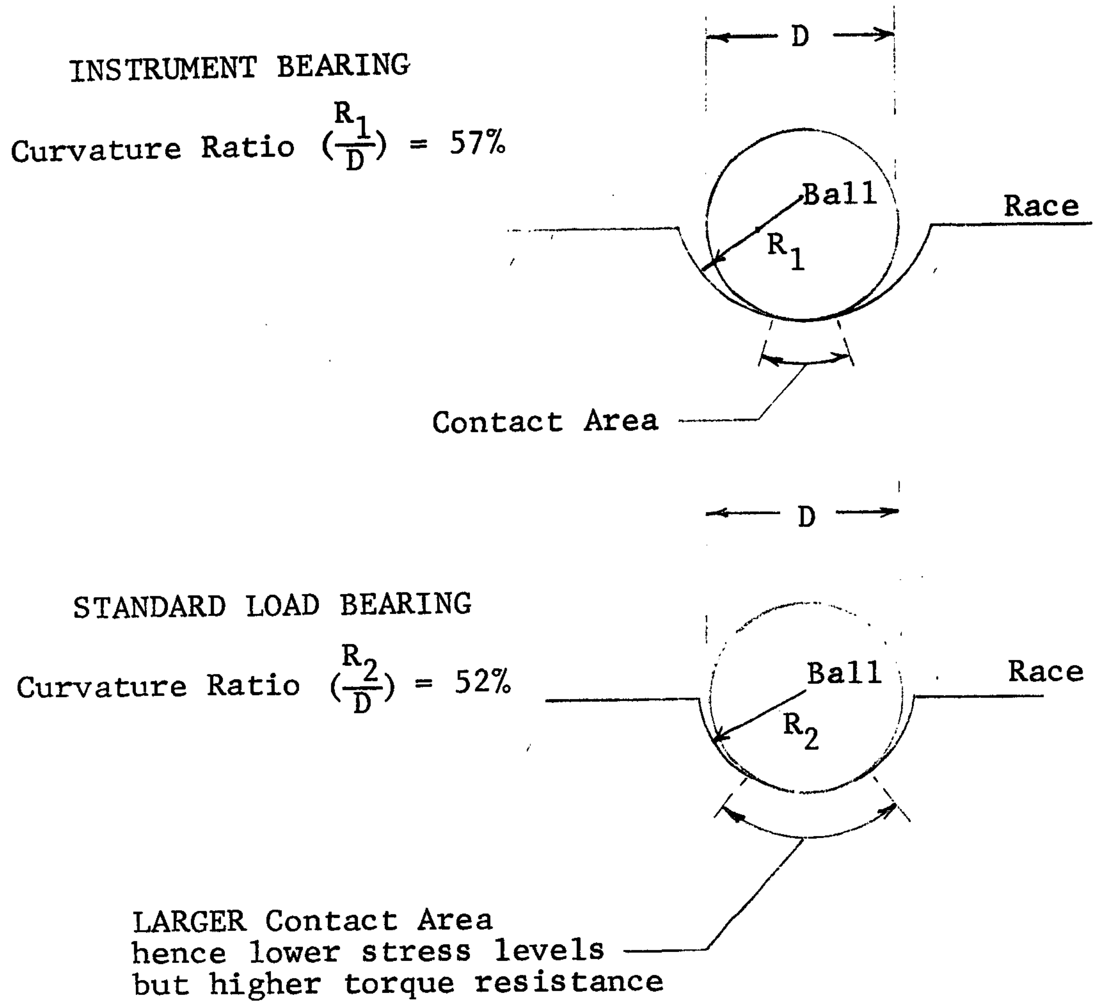

Figure 59

CURVATURE RATIOS FOR STANDARD AND INSTRUMENT BEARINGS

- Designing for installation, that is, specifying installation practices which do not contribute excessive installation loads and hence only bearing failure.
- Use under a limiting contact stress for both short term loads, e.g., high "g" shock loads, and the operating loads resulting from pre-loads and tape tensions.
- Lubricant system design for long term effectiveness.
- Final bearing selection after bearing testing.

Relative to the above, the following sections elaborate on the basic technology and specify a recommended design and testing procedure for the total bearing system, i.e., bearing and lubricant.

3.5.1 Bearing Contact Stresses

3.5.1.1 General

Loads between balls and races produce large stresses because of the resulting small contact areas. Due to the effects of surface curvature, the inner race will generally experience larger stress levels than the outer race. To quantitize these stress levels, investigations have utilized Hertzian contact stress theory that specifies the contact area as a portion of the surface of an ellipsoid of revolution. From this type of analysis, stress levels of 200,000 to 500,000 psi can be rationalized, previous use of point loads did not yield direct insight into the mechanics within the ball to race contact region. Because of the analytical complexity associated with the elasticity analysis of ball bearings, a vast assemblage of analytical and experimental data has been developed to predict the stress distributions throughout the bearing set. Most of this experimental data focuses on determining the magnitude of the contact region for a range of bearing parameters, and also on developing approximate stress and load formulae. To these results, the following sections are addressed.

3.5.1.2 Contact Stresses Under Combined Radial and Axial Loads

For the applications to the five-year transport, bearing assemblies will be subjected to both radial and axial loads. Normal transport loads result from tape tensions (radial forces) and pre-load forces (axial forces). During launch, shock and vibration can produce stress levels several times greater than those ordinarily encountered. Hence, its imperative that stresses be evaluated for the launch as well as the orbiting modes. For the short term loads, industry practice recommends contact stresses no more than 300,000 psi; whereas, for the long term operating conditions, maximum stresses of about 200,000 psi are recommended. To calculate these stresses, the following equations are provided:

$$\bar{Q} = \frac{F_r}{J_r Z \cos \alpha} = \frac{F_a}{J_a Z \sin \alpha} \tag{120}$$

where

$\bar{Q}$ = max contact load

F_r = applied radial load

F_a = applied axial load

Z = number of balls

α = contact angle during load

J_r = radial bearing parameter[9]

J_a = axial bearing parameter[9]

The dimensionless bearing parameters J_r, J_a, are tabulated for various values of $\frac{F_r}{F_a} \tan \alpha$.

Using $\overline{Q}$ from equation 120 the following relationship from Hertzian contact stress theory is employed to determine the maximum stress, e.g.:

$$\overline{\sigma} = \frac{\overline{Q}}{2\pi ab} \tag{121}$$

where

σ = maximum compressive stress, psi

a,b = contact area parameters for various ball and race curvatures and $\overline{Q}$. These parameters are also tabulated in Harris[7].

Thus, by determining the applied loads for normal operation as well as during launch, the resulting stresses can be calculated and then compared to the following criteria for long life:

$$\begin{aligned} &\overline{\sigma} < 200{,}000 \text{ psi} && \text{normal loads - both radial and pre-load} \\ &\overline{\sigma} < 300{,}000 \text{ psi} && \text{normal transport loads plus shock and vibration loads} \end{aligned} \tag{122}$$

3.5.1.3 <u>Preload Effects</u>

The techniques of pre-loading bearings have been employed in transport technology as a basic method for removing radial and axial play, and thereby assuring greater rotational accuracy of the rotating shaft. Originally, stringent wow and flutter requirements dominated the design to the point where substantial emphasis was placed upon achieving a high degree of mechanical accuracy. By selecting Precision Class 7 or 9 instrument bearings and then utilizing pre-loading and precise machining practices, the requirements for dimensional accuracy were largely attained. Pre-loading produces further advantages by developing a smoother running bearing. Reduced torque pulsations result because the ball-race geometrical relationships remain essentially constant under varying loads; and further, self-excited oscillations between balls and races are diminished.

In the development of a five-year transport, extremely fine running bearings are not nearly as important as assuring a high probability of survival for the mission life. Hence, the balance between wow and flutter performance and reliability must be established. For this case, a direct link exists between life and pre-loading. Figure 60 illustrates the maximum contact stress resulting pre-loading a R4B ball bearing. It is seen that for relatively small axial loads, rather appreciable stresses ($\overline{\sigma} > 200{,}000$ psi) occur. For maximum life, minimization of $\overline{\sigma}$ must also be considered in balance with the necessity for eliminating self-excited oscillations. These oscillations contribute to the reduction of operational life by increasing the number of applied load cycles. To obtain smooth operation, a rule of thumb is to apply an axial pre-load of not more than 10% of the bearings dynamic load capacity. This load level is essentially a limitation on loading because of the effects on fatigue life. In recorder applications, it has been generally found that 1% of the dynamic capacity is sufficient, but this load should be verified experimentally for each case.

The two methods of preloading, that is, shimming (mechanical interference) and spring loading, require thorough analysis prior to their adaptation to the transport system. If shock and vibration isolation between the transport and space vehicle is not possible, shim pre-loading is essential as resonance of the spring loading would result. Resonance must be circumvented because unacceptably large contact stresses will be produced. In general, where large thermal gradiants are encountered, spring pre-loading is mandatory to accommodate differential expansion. Thus, the mission environment from launch through orbital operation dictates the bearing configuration; and further, it must be recognized that conflicting requirements will lead to trades and modifications of the original goals. As an example, if thermal gradiants of 60°C are possible,

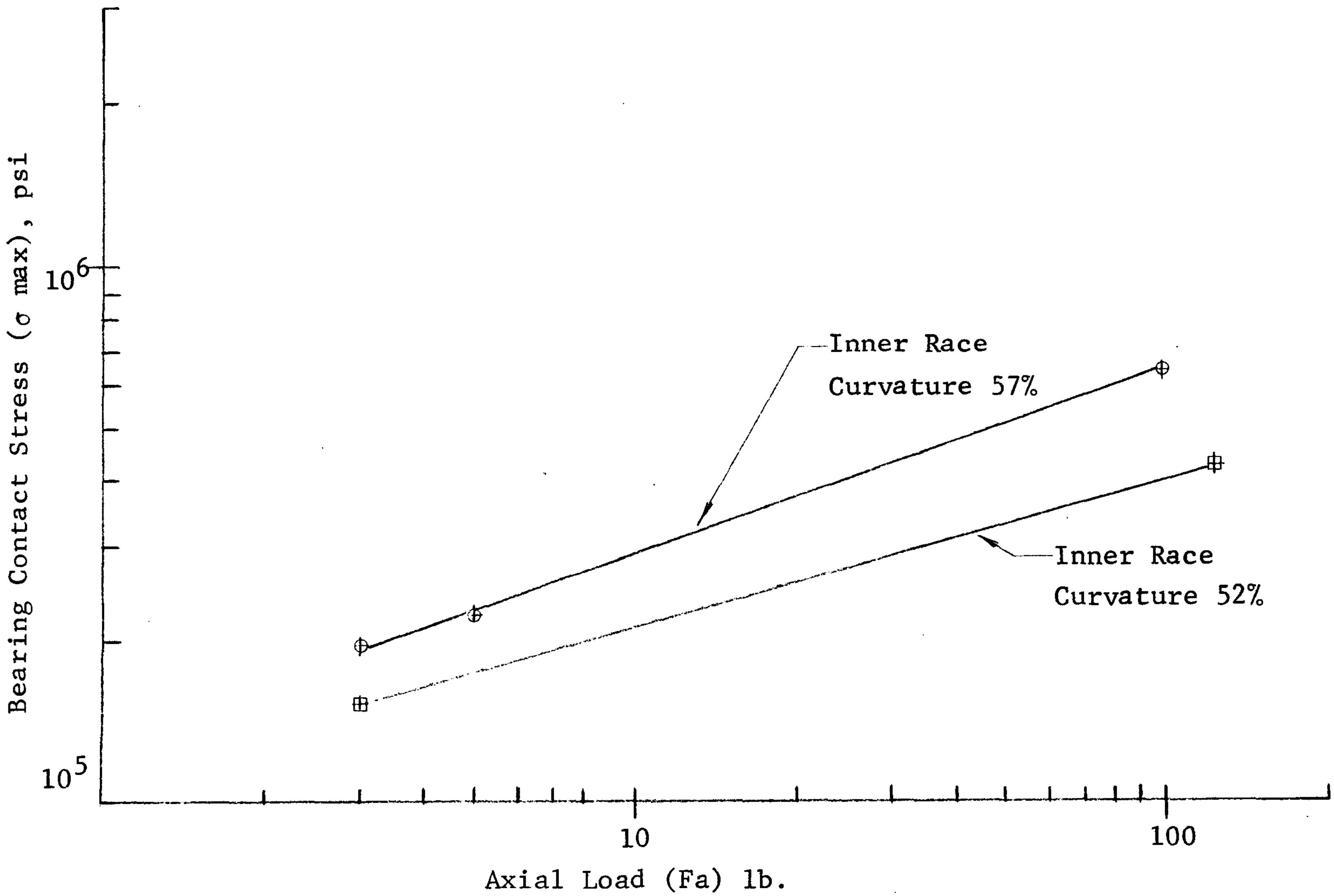

Figure 60

CONTACT STRESS OF R4B SIZE BEARING FOR TWO BEARING CURVATURES it will be necessary to use spring pre-loading and thus shock and vibration isolation techniques must be implemented to maintain the shock and vibration disturbances to low amplitude and frequency levels.

3.5.1.4 Shaft Misalignment

A recent paper in "Wear"[10] illustrates quite graphically the deliterious effects of bearing misalignment. At approximately 5 milli-radians of misalignment the stress on the cage pockets increases rapidly. The article recommends the maintenance of less than 2 milli-radians misalignment which amounts to 2×10^{-3} inches in off axis center. The bearing used for the experimental study reported on in the paper had a one-inch bore and thus could accommodate greater misalignment than the instrument sized bearings which would be used in a recorder. The bearing alignment should be accomplished by through boring the bearing housing. In any case the greatest misalignment that could be accepted is less 0.3 milli-radians or 3×10^{-4} inches off center per axial inch length of shaft.

3.5.2 Bearing Torque

The torque resistant of a bearing - assuming adequate lubrication - can be determined from:

$$M = f_1 \quad F_B d_m \tag{123}$$

where

M = bearing torque

f_1 = coefficient of friction (empirically based calculation)

F_B = combined bearing load

d_m = ball pitch diameter

and

$$f_1 = Z\left(\frac{F_s}{C_s}\right)^y \quad \text{(Ref. 11)} \tag{124}$$

where

F_s = bearing static equivalent load
C_s = bearing static capacity
z and y are functions of the bearing design and are related to the bearing type and bearing construction.

The value of z for ball bearings ranges from 0.003 to 0.0013 and y ranges from 0.33 to 0.4 thus the coefficient of friction, f_1, could range from 1.2×10^{-4} to 6×10^{-4} for $\frac{F_s}{C_s} = 0.1$. The lower coefficient of friction applies to a self-aligning bearing $\alpha = 10°$, and the higher coefficient of friction applies to a deep groove bearing where $\alpha = 0°$. These represent two distinct bearing types.

The bearing equivalent load for bearing friction resistance torque evaluation is:

$$F_B = 0.9\ F_A \cot\alpha - 0.1\ F_r \quad \text{(Ref. 12)} \tag{125}$$

or

$$F_B = F_r \tag{126}$$

where the one yielding the larger value of F_B is used.

As an illustrative example the R4B bearing is selected. Basic parameters of this bearing type are:

$\alpha = 16°$
$d_m = .434$ in.
$F_a = 3$ lb.
$F_r = 16$ oz. = 1 lb.

$F_s \approx 3.2$ lb.
$C_s = 70$ lb.
$\left.\begin{array}{l} Z \approx 0.0005 \\ Y \approx 0.36 \end{array}\right\}$ Table 14.1 Ref. 11

Then from equations 124 and 125

$$F_B = 8.4 \text{ lb.}$$

and

$$f_1 = 0.00047$$

from equation 123

$$M = f_1 \ F_B \ d_m$$
$$= 1.72 \times 10^{-3} \text{ lb.in.}$$
$$= 27.5 \times 10^{-3} \text{ oz.in.}$$

The power required for the bearing friction resistance operating at a shaft speed of 2,000 rpm ($\omega = 209$ rad/s) is:

$$P = \omega M \tag{127}$$

or

$$P = 40.8 \times 10^{-3} \text{ watts/bearing}$$

Obviously if the radial load (F_r in equation 125) is the major component of the loading then any perturbation of the tape tension will be reflected directly in the bearing friction torque. If, on the other hand, the radial load is a fraction of the axial load then any tape tension perturbation would have a very weak effect on the bearing friction resistance. The bearing frictional resistance due to the windage effect of the lubricant oil is approximately one order of magnitude less than resistance due to the bearing loadings.

3.5.3 Bearing Life Prediction

Bearing life prediction is based on the experimental data developed by the bearing manufacturers. All of the bearing manufacturer's catalogue data is based on the L_{10} life. The L_{10} life is the life that 90% of the bearing would exhibit if loaded and cycled in an identical manner, i.e., speed, load, lubricant, and temperature.

The basic dynamic capacity for both the outer and inner race of a ball bearing is given by:

(Ref. 13)

$$Q_c = A \left(\frac{2f}{2f-1}\right)^{0.41} \cdot K \left(\frac{\gamma}{\cos \alpha}\right)^{0.3} (D)^{1.8} \quad (Z)^{-0.33} \quad \text{lbs.} \tag{128}$$

where

A = material constant

f = curvature (r/D)

r = raceway groove radius

D = ball diameter

$\gamma = \dfrac{D \cos \alpha}{dm}$

dm = pitch diameter

α = contact angle

Z = number of balls

$K = \dfrac{(1 - \gamma)^{1.39}}{(1 + \gamma)^{0.333}}$ for inner race contact

$K = \dfrac{(1 + \gamma)^{1.39}}{(1 - \gamma)^{0.333}}$ for outer race contact

The smallest value of Q_c is that value of the contact load for which 90% of the bearing will withstand one million (10^6) revolutions without failure. The value of A is dependent on the type bearing and the type and hardness of the bearing steel. For single row ball bearings the value of A was determined to be 7450 from the statistical data, however, Palmgren[14] recommends that a value of 7080 should be used to account for manufacturing inaccuracies.

Once the maximum contact load is determined from equation 120 the life (L) in revolutions for the desired bearing load can be determined from:

$$L = \left(\frac{Q_c}{Q}\right)^3 \tag{129}$$

This life (L) in revolutions is the L_{10} life, i.e., the probability of survival for L revolutions is 90% since it is based on L_{10} life studies and analysis of the Weiball statistical life plots. Note that this life is, for the case considered, either inner or outer race contact. The life of the bearing is based on the probability of failure for both races. The life (L) in revolutions for both inner and outer race is:

$$L = (L_i^{-1.111} + L_o^{-1.111})^{-0.9} \tag{130}$$

where

L_i = L_{10} life of inner race

L_o = L_{10} life of outer race

Estimates must be made for a life rating beyond the L_{10} life. There are a number of methods that can be used[15]. The method which will be used is that presented by McCool[16]. If a survival probability of S is desired then the life (L_s) in revolutions is:

$$L_s = A_1 A_2 A_3 \left(\frac{Q_c}{Q}\right)^k \tag{131}$$

where

k = 3 for ball bearings

A_1 = reliability factor

A_2 = environment factor

A_3 = material factor

The reliability factor A_1 is the factor that pushes the extrapolation of the 90% experimental data supporting L_{10} bearing life. McCool[16] lists the desired probability of survival, s, in percent from 90 to 99 versus the A_1 factor as:

S%	90	95	96	97	98	99
A_1	1.0	.62	.53	.44	.33	.21

and gives the following equation which can be used to determine A_1 for $0.90 < S < .999$ as

$$A_1 = \frac{1}{K} \left(\ln \frac{1}{S}\right)^{\frac{1}{1.5}} \tag{132}$$

where K = 0.10536 for ball bearings.

Since the bearings will be fabricated from first class vacuum degassed special melts the use of $A_3 = 1$ is conservative. Actually the standard material 52100 produced by special process can result in an L_{10} life in excess of the L_{10} life predicted by the bearing standards. Such examples have been reported[16] where L_{10} life has been extended by a factor of 20.

The environment factor A_2 is equal to unity under standard conditions and is predominantly effected by the lubricant. If a full lubricant film can be maintained, then $A_2 = 1$ is conservative.

One can object to the use of the A_1, A_2, and A_3 factors (see discussion reference[16] , however until a considerable body of data for 99% probability of survival is developed one must extrapolate and this method separates out the important factors. The environmental factor A_2 is of particular interest for instrument bearings as it illustrates the importance of the lubricant.

3.5.4 Materials

For fatigue resistance, the best bearing steel is vacuumed processed 52100 steel. The steel is vacuum processed to take fullest advantage of the available technology. Essentially what is being paid for by vacuum processing is less dispersion on a Weibull life plot, which is the basis for the life estimate. The 52100 series steel is chosen in the absence of a corrosive atmosphere because of the greater technical background in the production of this alloy, and because its machinability characteristics are slightly superior to the other material candidate, 440C stainless steel.

Both 440C and 52100 steels are well within their preferred operating temperature range since the recorder has a range from -5° to +60°C. However, the recorder tape may have to operate in an environment of relatively high humidity. In this event the 440C stainless steel should be specified because of its greater resistance to corrosion.

For the five year life requirement, most of the common retainer materials such as brass and steel are immediately eliminated. Although these retainer materials can operate successfully over a wide temperature range they suffer from inherent wear pattern problems and a lack of retection of the oil source. The optimum retainer material choice within the temperature region of -5° to +60°C is at present a porous phenolic impregnated with the same oil as that used for lubrication. A possible challenger could be porous bronze, which is currently used for high speed, high temperature applications.

The ball retainer must also be chosen to enhance the overall bearing reliability. The advantages and disadvantages of porous phenolic and porous bronze retainers indicates that experimental validation is in order. With adequate lubrication, a phenolic retainer will exhibit minimal wear. The manner in which it wears is to smear the plastic from ball to raceway and finally seize the bearing because of reduced radial play. With a bronze retainer, the wear consists of small metallic particles which can be thrown out of the bearing. In any case, they do not exhibit the sticking that is shown by plastics. Thus, the bearing can continue rolling after a somewhat greater degree of wear takes place. Bronze also wears at a lower rate than does a phenolic. If one was attempting to extract the most life after an adequate lubricant replenishment was completely depleted, an oil filled porous bronze is a challenging candidate.

3.5.5 Lubrication and Environment

The weakest link in the life chain of an instrument bearing is lubrication. Typically, instrument bearings are lubricated and are on their way to a predictable end at an unpredictable time. Usually lubrication starvation does not cause the failure. Air borne contamination, improper cleaning procedures, and maintenance initiated deterioration are more likely to be the root of the problem.

If the design life objective was 1000 hours or less, then satisfactory lubrication could be obtained with a one-shot installation. However with a life requirement in the tens of thousands of hours, possibly operating continuously, lubricant replenishment must be incorporated into the recorder bearing design. Two schemes of lubricant replenishment are available; a reservoir of lubricant at each bearing and wick feed, or a central lubricant reservoir from which lubricant could be periodically pumped through capillary tubes to each bearing.

Andok C lubricating grease with a phenolic retainer has long been a standby in instrument bearing lubrication. Review of the differences between grease and "oil only lubrication" shows that the major difference is the mixture of small soap spheroids[17,18] in with the oil. The effect of the soap breakdown is to raise the apparent viscosity of the lubricating oil, thus increasing the minimum oil thickness separating the ball to race contact. As an example, the rolling speed of a 3/16 ball in a typical recorder application would range from 1 to 15 in./sec. With a Gl lithium hydroxysterate soap grease, the minimum film thickness would range from $h \approx 3 \times 10^{-6}$ in. to 12×10^{-6} in. while the base oil alone would generate a thickness range from $h \approx 2 \times 10^{-6}$ in. to 8×10^{-6} in. for the same load and speed conditions.

Considerations of oil film thickness -- particularly between the balls and the races -- is crucial to the success of the bearing system. Tallian[19] clearly illustrates the impact of film thickness on L_{10} life. He reports on the statistical evidence that a ratio of film thickness composite surface roughness, ξ_o, of less than a factor of two (2) results in major life reduction, e.g., a change in ξ from 2 to 1 produces a L_{10} reduction from 100% to 50%. Hence, a main design specification for the lubricant is that for the transport's bearing range of speeds, loads, and temperature, ξ should be maximized, i.e.,

$$\xi = \frac{\text{Minimum Film Thickness(h)}}{\text{Composite Surface Roughness(R)}} \tag{133}$$

$$\xi > 2 \quad (\text{preferably: } \xi \simeq 4,\ L_{10} \text{ increased } 200\%) \tag{134}$$

Numerically, this ratio represents a film thickness criteria of:

$$h \simeq 40 \times 10^{-6} \text{ in.}$$

since, for precision bearing, the surface roughness factor (R) is approximately

$$R \simeq 10 \times 10^{-6} \text{ in.}$$

In the work by Dyson and Wilson[17], bearing failures have been attributed to oil starvation. In one case, starvation occurred after 45 minutes of operation at a rather high rolling speed of 80 in./sec. The important parameters which effect film starvation are the oil viscosity and surface tension. Starvation does not necessarily imply a lack of oil in the general sense but more specifically the problem of oil supply at the inlet position of the ball. The correct amount of oil is more important than an excess of oil since an excess of oil can lead to churning, thus heating the oil, decreasing the viscosity, and wastefully absorbing power. At relatively slow ball speeds (a few in./sec.) expected in a recorder, it is unlikely that film oil starvation would be encountered. However, loss of oil may be experienced owing to the zero gravity effect. In such a case, minute amounts of oil may splash away from the ball, and not return to the bottom of the race. This "lost" oil must be minimized and replaced.

Oil loss can be minimized by presenting non-wetting surfaces in areas adjacent to the bearing (Fig. 61). Where oil is at a junction of a non-wetting surface and the bearing, the surface tension of the oil can be used to prevent further oil exit motion. A low surface energy layer such as Nye Bar[20] is commercially available and can be easily applied to surfaces adjacent to a bearing. A Teflon liner would also serve the same purpose.

Continuing the exploration of methods to ensure sufficient lubrication, one can consider the combination of zero gravity and wetting surfaces. Any splashed off oil from the bearings, will not have zero velocity. It will at least drift in the shaft housing until it hits the shaft housing or the shaft. If it hits the shaft it will experience a velocity change. Ultimately any drifting oil must contact the shaft housing wall. The shaft housing wall should have an oil wetting surface. Any oil that contacts such a surface would spread. The surface tension effect could then be used to return the "lost" oil to a central storage from where it could by recycled. In theory this scheme would work if the ancillary flow control problems do not produce a reliability penalty on the recycling of the lubricating oil.

The oil chosen as the lubricant must have a relatively flat viscosity curve with respect to temperature between -5°C and 60°C. It must be highly refined so that any varnish forming impurities are removed. It must not contain any oxidation preventive additives; since the complete recorder should be in an inert gas environment. The soap which carries the oil must be a non-caking type and investigation should be made into the effects of long term shelf life on any candidates; since, that is probably the closest test to setting in a bearing for long periods that can be made.

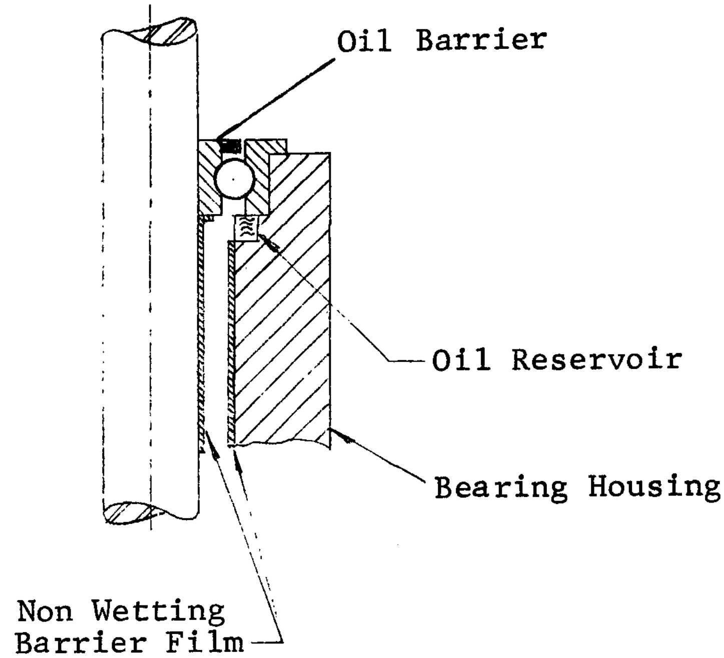

b) Oil Reservoir - Wick Feed Lubricant Replenishment

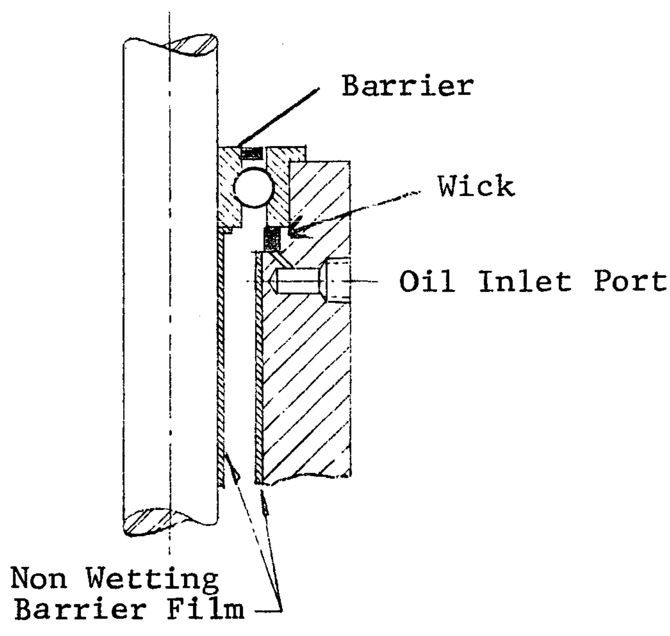

a) Pulsed Lubricant - Replenishment

Figure 61

SCHEMATIC OF LUBRICANT REPLENISHMENT CONCEPTS

The necessary gas environment to maximize reliability is therefore a low humidity, inert gas. An acceptable candidate is nitrogen with a trace of helium for leak checking. The consideration of over-riding importance is to insure the absence of oxygen. Essentially all lubricants are oxidized at a rate that is an exponential function of temperature. The operating temperature of the recorder is not severe, but the greatest environmental damage to lubricants is the development of the so called "brown sugar"; a result of lubricant oxidation. Continuing the discussion of the gas environment, it would be preferable to reduce the water content to zero. A conflicting requirement is the required humidity level of the tape. If the water level cannot be reduced to minimal levels -- say 5% relative humidity -- then the use of 52100 steel should be reevaluated and 440C stainless steel becomes preferable bearing material.

3.6 Kinetic Analysis

3.6.1 Modeling

The function of this analysis is to determine the changes in kinetic properties as magnetic tape is transferred from one tape reel (assumed to be on the right) to another tape reel (on the left) ignoring the effects of system friction and tape tension drag. The nomenclature is given in Table 13.

3.6.1.1 Rotational Velocities of the Tape Reels

The change in radius of the reel hubs plus tape over time is given by the expression:

$$r_L = \left(r_{HO}^2 + \frac{VT\delta}{\pi P_t}\right)^{\frac{1}{2}} \tag{135}$$

$$r_R = \left(r_{HO}^2 + \frac{\delta(L-VT)}{\pi P_t}\right)^{\frac{1}{2}} \tag{136}$$

The rotational velocities of the reels are:

$$\omega_L = \frac{V}{r_L} \tag{137}$$

$$\omega_R = \frac{V}{r_R} \tag{138}$$

3.6.1.2 Reel Inertia

$$I_H = \frac{\pi\rho_H W(r_{HO}^4 - r_{Hi}^4)}{2} \tag{139}$$

$$I_{LT} = \frac{\pi\rho_T W(r_L^4 - r_{HO}^4)}{2} \tag{140}$$

Table 13

KINETIC ANALYSIS NOMENCLATURE

r_L = outside radius of the left reel including tape

r_R = outside radius of the right reel including tape

r_{HO} = outside radius of the tape reel hub

r_{HI} = inside radius of the tape reel hub

V = tape velocity

T = time since analysis began

δ = thickness of tape

P_T = packing factor for tape

L = total length of tape

ω_L = rotational velocity of left reel

ω_R = rotational velocity of right reel

I_H = moment of inertia of the reel hubs

I_{LT} = moment of inertia of the tape on the left reel

I_{RT} = moment of inertia of the tape on the right reel

ρ_H = density of the hub material/g

ρ_T = density of the tape/g

W = width of the tape

I_L = moment of inertia of the left hub and tape (reel)

I_R = moment of inertia of the right hub and tape (reel)

α_L = angular acceleration of the left reel

α_R = angular acceleration of the right reel

Table 13 (Cont.)

KINETIC ANALYSIS NOMENCLATURE

τ_L = torque potential of left reel

τ_R = torque potential of right reel

E_L = rotational energy of the left reel

E_R = rotational energy of the right reel

P_L = rotational power of the left reel

P_R = rotational power of the right reel

$$I_{RT} = \frac{\pi\rho_T W(r_R^4 - r_{HO}^4)}{2} \tag{141}$$

$$I_L = I_H + I_{LT} \tag{142}$$

$$I_R = I_H + I_{RT} \tag{143}$$

3.6.1.3 Torque Determination

$$\alpha_L = \dot{\omega}_L \simeq \frac{\omega_{L2} - \omega_{L1}}{T2 - T1} \tag{144}$$

$$\alpha_R = \dot{\omega}_R \simeq \frac{\omega_{R2} - \omega_{R1}}{R2 - R1} \tag{145}$$

$$\tau L = I_L\alpha_L \tag{146}$$

$$\tau R = I_R\alpha_R \tag{147}$$

3.6.1.4 Angular Momentum

$$M_L = I_L\omega_L \tag{148}$$

$$M_R = I_R\omega_R \tag{149}$$

3.6.1.5 Rotational Energy

$$E_L = \frac{I_L \omega_L^{\ 2}}{2} \tag{150}$$

$$E_R = \frac{I_R \omega_R^{\ 2}}{2} \tag{151}$$

3.6.1.6 Rotational Power

$$P_L = \dot{E}_L \simeq \frac{E_{L2} - E_{L1}}{T_2 - T_1} \tag{152}$$

$$P_R = \dot{E}_R \simeq \frac{E_{R2} - E_{R1}}{T_2 - T_1} \tag{153}$$

3.6.2 Computation and Documentation

The preceding formulas were programmed on the digital computer in order of their appearance. The required input data is shown in Figure 62, and the computer program in Figure 63. The input/output data is shown in Figure 64 where the results can be read directly from the computer printout. The example shown illustrates the change of the various kinetic properties in five second time increments at a tape speed of 32.0 inches per second.

Code	Nomenclature	Field	Format	Units
RH	Inside Hub Radius	1-7	10F7.0	ins
RHO	Outside Hub Radius	8-14	10F7.0	ins
DH	Hub Density	15-21	10F7.0	lb in^{-3}
D	Tape Length	22-28	10F7.0	ft
W	Tape Width	29-35	10F7.0	ins
DE	Tape Thickness	36-42	10F7.0	ins
PT	Packing Factor	43-49	10F7.0	%
V	Tape Velocity	50-56	10F7.0	in sec^{-1}
T	Time Increment	57-63	10F7.0	sec
DT	Tape Density	64-70	10F7.0	lb in^{-3}

Figure 62

KINETIC ANALYSIS INPUT DATA

Figure 63

KINETIC ANALYSIS COMPUTER PROGRAM

```
      READ 20,RH,RHO,DH,D,W,DE,PT,V,T,DT
   20 FORMAT ( 10F7.0 )
      PY = 3.14159
      E = D* 12.0
      A = 0.0
      OL = 0.0
      OR = 0.0
      ELO = 0.0
      ERO = 0.0
   40 B = V * A
      RL = ((RHO)**2.0 + ((B*DE) / (PT*PY)))**0.5
      RR = ((RHO)**2.0 + ((DE*(E-B)) / (PT*PY)))**0.5
      C = RL + RR
      OMEGL = V/RL
      OMEGR = V/RR
      AIH =  (PY*DH*W* ((RHO**4.0) - (RH**4.0 ))) /(2.0* 386.088 )
      AITL = ( PY*DT*W*(( RL**4.0 ) - ( RHO**4.0 ))*PT) /(2.0* 386.088 )
      AITR = ( PY*DT*W* ((RR**4.0) - (RHO**4.0))*PT) /(2.0* 386.088 )
      AIL = AIH + AITL
      AIR = AIH + AITR
      DOMEGL = OMEGL - OL
      OL = OMEGL
      DOMEGR = OMEGR - OR
      OR = OMEGR
      ALPHAL = DOMEGL / T
      ALPHAR = DOMEGR / T
      TORQL = AIL * ALPHAL
      TORQR = AIR * ALPHAR
      OMEGIL = AIL *OMEGL
      OMEGIR = AIR*OMEGR
      EL =  (AIL*(OMEGL**2.0)) / 2.0
      ER = ( AIR * (OMEGR**2.0)) / 2.0
      ET = EL + ER
      DEL = EL - ELO
      ELO = EL
      DER = ER - ERO
      ERO = ER
      PWRL = DEL / T
      PWRR = DER / T
      IF ( AA - 4.0 ) 220, 240, 240
  220 PRINT 230
  230 FORMAT(132H TIME LENGTH RAD.L RAD.R CTR.D OMEGA L OMEGA R INERT L
     1INERT R IOMEG L IOMEG R ERG L ERG R ERG T TORQUE L TORQUE R  POWER
     2 L POWER R      )
      PRINT 235
  235 FORMAT(132H SEC. INCHES  IN.   IN.   IN.  RAD/SEC RAD/SEC INLBSC2
     1INLBSC2 INLBSEC INLBSEC IN.LB IN.LB IN.LB  IN.LBS.  IN.LBS. INLB/S
     2EC INLB/SEC          / )
      AA = 5.0
  240 PRINT 250,(A,B,RL,RR,C,OMEGL,OMEGR,AIL ,AIR ,OMEGIL,OMEGIR,EL,ER,
     1ET,TORQL,TORQR,PWRL,PWRR )
  250 FORMAT ( F5.0,F7.0,3F6.3,6E8.3,3F6.3,4E9.4 )
      A = A + T
      IF ( B - E ) 40, 270, 270
  270 PRINT 280
  280 FORMAT ( 102H  IR HUB    OR HUB   DENS.HUB  LGT.TAPE  WDT.TAPE  TH
     1K.TAPE  PK FCTR   TAPE VEL  TIME INCR DENS.TAPE     /)
      PRINT 285
  285 FORMAT ( 105H  INCHES    INCHES   LBW/IN 3  FEET      INCHES    IN
     1CHES   DEC.PCT.  IN/SEC    SEC.      LBW/IN 3              /)
      PRINT 300, (RH,RHO,DH,D,W,DE,PT,V,T,DT )
  300 FORMAT ( 10E10.5 )
      END
```

1

INPUT DATA

IR HUB INCHES	OR HUB INCHES	DENS.HUB LBW/IN 3	LGT.TAPE FEET	WDT.TAPE INCHES	THK.TAPE INCHES	PK FCTR DEC.PCT.	TAPE VEL IN/SEC	TIME INCR SEC.	DENS.TAPE LBW/IN 3
.15000+01	.20000+01	.10000+00	.12000+04	.50000-00	.10000-02	.95000-00	.32000+02	.50000+01	.50000-01

OUTPUT DATA

TIME SEC.	LENGTH INCHES	RAD.L IN.	RAD.R IN.	CTR.D IN.	OMEGA L RAD/SEC	OMEGA R RAD/SEC	INERT L INLBSC2	INERT R INLBSC2	IOMEG L INLBSEC	IOMEG R INLBSEC	ERG L IN.LB	ERG R IN.LB	ERG T IN.LB	TORQUE L IN.LBS.	TORQUE R IN.LBS.	POWER L INLB/SEC	POWER R INLB/SEC
0.	0.	2.000	2.971	4.971	.160+02	.108+02	.222-02	.820-02	.356-01	.884-01	.285	.476	.761	.7120-02	.1767-01	.5696-01	.9520-01
5.	160.	2.013	2.962	4.975	.159+02	.108+02	.227-02	.811-02	.360-01	.877-01	.286	.474	.760	-.4812-04	.5333-04	.3006-03	-.4823-03
10.	320.	2.027	2.953	4.979	.158+02	.108+02	.231-02	.802-02	.365-01	.869-01	.288	.471	.759	-.4806-04	.5322-04	.3066-03	-.4817-03
15.	480.	2.040	2.943	4.983	.157+02	.109+02	.235-02	.793-02	.369-01	.862-01	.289	.469	.758	-.4800-04	.5311-04	.3124-03	-.4811-03
20.	640.	2.053	2.934	4.987	.156+02	.109+02	.240-02	.784-02	.373-01	.855-01	.291	.466	.757	-.4795-04	.5300-04	.3179-03	-.4805-03
25.	800.	2.066	2.925	4.991	.155+02	.109+02	.244-02	.775-02	.378-01	.848-01	.293	.464	.757	-.4791-04	.5289-04	.3232-03	-.4799-03
30.	960.	2.079	2.916	4.995	.154+02	.110+02	.248-02	.767-02	.382-01	.841-01	.294	.462	.756	-.4787-04	.5279-04	.3284-03	-.4792-03
35.	1120.	2.092	2.907	4.999	.153+02	.110+02	.253-02	.758-02	.387-01	.834-01	.296	.459	.755	-.4784-04	.5268-04	.3333-03	-.4786-03
40.	1280.	2.104	2.898	5.002	.152+02	.110+02	.257-02	.749-02	.391-01	.827-01	.298	.457	.754	-.4782-04	.5257-04	.3381-03	-.4779-03
45.	1440.	2.117	2.888	5.006	.151+02	.111+02	.262-02	.740-02	.396-01	.820-01	.299	.454	.754	-.4780-04	.5246-04	.3427-03	-.4772-03
50.	1600.	2.130	2.879	5.009	.150+02	.111+02	.267-02	.732-02	.401-01	.813-01	.301	.452	.753	-.4778-04	.5235-04	.3471-03	-.4765-03
55.	1760.	2.142	2.870	5.012	.149+02	.112+02	.271-02	.723-02	.405-01	.806-01	.303	.450	.752	-.4778-04	.5224-04	.3514-03	-.4758-03
60.	1920.	2.155	2.860	5.015	.149+02	.112+02	.276-02	.715-02	.410-01	.800-01	.305	.447	.752	-.4777-04	.5214-04	.3556-03	-.4751-03
65.	2080.	2.167	2.851	5.018	.148+02	.112+02	.281-02	.706-02	.415-01	.793-01	.306	.445	.751	-.4778-04	.5203-04	.3596-03	-.4744-03
70.	2240.	2.180	2.842	5.021	.147+02	.113+02	.286-02	.698-02	.420-01	.786-01	.308	.443	.751	-.4778-04	.5192-04	.3634-03	-.4737-03
75.	2400.	2.192	2.832	5.024	.146+02	.113+02	.291-02	.690-02	.425-01	.779-01	.310	.440	.750	-.4779-04	.5181-04	.3671-03	-.4729-03
80.	2560.	2.204	2.823	5.027	.145+02	.113+02	.296-02	.681-02	.430-01	.772-01	.312	.438	.750	-.4781-04	.5171-04	.3707-03	-.4721-03
85.	2720.	2.216	2.813	5.029	.144+02	.114+02	.301-02	.673-02	.435-01	.766-01	.314	.435	.749	-.4783-04	.5160-04	.3742-03	-.4713-03
90.	2880.	2.228	2.804	5.032	.144+02	.114+02	.306-02	.665-02	.440-01	.759-01	.316	.433	.749	-.4785-04	.5150-04	.3776-03	-.4705-03
95.	3040.	2.240	2.794	5.034	.143+02	.115+02	.311-02	.657-02	.445-01	.752-01	.318	.431	.748	-.4788-04	.5139-04	.3809-03	-.4697-03
100.	3200.	2.252	2.784	5.037	.142+02	.115+02	.316-02	.649-02	.450-01	.745-01	.319	.428	.748	-.4791-04	.5128-04	.3840-03	-.4689-03
105.	3360.	2.264	2.775	5.039	.141+02	.115+02	.322-02	.641-02	.455-01	.739-01	.321	.426	.747	-.4794-04	.5118-04	.3871-03	-.4680-03
110.	3520.	2.276	2.765	5.041	.141+02	.116+02	.327-02	.633-02	.460-01	.732-01	.323	.424	.747	-.4798-04	.5108-04	.3901-03	-.4671-03
115.	3680.	2.288	2.755	5.043	.140+02	.116+02	.333-02	.625-02	.465-01	.726-01	.325	.421	.747	-.4802-04	.5097-04	.3929-03	-.4662-03
120.	3840.	2.299	2.746	5.045	.139+02	.117+02	.338-02	.617-02	.470-01	.719-01	.327	.419	.746	-.4806-04	.5087-04	.3957-03	-.4653-03
125.	4000.	2.311	2.736	5.047	.138+02	.117+02	.343-02	.609-02	.476-01	.713-01	.329	.417	.746	-.4811-04	.5077-04	.3984-03	-.4644-03
130.	4160.	2.322	2.726	5.048	.138+02	.117+02	.349-02	.601-02	.481-01	.706-01	.331	.414	.746	-.4816-04	.5066-04	.4011-03	-.4634-03
135.	4320.	2.334	2.716	5.050	.137+02	.118+02	.355-02	.594-02	.486-01	.700-01	.333	.412	.745	-.4821-04	.5056-04	.4036-03	-.4625-03
140.	4480.	2.345	2.706	5.052	.136+02	.118+02	.360-02	.586-02	.492-01	.693-01	.335	.410	.745	-.4826-04	.5046-04	.4061-03	-.4615-03
145.	4640.	2.357	2.696	5.053	.136+02	.119+02	.366-02	.579-02	.497-01	.687-01	.337	.407	.745	-.4831-04	.5036-04	.4085-03	-.4604-03
150.	4800.	2.368	2.686	5.055	.135+02	.119+02	.372-02	.571-02	.502-01	.680-01	.339	.405	.745	-.4837-04	.5026-04	.4108-03	-.4594-03
155.	4960.	2.379	2.676	5.056	.134+02	.120+02	.378-02	.564-02	.508-01	.674-01	.342	.403	.744	-.4843-04	.5016-04	.4131-03	-.4583-03
160.	5120.	2.391	2.666	5.057	.134+02	.120+02	.384-02	.556-02	.513-01	.668-01	.344	.401	.744	-.4849-04	.5006-04	.4153-03	-.4573-03
165.	5280.	2.402	2.656	5.058	.133+02	.120+02	.389-02	.549-02	.519-01	.661-01	.346	.398	.744	-.4856-04	.4996-04	.4174-03	-.4561-03
170.	5440.	2.413	2.646	5.059	.133+02	.121+02	.395-02	.542-02	.524-01	.655-01	.348	.396	.744	-.4863-04	.4986-04	.4195-03	-.4550-03
175.	5600.	2.424	2.636	5.060	.132+02	.121+02	.402-02	.534-02	.530-01	.649-01	.350	.394	.744	-.4869-04	.4977-04	.4215-03	-.4538-03
180.	5760.	2.435	2.626	5.061	.131+02	.122+02	.408-02	.527-02	.536-01	.643-01	.352	.392	.744	-.4876-04	.4967-04	.4235-03	-.4527-03

Figure 64

KINETIC ANALYSIS - OUTPUT DATA

185.	5920.	2.446	2.616	5.062	.131+02	.122+02	.414-02	.520-02	.541-01	.636-01	.354	.389	.743-.4883-04	4958-04	.4254-03-.4514-03
190.	6080.	2.457	2.605	5.062	.130+02	.123+02	.420-02	.513-02	.547-01	.630-01	.356	.387	.743-.4891-04	4948-04	.4273-03-.4502-03
195.	6240.	2.468	2.595	5.063	.130+02	.123+02	.426-02	.506-02	.553-01	.624-01	.358	.385	.743-.4898-04	4939-04	.4291-03-.4489-03
200.	6400.	2.479	2.585	5.063	.129+02	.124+02	.433-02	.499-02	.559-01	.618-01	.361	.383	.743-.4906-04	4929-04	.4309-03-.4476-03
205.	6560.	2.490	2.574	5.064	.129+02	.124+02	.439-02	.492-02	.564-01	.612-01	.363	.380	.743-.4914-04	4920-04	.4326-03-.4463-03
210.	6720.	2.500	2.564	5.064	.128+02	.125+02	.446-02	.485-02	.570-01	.606-01	.365	.378	.743-.4921-04	4911-04	.4343-03-.4449-03
215.	6880.	2.511	2.553	5.064	.127+02	.125+02	.452-02	.479-02	.576-01	.600-01	.367	.376	.743-.4930-04	4902-04	.4359-03-.4435-03
220.	7040.	2.522	2.543	5.065	.127+02	.126+02	.459-02	.472-02	.582-01	.594-01	.369	.374	.743-.4938-04	4893-04	.4375-03-.4420-03
225.	7200.	2.532	2.532	5.065	.126+02	.126+02	.465-02	.465-02	.588-01	.588-01	.371	.371	.743-.4946-04	4884-04	.4390-03-.4406-03
230.	7360.	2.543	2.522	5.065	.126+02	.127+02	.472-02	.459-02	.594-01	.582-01	.374	.369	.743-.4954-04	4876-04	.4406-03-.4390-03
235.	7520.	2.553	2.511	5.064	.125+02	.127+02	.479-02	.452-02	.600-01	.576-01	.376	.367	.743-.4963-04	4867-04	.4420-03-.4375-03
240.	7680.	2.564	2.500	5.064	.125+02	.128+02	.485-02	.446-02	.606-01	.570-01	.378	.365	.743-.4971-04	4859-04	.4435-03-.4359-03
245.	7840.	2.574	2.490	5.064	.124+02	.129+02	.492-02	.439-02	.612-01	.564-01	.380	.363	.743-.4980-04	4850-04	.4449-03-.4343-03
250.	8000.	2.585	2.479	5.063	.124+02	.129+02	.499-02	.433-02	.618-01	.559-01	.383	.361	.743-.4989-04	4842-04	.4463-03-.4326-03
255.	8160.	2.595	2.468	5.063	.123+02	.130+02	.506-02	.426-02	.624-01	.553-01	.385	.358	.743-.4998-04	4834-04	.4476-03-.4309-03
260.	8320.	2.605	2.457	5.062	.123+02	.130+02	.513-02	.420-02	.630-01	.547-01	.387	.356	.743-.5007-04	4826-04	.4489-03-.4291-03
265.	8480.	2.616	2.446	5.062	.122+02	.131+02	.520-02	.414-02	.636-01	.541-01	.389	.354	.743-.5016-04	4818-04	.4502-03-.4273-03
270.	8640.	2.626	2.435	5.061	.122+02	.131+02	.527-02	.408-02	.643-01	.536-01	.392	.352	.744-.5025-04	4811-04	.4514-03-.4254-03
275.	8800.	2.636	2.424	5.060	.121+02	.132+02	.534-02	.402-02	.649-01	.530-01	.394	.350	.744-.5035-04	4803-04	.4527-03-.4235-03
280.	8960.	2.646	2.413	5.059	.121+02	.133+02	.542-02	.395-02	.655-01	.524-01	.396	.348	.744-.5044-04	4796-04	.4538-03-.4215-03
285.	9120.	2.656	2.402	5.058	.120+02	.133+02	.549-02	.389-02	.661-01	.519-01	.398	.346	.744-.5053-04	4789-04	.4550-03-.4195-03
290.	9280.	2.666	2.391	5.057	.120+02	.134+02	.556-02	.384-02	.668-01	.513-01	.401	.344	.744-.5063-04	4782-04	.4561-03-.4174-03
295.	9440.	2.676	2.379	5.056	.120+02	.134+02	.564-02	.378-02	.674-01	.508-01	.403	.342	.744-.5073-04	4775-04	.4573-03-.4153-03
300.	9600.	2.686	2.368	5.055	.119+02	.135+02	.571-02	.372-02	.680-01	.502-01	.405	.339	.745-.5082-04	4768-04	.4583-03-.4131-03
305.	9760.	2.696	2.357	5.053	.119+02	.136+02	.579-02	.366-02	.687-01	.497-01	.407	.337	.745-.5092-04	4762-04	.4594-03-.4108-03
310.	9920.	2.706	2.345	5.052	.118+02	.136+02	.586-02	.360-02	.693-01	.492-01	.410	.335	.745-.5102-04	4756-04	.4604-03-.4085-03
315.	10080.	2.716	2.334	5.050	.118+02	.137+02	.594-02	.355-02	.700-01	.486-01	.412	.333	.745-.5112-04	4750-04	.4615-03-.4061-03
320.	10240.	2.726	2.322	5.048	.117+02	.138+02	.601-02	.349-02	.706-01	.481-01	.414	.331	.746-.5121-04	4744-04	.4625-03-.4036-03
325.	10400.	2.736	2.311	5.047	.117+02	.138+02	.609-02	.343-02	.713-01	.476-01	.417	.329	.746-.5131-04	4739-04	.4634-03-.4011-03
330.	10560.	2.746	2.299	5.045	.117+02	.139+02	.617-02	.338-02	.719-01	.470-01	.419	.327	.746-.5141-04	4734-04	.4644-03-.3984-03
335.	10720.	2.755	2.288	5.043	.116+02	.140+02	.625-02	.333-02	.726-01	.465-01	.421	.325	.747-.5151-04	4729-04	.4653-03-.3957-03
340.	10880.	2.765	2.276	5.041	.116+02	.141+02	.633-02	.327-02	.732-01	.460-01	.424	.323	.747-.5162-04	4724-04	.4662-03-.3929-03
345.	11040.	2.775	2.264	5.039	.115+02	.141+02	.641-02	.322-02	.739-01	.455-01	.426	.321	.747-.5172-04	4720-04	.4671-03-.3901-03
350.	11200.	2.784	2.252	5.037	.115+02	.142+02	.649-02	.316-02	.745-01	.450-01	.428	.319	.748-.5182-04	4716-04	.4680-03-.3871-03
355.	11360.	2.794	2.240	5.034	.115+02	.143+02	.657-02	.311-02	.752-01	.445-01	.431	.318	.748-.5192-04	4712-04	.4689-03-.3840-03
360.	11520.	2.804	2.228	5.032	.114+02	.144+02	.665-02	.306-02	.759-01	.440-01	.433	.316	.749-.5203-04	4708-04	.4697-03-.3809-03
365.	11680.	2.813	2.216	5.029	.114+02	.144+02	.673-02	.301-02	.766-01	.435-01	.435	.314	.749-.5213-04	4705-04	.4705-03-.3776-03
370.	11840.	2.823	2.204	5.027	.113+02	.145+02	.681-02	.296-02	.772-01	.430-01	.438	.312	.750-.5223-04	4702-04	.4713-03-.3742-03
375.	12000.	2.832	2.192	5.024	.113+02	.146+02	.690-02	.291-02	.779-01	.425-01	.440	.310	.750-.5234-04	4700-04	.4721-03-.3707-03
380.	12160.	2.842	2.180	5.021	.113+02	.147+02	.698-02	.286-02	.786-01	.420-01	.443	.308	.751-.5244-04	4698-04	.4729-03-.3671-03
385.	12320.	2.851	2.167	5.018	.112+02	.148+02	.706-02	.281-02	.793-01	.415-01	.445	.306	.751-.5255-04	4697-04	.4737-03-.3634-03
390.	12480.	2.860	2.155	5.015	.112+02	.149+02	.715-02	.276-02	.800-01	.410-01	.447	.305	.752-.5265-04	4695-04	.4744-03-.3596-03
395.	12640.	2.870	2.142	5.012	.112+02	.149+02	.723-02	.271-02	.806-01	.405-01	.450	.303	.752-.5276-04	4695-04	.4751-03-.3556-03
400.	12800.	2.879	2.130	5.009	.111+02	.150+02	.732-02	.267-02	.813-01	.401-01	.452	.301	.753-.5286-04	4695-04	.4758-03-.3514-03
405.	12960.	2.888	2.117	5.006	.111+02	.151+02	.740-02	.262-02	.820-01	.396-01	.454	.299	.754-.5297-04	4695-04	.4765-03-.3471-03
410.	13120.	2.898	2.104	5.002	.110+02	.152+02	.749-02	.257-02	.827-01	.391-01	.457	.298	.754-.5307-04	4696-04	.4772-03-.3427-03
415.	13280.	2.907	2.092	4.999	.110+02	.153+02	.758-02	.253-02	.834-01	.387-01	.459	.296	.755-.5318-04	4697-04	.4779-03-.3381-03
420.	13440.	2.916	2.079	4.995	.110+02	.154+02	.767-02	.248-02	.841-01	.382-01	.462	.294	.756-.5329-04	4699-04	.4786-03-.3333-03
425.	13600.	2.925	2.066	4.991	.109+02	.155+02	.775-02	.244-02	.848-01	.378-01	.464	.293	.757-.5339-04	4701-04	.4792-03-.3284-03
430.	13760.	2.934	2.053	4.987	.109+02	.156+02	.784-02	.240-02	.855-01	.373-01	.466	.291	.757-.5350-04	4704-04	.4799-03-.3232-03
435.	13920.	2.943	2.040	4.983	.109+02	.157+02	.793-02	.235-02	.862-01	.369-01	.469	.289	.758-.5361-04	4708-04	.4805-03-.3179-03
440.	14080.	2.953	2.027	4.979	.108+02	.158+02	.802-02	.231-02	.869-01	.365-01	.471	.288	.759-.5372-04	4713-04	.4811-03-.3124-03
445.	14240.	2.962	2.013	4.975	.108+02	.159+02	.811-02	.227-02	.877-01	.360-01	.474	.286	.760-.5382-04	4718-04	.4817-03-.3066-03
450.	14400.	2.971	2.000	4.971	.108+02	.160+02	.820-02	.222-02	.884-01	.356-01	.476	.285	.761-.5393-04	4724-04	.4823-03-.3006-03

Figure 64 (Cont.)

KINETIC ANALYSIS - OUTPUT DATA

3.7 Alternate Motor Speed Reducer

The requirement of providing different tape speeds for the record and reproduce mode of an operable transport has historically been accomplished by using either gear or belt pulley assemblies. Such speed reducers coupled with capstan diameters in the order of 0.5 inches or less have allowed reasonably high rotational motor speeds to be used.

The use of this type of speed reducer was eliminated with the decision to minimize all possible critical components within the transport including gears and belts. A direct drive strategy was adopted where the capstan became an integral part of the drive motor in a modularized form.

A further requirement of minimizing stress levels within the tape demanded a substantial increase in the diameter of the drive capstans up to a minimum of 1.0 inch diameter. These two requirements coupled with an assumed low tape speed in the order of 1.5 inches per second result in a low motor speed of approximately 20 rpm.

Although the use of such a low motor speed is not considered to be detrimental to the overall life of the transport at this time, a design was conceived for an alternate slow speed capstan in which a six to one reducer allows a motor speed of approximately 120 rpm to be maintained for a tape speed of 1.5 inches per second.

The mechanical reducer illustrated in Figure 65 is an integral part of the capstan/motor assembly and situated between them. Three disks (steel rim mounted on an elastomer support) are driven by the motor shaft through friction, enough force is obtained between the disks and the drive shaft to insure rolling and hence no slippage. Gear or belt pulsations are, of course, eliminated in this transmission, as the outer diameter of the disks drive the capstan from the inside. A unique feature of this drive is the method for decoupling the reducer during the high speed mode. During playback at high speed, the slow speed capstan would drive the slow motor at a 24:1 increase in its normal speed. To circumvent this condition, the cage that couples the planetary disks is unlocked during the high speed mode. This unlocking of the cage permits the planetary disks to freely rotate and hence allows the drive to operate at a speed ratio of 1:1.

It is obvious from the underlying philosophy adopted throughout this design study that the concept of direct drive even at low motor speeds is desirable owing to the complexity of this arrangement. In the event, however, that the required motor characteristics are not obtainable at extremely low rotational speeds, this assembly is considered to be the most desirable alternative to obtaining reliable operation at low tape speeds.

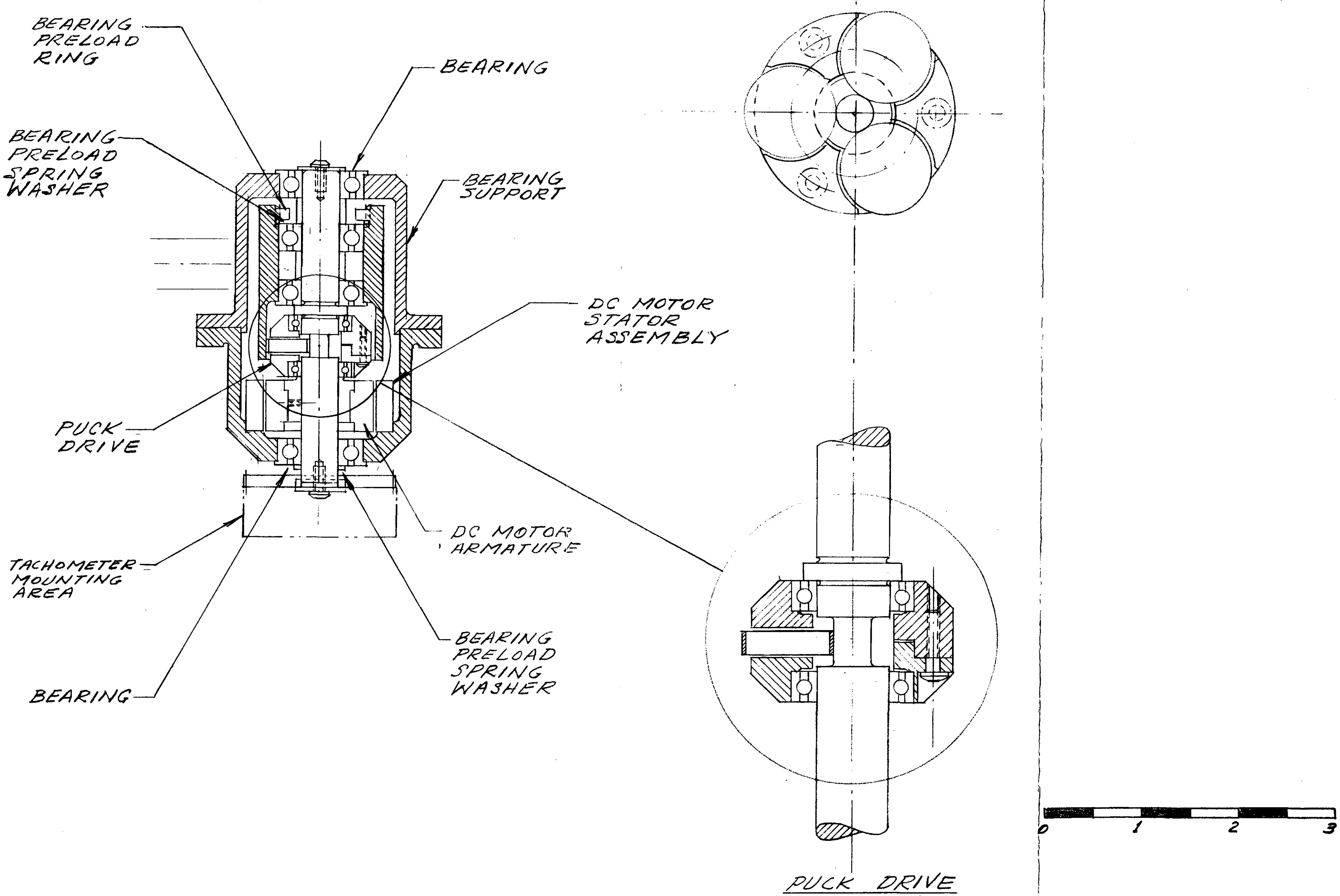

FIGURE 65 ALTERNATE MOTOR SPEED REDUCER

Preceding page blank

REFERENCES

1. Scopelite, T.M., Error Analysis of Tape Transport Systems, IIT Research Institute, Project No. K1039, September 1967.

2. Owen, R.J., Magnetic Head/Tape Interface Study for Satellite Tape Recorders, Contract No. NAS5-11622, IIT Research Institute, Project E6134, February 1971.

3. Owen, R.J., Five Year Magnetic Tape for Unattended Satellite Tape Recorders, Contract No. NAS5-21623, IIT Research Institute, Project E6205, to be published.

4. Benn. G.S.L., Mariner Mars-71 Head/Tape Stick-Slip Study, J.P.L. Contract No. 952832, IIT Research Institute, Project E6169, February 1971.

5. Eshleman, R.L. and Rao, P.N., "The Response of Mechanical Shock Isolation Elements to High Rate Input Loading," Shock and Vibration Bulletin, No. 40, p. 5, December 1969, pp. 217-234.

6. Davies, G.L., "Magnetic Tape Instrumentation," McGraw-Hill, New York, 1961.

7. Eschman, P., "Roller Bearing Wear Life," ASME, 1967.

8. Magnetic Tape Study, ASTM Report No. AD 238 884L, January 31, 1960.

9. Harris, T.A., "Roller Bearing Analysis," 1st Edition 1966 - J. Wiley and Son, New York, p. 171.

10. Crawford, T.S., "The Experimental Determination of Ball Bearing Cage Stress," Wear (16), 1970, pp. 43-52.

11. Harris, op. cit., p. 446.

12. Ibid., p. 477.

13. Ibid., p. 350.

14. Palmgren, A., "Ball and Roller Bearing Engineering," 3rd Edition, Burbank, 1959.

15. Harris, op. cit., pp. 412-415.

16. McCool, J.L., "Load Ratings and Fatigue Life Prediction for Ball and Roller Bearings," ASME Trans., J. Lube Tech., January 1970.

17. Dyson, A., Wilson, A.R., Film Thickness in Elastohydrodynamic Lubrication of Rollers by Grease, Inst. of Mech. Eng. Symposium on the Use of Grease as an Engineering Component, London, February 19-20, 1970.

18. Wedeven, L.D., et al,"Optical Analysis of Ball Bearing Starvation," ASME, 70-LUB-19.

19. Tallian, T.E., "On Computing Concept Modes in Rolling Contact," ASLE Trans., V. 10, 1967, pp. 418-439.

20. William F. Nye, Inc., Bedford, Massachusetts.